DISSERTATIONES
CHIMICAE
UNIVERSITATIS
TARTUENSIS
228

KERLI MARTIN

Recognition of carboxylates by synthetic receptors – from structure-affinity studies to solid-contact anion-selective electrode prototyping

DISSERTATIONES CHIMICAE UNIVERSITATIS TARTUENSIS
228

DISSERTATIONES CHIMICAE UNIVERSITATIS TARTUENSIS
228

KERLI MARTIN

Recognition of carboxylates by synthetic receptors – from structure-affinity studies to solid-contact anion-selective electrode prototyping

UNIVERSITY OF TARTU
Press
1632

Institute of Chemistry, Faculty of Science and Technology, University of Tartu, Estonia

The dissertation is accepted for the commencement of the degree of Doctor of Philosophy in Chemistry on 11 June 2024, by the Council of the Institute of Chemistry, University of Tartu.

Supervisor:	Professor Ivo Leito, PhD Institute of Chemistry, University of Tartu, Estonia
Opponent:	Professor Claudia Caltagirone, PhD University of Cagliari, Italy
Commencement:	7 August 2024 at 10:15 AM. Auditorium 1020, Ravila 14a, Tartu

Publication of this dissertation is granted by University of Tartu, Estonia.

This work has been partially supported by Graduate School of Functional materials and technologies receiving funding from the European Regional Development Fund in University of Tartu, Estonia.

ISSN 1406-0299 (print)
ISBN 978-9916-27-582-5 (print)
ISSN 2806-2159 (pdf)
ISBN 978-9916-27-583-2 (pdf)

University of Tartu Press
www.tyk.ee

CONTENTS

LIST OF PUBLICATIONS

The current dissertation is based on the following publications referred to in the text by their Roman numerals:

I. Kadam, S. A.; **Martin, K.**; Haav, K.; Toom, L.; Mayeux, C.; Pung, A.; Gale, P. A.; Hiscock, J. R.; Brooks, S. J.; Kirby, I. L.; Busschaert, N.; Leito, I. Towards the Discrimination of Carboxylates by Hydrogen-Bond Donor Anion Receptors. *Chem. Eur. J.* **2015**, *21* (13), 5145–5160.

II. **Martin, K.**; Nõges, J.; Haav, K.; Kadam, S. A.; Pung, A.; Leito, I. Exploring Selectivity of 22 Acyclic Urea-, Carbazole- and Indolocarbazole-Based Receptors towards 11 Monocarboxylates: Exploring Selectivity of 22 Acyclic Urea-, Carbazole- and Indolocarbazole-Based Receptors towards 11 Monocarboxylates. *Eur. J. Org. Chem.* **2017**, *2017* (35), 5231–5237.

III. **Martin, K.**; Kadam, S. A.; Mattinen, U.; Bobacka, J.; Leito, I. Solid-Contact Acetate-Selective Electrode Based on a 1,3-Bis(Carbazolyl)Urea-Ionophore. *Electroanalysis* **2019**, *31* (6), 1061–1066.

Author's contribution to the publications

Publication I: The author performed the experimental work together with one of the co-authors, contributed to the planning of the experiments and the writing of the manuscript's experimental section, and participated in the manuscript's revision.

Publication II: The author performed the experimental work together with one of the co-authors, was the primary person responsible for the planning of the experiments and evaluation of the results, performed part of the computational work, and wrote the manuscript's first version. The finalisation of the manuscript was carried out together with the co-authors.

Publication III: The author performed all the experimental work, evaluated the results and wrote the manuscript's first version. The finalisation of the manuscript was carried out together with the co-authors.

ABBREVIATIONS

ASS-ISE	All-solid-state ion-selective electrode
CE	Counter electrode
COSMO-RS	Conductor-like screening model for real solvents
CP	Conductive polymer
CWE	Coated wire electrode
DMSO	Dimethyl sulfoxide
DMSO-d_6	Deuterated dimethyl sulfoxide
EIS	Electrochemical impedance spectroscopy
emf	Electromotive force
E_{R}	Repulsive energy
FIM	Fixed interference method
GC	Glassy carbon
HB	Hydrogen bond
HBA	Hydrogen bond acceptor
HBD	Hydrogen bond donor
HEPES	4-(2-hydroxyethyl)-1-piperazineethanesulfonic acid
ICZ	Indolocarbazole
ISE	Ion-selective electrode
ISM	Ion-selective membrane
IUPAC	International Union of Pure and Applied Chemistry
K_{ass}	Binding constant (association constant)
$K_{i,j}^{pot}$	Potentiometric selectivity coefficient
LC	Liquid-contact
$\log K_{\mathrm{ass}}$	Logarithm of binding constant
$\log P_{\mathrm{o-w}}$	Logarithm of octanol-water partition coefficient
NMR	Nuclear magnetic resonance
o-NPOE	2-nitrophenyl octyl ether
PCA	Principal component analysis
PEDOT	Poly(3,4-ethylenedioxythiophene)
pK_{a}	Negative logarithm of acid dissociation constant
PVC	Poly(vinyl chloride)
RE	Reference electrode
SC	Solid contact
SC-ISE	Solid-contact ion-selective electrode
SP-ISE	Single-piece ion-selective electrode
SSM	Separate solution method
TBA	Tetrabutylammonium
TDMACl	Tridodecylmethylammonium chloride
THF	Tetrahydrofuran
UV-Vis	Ultraviolet-visible
WE	Working electrode

INTRODUCTION

Ions play a critical role in both environmental systems and biological processes. Any imbalance in ion levels can lead to significant adverse effects: environmental imbalances result in pollution, while imbalances within the human body contribute to diseases. Various analytical techniques, including chromatography, mass spectrometry, fluorescence, and electrochemical methods, such as solid-contact ion-selective electrodes (SC-ISEs), are frequently used to detect and quantify ions. SC-ISEs offer unique advantages, such as being easily portable, cost-effective, and compatible with microfabrication and miniaturisation due to their small size. However, SC-ISEs for carboxylate ions are rare because of the lack of ionophores that selectively bind carboxylates.

This dissertation aims to study the binding of small carboxylates to synthetic receptors (potential ionophores) in order to identify the most suitable binding groups for designing synthetic receptors for carboxylate anions. Furthermore, this research seeks to incorporate one of the best-binding receptors into the SC-ISE's polymeric membrane as an ionophore.

To predict a carboxylate receptor that would function effectively as an ionophore in an electrode prototype, it is necessary to understand the supramolecular receptor-anion binding processes at a fundamental level and determine the binding affinities of the receptors under investigation. Previous studies have demonstrated good affinity and moderate selectivity of synthetic receptors towards different carboxylates. However, a comprehensive analysis of the structural features of carboxylates in relation to their binding to synthetic receptors is lacking. Studies with a small number of receptors and anions in different solvent media provide limited opportunities for generalisation and make meaningful comparisons of binding data difficult. Additionally, only a few carboxylate receptors have been incorporated into the membranes of ISEs.

This work aims to quantitatively characterise (with $\log K_{\mathrm{ass}}$ values) the binding of monocarboxylate anions to a diverse series of synthetic multidentate hydrogen-bond donor receptors. In the Supramolecular Analytical Chemistry research group, an established, highly accurate relative NMR-based measurement method is used to characterise the receptor-anion interaction quantitatively. Using this method, I measured the binding affinities of 44 acyclic urea-, indole-, carbazole-, thiourea- and indolocarbazole-based synthetic receptors. In total, I constructed binding affinity ladders for eight anions and studied the differential binding of 11 carboxylates (formate, acetate, pivalate, lactate, naproxen, ibuprofen, ketoprofen, glucuronate, hexanoate, sorbate, and benzoate). Furthermore, I evaluated the ability of selected receptors to discriminate between anions based on structural features (hydrophilicity, substitution at the α-carbon, etc.). Finally, I used a 1,3-bis(carbazolyl)urea derivative as a neutral hydrogen-bonding ionophore, constructed solid-contact acetate-selective electrode prototypes, and studied their performance in determining acetate anions.

1. LITERATURE OVERVIEW

1.1. Supramolecular chemistry

Most people know what analytical and organic chemistry are and what is being studied in these areas. Supramolecular chemistry is a somewhat newer and not so-widely known field. In 1967, an American organic chemist, Charles John Pedersen, described the method of synthesising dibenzo[18]crown-6, a crown ether that binds various metal cations.[1] In 1978, a French chemist, Jean-Marie Lehn, synthesised cage-like molecules – cryptands – that are suited for recognising spherical cations.[2] Some years later, Pedersen's work was expanded by an American chemist, Donald James Cram, who synthesised cyclic polyethers (spherands), which encapsulate metal cations in their small cavity.[3] These three men were the principal founders of supramolecular chemistry and were awarded the Nobel Prize in Chemistry in 1978. Since then, supramolecular chemistry has been a distinct area that studies systems involving assemblies of molecules or ions held together by non-covalent interactions. Depending on the size and shape of the interacting molecules, supramolecular chemistry can be, somewhat arbitrarily, divided into two broad categories: host-guest chemistry and self-assembly.[4] As the name suggests, in host-guest chemistry, one molecule or ion (the host) is significantly larger than another, and it can form a cavity to encapsulate the smaller molecule or ion (the guest).[5] For example, when a crown ether binds a metal cation, the crown ether acts as a host, and the metal cation acts as a guest. By non-covalent interactions, they form a supermolecule (the host-guest complex). In the case of self-assembly, there is no significant difference in size, and two or more complementary molecules or ions form a supermolecule (self-assembled aggregate) spontaneously by the non-covalent joining. In either of the two categories, supramolecular chemists explore different aspects of these supramolecular systems that can be used in various areas, such as molecular sensors and machines, chemical catalysis, extraction, and drug delivery[6,7]. The area that mainly focuses on the creation and application of sensors is called supramolecular analytical chemistry.[8]

In this dissertation, supramolecular systems are explored from the viewpoint of molecular recognition, where a synthetic receptor (the host) forms a complex with an anion (the guest) through supramolecular interactions.

Supramolecular interactions

Non-covalent interactions hold supramolecular systems together, and thus, all non-covalent interactions can be regarded as supramolecular interactions. There are several different non-covalent interactions, such as electrostatic interactions, hydrogen bonding, cation/anion-π interactions, π-π interactions, dispersion interactions, and hydrophobic effects. They are typically considerably weaker than covalent interactions, with energies ranging from 300 kJ mol^{-1} for ion-ion interactions to 1–3 kJ mol^{-1} per CH_2 for solvophobic interactions.[9,10] However, when

the binding between two or more molecules or ions is mediated simultaneously by several non-covalent bonds cooperatively, it leads to *molecular recognition*. Some examples of supramolecular interactions are illustrated in Figure 1, using the structures of well-known supramolecular systems.[1,11–14]

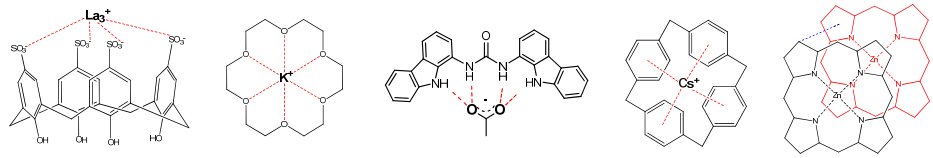

(a) (b) (c) (d) (e)

Figure 1. Examples of supramolecular interactions: (a) ion-ion interaction in the lanthanum complex of p-sulfonatocalix[4]arene; (b) ion-dipole interaction in the potassium complex of [18]crown-6; (c) hydrogen bonding in the acetate complex of bis(carbazolyl)urea; (d) cation-π interaction in the cecium complex of [1.1.1]-paracyclophane; (e) π-π interaction (blue line) in the zinc porphyrin-zinc porphyrin complex.

In addition, hydrophobic effects also contribute to molecular recognition, especially in supramolecular systems where host molecules possess large non-polar regions and/or intramolecular cavities. An example of such a hydrophobic effect would be binding the cyclophane host with a pyrene molecule, during which a nonpolar pyrene molecule replaces the high-energy water molecules in the hydrophobic cyclophane cavity.[15] Water near nonpolar surfaces or within cavities can exhibit unfavourable free energy characteristics due to a combination of enthalpy and entropy effects.[16] In such systems, dispersion interactions also become considerable.

Apart from the strength of the supramolecular interactions, the directionality affecting supermolecule formation is also essential. Supramolecular interactions can be both directional and non-directional.[9] For example, ion-ion interactions are non-directional because the charge is uniform in all directions, and thus, the interaction can occur in any direction. Non-directional interactions can stabilise supermolecules, but they do not promote selective binding. As another example, hydrogen bonds (HB) are highly directional because they are stronger when the hydrogen atom is aligned with the two electronegative atoms. Thus, the interaction can occur in a definite direction. Directional interactions can align the molecules into supramolecular systems and feature highly in supramolecular design.[17]

Supramolecular interactions can enable chemists to develop host molecules that selectively bind the target guest molecules (depending on the context, also called analytes, ligands, or substrates). To design a host for a specific guest, it is necessary to know the guest molecule's size, shape, and chemical properties. Strong and selective binding is achieved when the binding sites of both partners are complementary – interaction sites match spatially and electronically.[5,9] This kind of *complementarity* with the analyte can be created by the strategic design and synthesis of synthetic receptors[18].

Aspects of anion recognition

The history of synthetic anion receptor chemistry dates back to 1968 when Park and Simmons[19] reported that deprotonated 1,11-diazabicyclo[9.9.9]nonacosane binds selectively Cl^- anions. The field of anion recognition started intense development in 1976 when Graf and Lehn[20] characterised tetraprotonated spheroidal cryptands that encapsulate F^-, Br^- and Cl^- anions. For more than 40 years, the field has developed into a very diverse and challenging area.[21–24] Beer and Gale[25] have proposed a practical way of categorising anion receptors by considering the types of noncovalent interaction used to complex the anionic guest (electrostatic interactions, hydrogen bonding, hydrophobicity, coordination to a metal ion, and combinations of these interactions). Anions can be recognised by either positively charged or neutral synthetic receptors. Positively charged receptors bind anions through stronger electrostatic interactions and metal-anion complexation, but this can make it challenging to maintain consistent selectivity. Neutral receptors primarily rely on weaker but more directional interactions such as hydrogen-bonding, π-π stacking, and van der Waals forces, which can lead to high selectivity.[25] Additionally, positively charged receptors (such as those based on ammonium or guanidinium) are highly sensitive to changes in pH.[23] In contrast, neutral receptors are less influenced by pH variations. This work focuses on **neutral hydrogen-bond donor (HBD) anion receptors**.

Anions are generally larger than their respective cations and the larger size allows for more flexibility in their geometric arrangements. Consequently, electrostatic binding interactions are less effective for anions and the complementarity of anion receptors tends to be more challenging to achieve.[25] Anions exhibit also a higher degree of solvation in various mediums when compared to cations. In non-polar solvents, solvation is weaker, leading to stronger binding between the receptor and anion. However, in non-polar solvents, significant ion-pairing can occur. Furthermore, the behaviour of anions can be influenced by pH values, as they may become protonated at low pH.[23]

Although chemical structures and physicochemical properties of the receptor and anion largely determine the success of the molecular recognition, it is also affected by temperature, and solvent employed. The solvent will affect the conformations of receptor and/or anion and may affect the accessibility of one to the other.[21] Increasing the dielectric constant of the solvent makes most of the noncovalent interactions, electrostatic by nature, weaker.[26] In the case of a complex medium, it is necessary to consider which competing molecules may be present in the solution. The suitable choice of the solvent and exclusion of competing molecules from the binding allow to optimise selectivity.[27]

Achieving high-affinity anion binding using neutral HBD receptors in pure water remains challenging.[28] The primary obstacles include the intense competition from water molecules – via solvating both the anions and the receptors – and the limited solubility of receptors in water. Therefore, many receptor-anion complexes have been studied in less competitive solvents, mainly aprotic solvents such as $CHCl_3$, MeCN, and DMSO.

1.2. Carboxylate binding

Carboxylate anions

Carboxylic acids, one of the major classes of organic compounds, feature the carboxyl group(s) ($-\mathrm{COOH}$), which is a prevalent functional group in both biological and synthetic organic molecules. Many carboxylic acids are called by their common names such as acetic acid (IUPAC name is ethanoic acid) or ibuprofen (IUPAC name is 2-(4-isobutylphenyl) propionic acid). Carboxylic acids can dissociate in aqueous solution into carboxylate ions (carboxylates) and protons. Monobasic carboxylic acids typically have pK_a values between 3 and 5.[29] Thus, carboxylic acids in neutral and basic environments (i.e., $\mathrm{p}H \gg \mathrm{p}K_\mathrm{a}$) will exist predominantly in their ionised, conjugate base form ($\mathrm{RCOO^-}$) and exhibit strong solvation in hydrogen-bond-donating solvents, particularly in water.[30] Due to the structural changes accompanying carboxylic acid ionisation, the negative charge in carboxylate anions is dispersed by the inductive effect and resonance effect of the carbonyl group. As a result of these mechanisms, the carboxylate anion adopts a Y-shaped structure, where both carbon-oxygen distances become equal.[31] This stabilised anionic centre can interact with ions and dipoles, and act as a hydrogen bond acceptor (HBA) site.[21]

The R groups attached to the carboxyl group exhibit significant variability in terms of size, geometry, and the presence of additional functional groups. As a result, they greatly vary in properties such as basicity, chirality, hydrophobicity/ hydrophilicity, and polarisability. The structures and characteristic values of the carboxylate ions investigated in this work – formate, acetate, pivalate (trimethylacetate), lactate, naproxen, ibuprofen, ketoprofen, glucuronate, hexanoate, sorbate, and benzoate – are shown in Figure 2. The extent of ionisation of the corresponding acids is described by their $\mathrm{p}K_\mathrm{a}$ values in water.[29,32–37] The $\mathrm{p}K_\mathrm{a}$ values in DMSO have been reported for formic acid, acetic acid, pivalic acid, and benzoic acid.[38–40] Hydrophilicity of carboxylates is described using the n-octanol-water partition coefficient ($\log P_{\mathrm{o-w}}$) of the respective acids.[41] The steric demand of carboxylate anions can be characterised by the E_R value, which describes the repulsive energies of the R group.[42] HBA parameter (β) values have been determined for acetate and benzoate.[43]

Formate

$pK_a(H_2O) = 3.74$[29]
$pK_{a\ exp}(DMSO) = 10.3$[38]
$\log P_{o-w} = -0.54$[41]
$E_R = 0$[42]

Acetate

$pK_a(H_2O) = 4.76$[29]
$pK_{a\ exp}(DMSO) = 12.3$[39]
$\log P_{o-w} = -0.17$[41]
$E_R = 17$[42]

Pivalate

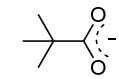

$pK_a(H_2O) = 5.03$[32]
$pK_{a\ exp}(DMSO) = 12.9$[40]
$\log P_{o-w} = 1.47$[41]
$E_R = 59$[42]

Lactate

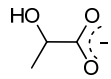

$pK_a(H_2O) = 3.86$[29]
$pK_{a\ calc}(DMSO) = 9.0$[II]
$\log P_{o-w} = -0.72$[41]
$E_R = 48$[42]

Naproxen

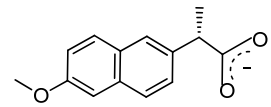

$pK_a(H_2O) = 4.15$[33]
$pK_{a\ calc}(DMSO) = 11.7$[II]
$\log P_{o-w} = 3.34$[41]
$E_R = 66$[42]

Ibuprofen

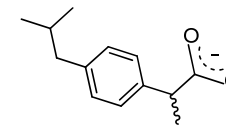

$pK_a(H_2O) = 4.40$[34]
$pK_{a\ calc}(DMSO) = 11.6$[II]
$\log P_{o-w} = 4.5$[41]
$E_R = 66$[42]

Ketoprofen

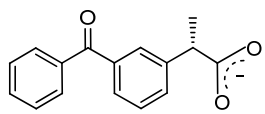

$pK_a(H_2O) = 4.30$[35]
$pK_{a\ calc}(DMSO) = 11.1$[II]
$\log P_{o-w} = 3.12$[41]
$E_R = 66$[42]

Glucuronate

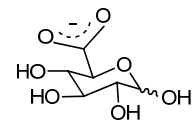

$pK_a(H_2O) = 3.28$[36]
$pK_{a\ calc}(DMSO) = 8.3$[II]
$\log P_{o-w} = -2.57$[41]
$E_R = 57$[II]

Hexanoate

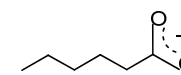

$pK_a(H_2O) = 4.88$[32]
$pK_{a\ calc}(DMSO) = 12.5$[II]
$\log P_{o-w} = 1.92$[41]
$E_R = 36$[42]

Sorbate

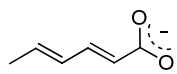

$pK_a(H_2O) = 4.50$[37]
$pK_{a\ calc}(DMSO) = 12.4$[II]
$\log P_{o-w} = 1.33$[41]
$E_R = 36$[II]

Benzoate

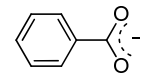

$pK_a(H_2O) = 4.20$[29]
$pK_{a\ exp}(DMSO) = 11.1$[39]
$\log P_{o-w} = 1.87$[41]
$E_R = 45$[II]

Figure 2. The structures of investigated anions $R-COO^-$ together with pK_a values of $R-COOH$ in water (experimental) and DMSO (exp–experimental, calc–computational), $\log P_{o-w}$ values of $R-COOH$ and substituent repulsive energies E_R (kcal mol^{-1}) as estimators of the steric demand of X.

Carboxylate anions play a significant role in environmental, biological, and industrial contexts. Acetate and formate are major fermentation products and for that matter, important electron donors in microbial fuel cells.[44] Benzoate and sorbate are used as chemical preservatives and flavouring agents in foods, cosmetics, and hygiene products.[45,46] Ibuprofen, ketoprofen, and naproxen are commonly used nonsteroidal anti-inflammatory drugs (NSAIDs).[47] Lactate and glucuronate are metabolites produced by microbes during fermentation and can be found in kefir and kombucha, respectively.[48]

Current carboxylate detection methods generally require preconcentration of the sample by solid-phase extraction or solvent extraction, its separation by liquid or gas chromatography, and detection by mass spectrometry or fluorescence techniques.[49–51] In the context of food products, fluorescence polarisation immunoassay (FPIA) can be used to detect benzoate[52]. Sigma-Aldrich offers a Colorimetric Acetate Assay Kit for research and development, where acetate concentration is determined by a coupled enzyme assay; this process requires a spectrophotometer with a 96-well plate reader. Despite these options, there are still no commercial ISEs available for small carboxylates.

Neutral synthetic receptors for carboxylate recognition

Neutral synthetic receptors interact with the carboxylate group through hydrogen bonding. The most common approach to designing a new receptor is to try to arrange binding sites with appropriate symmetry according to the functional groups and topology of the anion to be determined. The most extensively used H-bond donor groups are N-H fragments from amide[53,54], urea[55–57], thiourea[55], pyrrole[58–60], indole[61,62], carbazole[62,63], indolocarbazole[62,64,65] or squaramide[66] subunits. These subunits have been used to construct both flexible acyclic and preorganised macrocyclic receptors.[67]

Suitable HB donor groups should be able to form strong hydrogen bonds without undergoing deprotonation. For instance, this is why $-OH$ groups are not commonly used, as they tend to deprotonate easily. Tshepelevitsh *et al.* [68] studied the hydrogen-bond donicity of various HB donors and showed that bidentate HB donors have an important advantage in anion recognition because they are characterised by higher HB donicity than could be expected from their acidity.

Achieving high affinity toward carboxylates is relatively straightforward due to the uniform geometry and charge distribution within the carboxylate group. However, distinguishing carboxylates from each other poses a more challenging task. To accomplish this, the receptor (or multiple receptors in differential sensing) must also recognise the characteristic “tail” of the specific carboxylate. The receptor should not only be able to differentiate between similar carboxylates but also between other anionic species and be capable of overcoming solvent and counterion competition.

1.3. Quantifying the binding affinity

The receptor-anion complex RA^- formation between receptor R and an anion A^-, according to 1:1 stoichiometry, is described by the following reversible reaction:

$$R + A^- \rightleftarrows RA^- \quad (1)$$

The equilibrium constant of this reaction – the association constant K_{ass} (also denoted as binding constant or affinity constant) describes how readily the receptor forms a stable complex with the anion. It can be calculated using the activities of the receptor (a_R), anion (a_{A^-}), and the receptor-anion complex (a_{RA^-}):

$$K_{ass} = \frac{\alpha_{RA^-}}{\alpha_R \cdot \alpha_{A^-}} \quad (2)$$

In practical calculations of K_{ass}, since the activity coefficients are frequently unknown, the activities in Equation (2) are often replaced with the respective equilibrium concentrations:

$$K_{ass} = \frac{[RA^-]}{[R] \cdot [A^-]} \quad (3)$$

The free energy of complexation ΔG_{ass} (also denoted as binding energy) associated with the binding reaction (1) quantifies the spontaneity of a complexation under specific conditions. It establishes the connection between the binding constant K_{ass}, the binding reaction enthalpy change ΔH_{ass}, the temperature T, and the binding reaction entropy change ΔS_{ass}:

$$\Delta G_{ass} = -RT \ln K_{ass} = \Delta H_{ass} - T\Delta S_{ass} \quad (4)$$

The binding constant quantifies the thermodynamic stability of a receptor-anion complex in a specific solvent at a given temperature. ΔG_{ass} and K_{ass} are interconnected and both can be used to quantify the binding affinity. Theoretically, determination of the binding constants at different temperatures enables to calculate the thermodynamic parameters as the slope and the intercept of the van't Hoff equation:[69]

$$\ln K_{ass} = -\frac{\Delta H_{ass}}{RT} + \frac{\Delta S_{ass}}{R} \quad (5)$$

Direct measurement of the thermodynamic quantities can be carried out only with isothermal titration calorimetry (ITC).[21,70] Other experimental techniques, such as UV-Vis, NMR, fluorescence or potentiometry are commonly used to determine the K_{ass} value from the titration experiments and regression, where the complex concentration at equilibrium ($[RA^-]$) is evaluated. Usually, the concentration of the receptor is fixed, while the concentration of the anion is varied. Different physical observables (such as optical absorbance and chemical shift), that correlate with the receptor-anion complex concentration, can be utilised to determine $[RA^-]$ and stoichiometry of the binding reaction. This monitored physical change is plotted as a function of the amount of anion added and the

resulting titration curve (the binding isotherm) is then fitted to the developed mathematical model.[71]

In quantitative analysis of receptor-anion complexation, a critical aspect is reliably determining the binding constant.[21] Keiji Hirose[69] gives practical guidelines how to determine stoichiometry, evaluate the complex concentration, choose the reliable concentration regions for K_{ass} determination, and how to treat the collected data.

Pall Thordarson[71] has listed fourteen dos and don'ts in supramolecular titration experiments. Out of all the very practical suggestions, the following recommendations could be highlighted: all possible stoichiometries should be considered, titrations should be repeated, the measurement uncertainties should be estimated and programs that can handle the data analysis should be used.

When determining stoichiometry of the reaction (1), it usually involves assuming a simple 1:1 stoichiometry and then seeking additional evidence to either support or challenge that assumption. For this purpose, Connors[72] outlines several methods like the method of continuous variations (Job's plot method), comparison of binding constants evaluated by different methods, considering the receptor-anion complex structure (e.g. molecular modelling), usage of isosbestic points and evaluating the constancy of stability concentration. Visualisation of the receptor-anion complex as well as predicting the most stable conformers of binding partners with COSMO-RS approach can be also valuable supporting information during binding studies.[73] When considering stoichiometry in a titration experiment, at the outset, when receptor molecules are in excess, the likelihood of 1:2 binding of anions to receptors is low because the binding of the second anion is obstructed if the binding pocket is already occupied by the first anion. Similarly, 2:1 binding is improbable as the binding to carboxylates is directional (receptor approaches the anion by the carboxyl group). Even towards the end, when there's excess titrant, 1:2 binding remains unlikely due to the absence of suitable second binding pocket, especially with planar and small receptors like substituted indolocarbazoles.

NMR spectrometry can be used in cases where the receptor-anion complexation equilibrium has a very slow exchange rate or a very fast exchange rate compared with the NMR time scale.[74] Under fast exchange conditions, the NMR peaks of the free receptor and the receptor-anion complex appear at the weighted average chemical shift. Compared to other techniques, the NMR spectra are rich in information content and can give additional information about the identity, purity, solubility, etc. When determining absolute binding constants, the choice of technique primarily hinges on the predicted magnitude of K_{ass}, because this value defines the appropriate range of titration concentrations. In order to accurately determine the proportion of unbound anion in solution, NMR spectroscopy is a suitable technique for assessing absolute binding constants up to K_{ass} values of 10^5 M^{-1}.[69] However, the NMR method employed in this study for determining relative binding affinities ($\Delta \log K_{\mathrm{ass}}$ values) extends beyond this limitation. It is elaborated upon in the following paragraph.

A new approach was developed in our research group, where differences in the affinities of two or more receptors are measured instead of determining the affinity of a single receptor. This method is versatile and can be applied to various host-guest bindings. Haav *et al.*[75] demonstrated this approach by using UV-Vis spectroscopy, and Kadam *et al.*[76] by NMR technique. The relative binding affinity ($\Delta \log K_{\mathrm{ass}}$) of two synthetic anion receptors towards the same anion was measured and described with the following Equations (6–8):

$$\mathrm{R_1} + \mathrm{R_2A^-} \rightleftarrows \mathrm{R_1A^-} + \mathrm{R_2} \tag{6}$$

$$\Delta \log K_{\mathrm{ass}} = \log K_{\mathrm{ass}}(\mathrm{R_1A^-}) - \log K_{\mathrm{ass}}(\mathrm{R_2A^-}) = \log \frac{\alpha_{\mathrm{R_1A^-}} \cdot \alpha_{\mathrm{R_2}}}{\alpha_{\mathrm{R_2A^-}} \cdot \alpha_{\mathrm{R_1}}} \tag{7}$$

$$\Delta \log K_{\mathrm{ass}} = \log \frac{[\mathrm{R_1A^-}] \cdot [\mathrm{R_2}]}{[\mathrm{R_2A^-}] \cdot [\mathrm{R_1}]} \tag{8}$$

When two receptors $\mathrm{R_1}$ and $\mathrm{R_2}$ are dissolved in the same solvent, it negates the necessity to determine the activity of the anion. Additionally, this approach mitigates various error sources, either partially or entirely: errors from volumetric procedures are entirely eliminated, as are those concerning the purity of compounds (assuming no peak overlap), the concentrations of receptors and the anion solution; the influence of solvent composition is partially reduced. Kadam *et al.*[76] showed that a binding affinity difference of less than 0.05 $\log K_{\mathrm{ass}}$ units can be determined with high accuracy. It was reported that $\Delta \log K_{\mathrm{ass}}$ values up to 1.5 units could be measured with reasonable accuracy, and the results from the NMR method agree with previous UV-Vis results[75]. Another benefit of this method is that it allows for the simultaneous determination of multiple $\Delta \log K_{\mathrm{ass}}$ values in a single measurement series. As a drawback, the spectra exhibit peaks from several receptors, which can overlap or merge. Consequently, careful interpretation of the spectra is necessary.

Binding **selectivity** describes how well a receptor discriminates between different anions based on their chemical properties and structural features. Binding selectivity is achieved by steric and electronic complementarity between anions and receptors. A thermodynamic selectivity coefficient for receptor $\mathrm{R_1}$ is defined as the ratio of the two equilibrium constants with anions $\mathrm{A_1^-}$ and $\mathrm{A_2^-}$:

$$K_{\mathrm{A_1,A_2}} = \frac{K_{\mathrm{ass}}(\mathrm{R_1A_2^-})}{K_{\mathrm{ass}}(\mathrm{R_1A_1^-})} \tag{9}$$

If $K_{\mathrm{A_1,A_2}} > 1$ ($K_{\mathrm{ass}}(\mathrm{R_1A_2^-}) > K_{\mathrm{ass}}(\mathrm{R_1A_1^-})$), then receptor $\mathrm{R_1}$ binds anion $\mathrm{A_2^-}$ better than anion $\mathrm{A_1^-}$. Equation (9) is applicable when both anions bind to the receptor with the same stoichiometry, under the same experimental conditions (most importantly, the same solvent), and no competing reactions occur.[77] Here lies the reason why the fundamental conclusions regarding receptor selectivity cannot be reliably drawn based solely on the binding affinities of individual receptors measured across different research groups or in varying solvent media. Therefore, comparable binding measurements of a more extensive set of receptors and anions in one solvent medium are necessary (Publications I and II).

Once a synthetic receptor's binding affinity and selectivity have been thoroughly assessed and deemed suitable for practical applications, a new phase of work towards a true sensor should begin. However, only slow progress is seen in this field[78], and most receptors designed for anions have never been implemented into sensors. Feedback gained from practical applications in a sensor prototype is usually more valuable than binding affinity measurements in pure single-phase organic solvents. Therefore, if the novel synthetic receptor is incorporated into the lipophilic phase in a potential application instead, it should also be investigated as an ionophore (Publication III). In chemical sensors, the input signal is the chemical composition of the media. If the output signal is electrical (voltage, current, capacitance), it is an electrochemical sensor.[79] This work focuses on the ion-selective electrodes giving potentiometric signals.

1.4. Ion-selective electrodes

A potentiometric ion-selective electrode (ISE) is an electroanalytical device used in conjunction with a reference electrode (RE), and the potential difference between these two is proportional to the logarithm of the activity of a specific ion in the solution.[80] In the context of an electrochemical cell, the ISE functions as an indicator electrode and obeys the Nernst equation:

$$\varphi = \varphi^0 + \frac{RT}{z_\mathrm{i}F} \ln a_\mathrm{i} \tag{10}$$

where φ is the electrode potential, φ^0 is the standard potential, R is the universal gas constant, T is the absolute temperature, z_i is the charge of the ion i, F is the Faraday constant, and a_i is the activity of the ion i. The potential of the ISE (E_ISE) is monitored relative to the reference electrode (e.g. Ag/AgCl/Cl^-) potential (E_RE). As the reference electrode's potential remains constant, the measured cell potential (E_cell) directly reflects the potential of the ISE[79], along with its practical response slope (S):

$$E_\mathrm{cell} = E_\mathrm{ISE} - E_\mathrm{RE} = E^0_\mathrm{cell} + S \log a_\mathrm{i} \tag{11}$$

where E^0_cell is the constant standard potential influenced by the ISE's specific design. It encompasses all the constant potential terms associated with the ISE and the reference electrode. The slope of the calibration curve (potential vs $\log a_\mathrm{i}$) is the sensitivity of the sensor. The ideal or so-called Nernstian slope value can be determined using the constants from Equation (10). Specifically, for monovalent ions at room temperature, the Nernstian slope is -59.16 mV per decade, and for divalent anions, it is -29.5 mV per decade. Real-world ISEs may deviate from Nernstian behaviour due to factors like interference, membrane fouling (deposition of contaminants on the surface of the membrane), or non-ideal selectivity. In such cases, slopes with lower absolute values are typically observed.

ISEs operate by sensing the activity of ions (a_i) in a solution, and it is related to its molar concentration (c_i) by the following equation:

$$a_{\mathrm{i}} = \gamma_{\mathrm{i}} c_{\mathrm{i}} \tag{12}$$

where γ_{i} is the single ion activity coefficient that can be calculated using the extended Debye-Hückel equation.[81]

ISEs are used in many different applications, including environmental analysis, clinical diagnosis, industrial process control, and food analysis, to name some.[6,82,83] Compared to spectroscopic methods, ISEs are easier to use, cheaper, faster, less destructive, and unaffected by colour or turbidity.[84,85] They are increasingly preferred in practical applications because they are easily portable, cost-effective, and compatible with microfabrication and miniaturisation due to their small size.[86]

Based on the ion-selective membrane (ISM) material, ISEs can be divided into glass, crystalline and polymeric membrane electrodes.[79] Based on the construction, ISEs are divided into conventional ISEs with internal filling solution (liquid-contact, LC) and all-solid-state ISEs (ASS-ISEs) without internal electrolyte solution. ASS-ISEs can be further categorised into coated wire electrodes (CWE), solid-contact ISEs (SC-ISEs), and single-piece ISEs (SP-ISEs).[87] A comparison of the construction of different electrodes is shown in Figure 3. This work focuses on the solid-contact polymeric membrane ISEs.

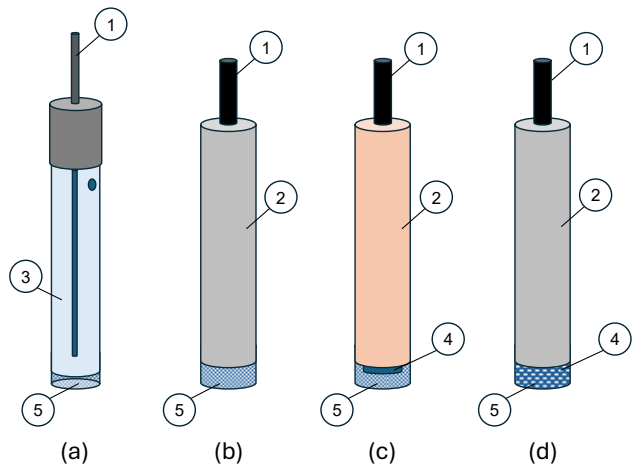

Figure 3. The construction of different types of ion-selective electrodes (ISEs): (a) conventional ISE with internal filling solution (LC-ISE); (b) disc-shaped coated wire electrode (CWE); (c) solid-contact ISE (SC-ISE); (d) single-piece ISE (SP-ISE) (1–electronic conductor, 2–electrode body, 3–internal filling solution, 4–solid contact, 5–ion-selective membrane).

Solid-contact ion-selective electrodes

Solid-contact ion-selective electrodes do not have an internal filling solution like conventional ion-selective electrodes. Therefore, they are more durable and easier to miniaturise. This has led to a widespread transition from LCs to SCs over the past decades, allowing ISEs to be used in integrated sensing systems in a wide variety of applications.[88–90]

Cattrall and Freiser[91] fabricated the first ISE without an internal solution in 1971. The invented coated-wire electrodes (CWEs), where the ISM is directly coated onto a metallic conductor, are extremely simple, inexpensive, and easy to prepare. However, CWEs and their descendants, disc-shaped CWEs, exhibit low potential stability resulting from the uncontrolled redox processes at the metal surface.[92,93] Currently, these electrodes are infrequently employed and are typically studied as comparative systems.[87]

To mitigate potential drift and improve stability, a solid-contact layer is introduced between the inner electrode (e.g. glassy carbon, GC) and the ISM.[94] This SC material can transfer the ion concentration to an electron signal and can be applied directly onto the inner electrode surface using drop casting or electrochemical deposition techniques.[92] Alternatively, conductive material can be dispersed or dissolved in the ISM. In this case, there is no distinct intermediate layer, and the electrode is referred to as a SP-ISE. The ideal SC material should exhibit high redox or double-layer capacitance, chemical stability, and reversible transition from ionic and electronic conductivity. It should also not participate in any side reactions.[79,92,94] Furthermore, SC should have hydrophobic properties to prevent the formation of a water layer between the polymeric membrane and the underlying solid contact.[93,95]

Conductive polymers (CPs) have been the pioneering choice[96] and continue to be widely used as solid-contact materials. Extensively studied CPs are polypyrrole (PPy), poly(3,4-ethylenedioxythiophene) (PEDOT), poly(3-octylothiophene) (POT), poly(N-methylpyrrole) (PNMP), and polyaniline (PANI).[84,92,97,98] CPs can be effectively attached to the surface of the inner electrode, exhibit highly reversible redox behaviour, and both electric and ionic conductivities. They offer versatility and ease of modification. For constructing anion-selective electrodes, partially oxidised CPs are doped with small anions.[99–101] While CPs have their advantages as SC, their sensitivity to environmental changes[102] and water layer formation can be limiting. To address these challenges, new electroactive materials are investigated, and a wide range of materials have been developed for solid contact in ISEs, such as carbon nanomaterials, metal nanoparticles, and composite or hybrid materials.[87,103] Nevertheless, when investigating a polymeric membrane utilising a novel ionophore, opting for a SC-ISE constructed with a well-known conductive polymer (such as PEDOT) is prudent. In this case, the ion selectivity is predominantly determined by the properties of the ISM, which can then be the main focus.[104]

SC-ISE, utilising PEDOT as the solid contact, contains three interfaces: GC/PEDOT, PEDOT/ISM, and ISM/sample. Interpreting the response of an ISE

with a phase boundary model[92,105], the SC-ISE potential (E_{ISE}) is the sum of the three interfacial potentials:

$$E_{\mathrm{ISE}} = E_{\mathrm{PEDOT}}^{\mathrm{GC}} + E_{\mathrm{ISM}}^{\mathrm{PEDOT}} + E_{\mathrm{sample}}^{\mathrm{ISM}} \quad (13)$$

Once the PEDOT is deposited on the GC rod and coated with ISM, the GC/ PEDOT and PEDOT/ISM interfacial potentials are constant and can be included in a constant E_{cell}^{0}. The signal is formed at the ISM/sample solution interface and is determined by the activity of the primary ion in the membrane phase $a_{\mathrm{i(ISM)}}$ and in the sample phase $a_{\mathrm{i(sample)}}$:[90]

$$E_{\mathrm{cell}} = E_{\mathrm{cell}}^{0} + S \log \frac{a_{\mathrm{i(sample)}}}{a_{\mathrm{i(ISM)}}} \quad (14)$$

To determine the unknown activity in the sample solution using Equation (11), the activity of the primary ion within the membrane phase must remain constant (in which case Equation (14) is equal to Equation (11)). This constancy is achieved through the ISM design, where the concentration of analyte ions in the membrane is determined by the amount of lipophilic ion-exchanger ions, which cannot leave the membrane.

For practical applications, SC-ISE's potential stability can be assessed with short-term and long-term potential stability studies. The potential stability can be evaluated by measuring the standard cell potential in a short time (few hours) or at constant intervals over an extended period (e.g. weeks and months), under no-current conditions and determining the potential drift as $\Delta E_{\mathrm{cell}}^{0}/\Delta t$. The second and even faster option is to use the Chronopotentiometry method[97], which, in addition to potential stability, can be used to estimate the capacitance and resistance of the electrodes.

Another technique commonly used to monitor electrodes' stability and performance together with their charge transport properties is Electrochemical Impedance Spectroscopy (EIS). In the EIS experiment, a potential wave with different frequencies is applied to the working electrode and the resulting current wave is recorded. The produced impedance is used to assess the membrane resistance, electric capacitance and charge transfer resistance between the ISM and the internal electronic conductor.[106,107]

In conclusion, recent advancements in SC-ISEs have demonstrated promising results through the modifications and enhancements of conducting polymers, e.g., by attaching them covalently[108] to the electrodes. These developments have yielded impressive standard potential values (E^{0}) comparable to LC-ISEs in use, facilitating the integration of SC-ISEs into chips and wearable sensors.[90] Moving forward, further research is warranted to develop suitable ionophores for accommodating new anions, thereby enhancing the versatility and applicability of SC-ISE technology.

Ionophore-based ion-selective membrane

Only a small number of analytes can be quantified when using electrodes with glass and crystalline membranes. However, ionophore-based polymeric membranes enable the quantification of over 70 different inorganic and organic ions.[109] And yet, a significant majority of membranes incorporate ionophores sensitive to cations. Conversely, the number of published ionophores for anions, particularly organic anions, remains relatively limited.[87] The essential components of the polymeric ISM (also called ISM cocktail) are the polymer matrix, plasticiser, lipophilic ion-exchanger, and ionophore. Each of these components contributes to the system's overall potential and affects the electrode's lifetime.[109]

The **polymer matrix** serves as the inert support for the ISM, providing mechanical stability and flexibility to the membrane. While poly(vinyl chloride) (PVC) is the most commonly used polymer, other materials such as polyurethane, polyacrylates, poly(vinylidene chloride), and polysiloxanes are also employed.[79]

Unfortunately, the low fluidity of polymer matrices restricts the mobility of ionophores within the membrane. To maintain rapid ion exchange kinetics, **plasticisers** like bis(2-ethylhexyl) sebacate (DOS) or 2-nitrophenyl octyl ether (*o*-NPOE) are incorporated (see structures in Figure 4). An effective plasticiser reduces the polymer's glass transition temperature, thereby contributing to the mechanical stability of the ISM.[109] Additionally, the plasticiser should dissolve readily within the matrix and exhibit lipophilic properties to prevent leaching. Most PVC-based ISMs typically comprise 30–33% PVC and 60–66% plasticiser.[79]

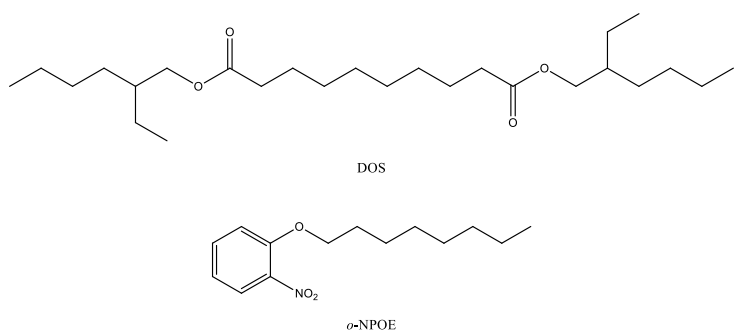

Figure 4. The structures of common plasticisers bis(2-ethylhexyl) sebacate (DOS) and 2-nitrophenyl octyl ether (*o*-NPOE) used in PVC-based membranes.

The lipophilic **ion-exchangers** are incorporated into the ISM cocktail to decrease the membrane's electric resistance, shorten the response time, and suppress the extraction of counterions from the sample solution into the ISM. This selective addition renders the membrane permeable only to ions of the same charge as the target ion, a phenomenon known as Donnan exclusion. Additionally, the intentional addition of ionic sites will dominate over the smaller proportion of ionic

sites arising from impurities in other membrane components. In cation-selective ISMs, tetraphenylborates are commonly employed for this purpose, while tetraalkylammonium salts, such as tridodecylmethylammonium chloride (TDMACl), find frequent use in anion-selective membranes.[110–113] In ISMs, the ion-exchanger-to-ionophore ratio is an essential variable parameter. Typically, this ratio is adjusted to ensure that the ion-exchanger constitutes 30–50 mol% relative to the ionophore.

The **ionophore** (receptor, ligand) is a key membrane component. It forms strong and reversible complexes with the target ion (primary ion) and weaker ones with interfering ions (secondary ions), which affect the selectivity of the electrode. The binding should not be too strong, as it would slow down the response time of the electrode due to the slow transfer of ions. For instance, ISEs rarely use rigid macrocycles because they have slow exchange kinetics. Excessive binding strength is also undesirable because it may result in the coextraction of the primary ion and an ion with the opposite charge from the aqueous phase. Therefore, the ion-binding properties of the ionophore can adjust the selectivity of ionophore-based ISEs. To ensure the electrode's sensitivity and selectivity, the ionophore must possess sufficient lipophilicity ($\log P_{\mathrm{o-w}} \geq 7.4$[79]) to prevent leakage from the membrane into the solution. The ionophore content in ISMs is usually 0.5–2% of the whole membrane mass.

All the ISM components are dissolved in a volatile organic solvent, most frequently in tetrahydrofuran (THF). The strength of adhesion between an ISM cocktail and the electrode body significantly depends on the material of the electrode body. In general, the adhesion of ISM to widely used PVC bodies is quite good. However, the adhesion weakens over prolonged use.[109,111] Recently, the delamination of the membrane has been prevented by covalently attaching the ISM to the electrode body.[108]

Characterising ionophore-based ISEs involves assessing their sensitivity (practical slope), response time, linear range (including lower limit of linearity), limit of detection, long-term stability, and most importantly, selectivity. In addition, conducting a water layer test[95], describing the effect of interfering substances, and providing information about potential drift and its possible causes are highly recommended.[113,114]

Selectivity of ion-selective electrodes

One of the most important response characteristics of an ISE is selectivity. The selectivity of an ISE refers to its ability to distinguish between the primary ion and interfering ions present in the sample solution.[79] Correctly determined electrode selectivity allows us to accurately predict how an ISE will respond in a real-world mixed sample. Equation (11) has been written on the assumption that the electrode responds only to the ion of interest, i. In practise, ISEs may also respond to other ions present in the sample solution and the selectivity coefficient is calculated according to the extended Nikolskii-Eisenman equation:

$$E_{\text{cell}} = E^0_{\text{cell}} + \frac{RT}{z_i F} \log\left(a_i + K^{\text{pot}}_{i,j} a_j^{z_i/z_j}\right) \quad (15)$$

where $K^{\text{pot}}_{i,j}$ is the selectivity coefficient and a_j is the activity of the interfering ion j. The selectivity coefficient quantifies the relative response of an ISE to interfering ions compared to the target ion. A lower value means a higher selectivity. Ideally, the selectivity coefficient should be zero, meaning that the ISE only responds to the ion of interest. However, this is rarely the case, and the selectivity coefficient depends on many factors, such as the membrane composition, the pH, the temperature, and the concentration of the ions. Therefore, the selectivity coefficient must be determined experimentally for each ISE and each application.[104]

The main two methods used to determine potentiometric selectivity coefficients are the Fixed Interference Method (FIM), and the Separate Solution Method (SSM).[80] In the FIM, the electrode function is measured in a mixed solution where the concentration of the target anion is varied while keeping the concentration of the interfering anion constant. The SSM, on the other hand, relies on measurements in pure solutions and, due to its simplicity, is the most popular method for determining potentiometric selectivity coefficients.[79] The SSM experiment is conducted as follows:

1. The electrode potential (E_i) is measured in a solution containing only the ions of interest, i.
2. Next, the electrode potential (E_j) is measured in a solution containing only the ions of interference j, whereas the activities of the primary ion and interfering ion in steps 1. and 2. are equal ($a_i = a_j$).
3. The potentiometric selectivity coefficient ($\log K^{\text{pot}}_{i,j}$) for monovalent anions is calculated using the following equation:

$$\log K^{\text{pot}}_{i,j} = \frac{E_j - E_i}{S} \quad (16)$$

   where the slope S can be obtained from the calibration experiments carried out in a solution containing only the ion of interest.
4. The potentiometric selectivity coefficient for divalent anions is calculated using the following equation:

$$\log K^{\text{pot}}_{i,j} = \frac{E_j - E_i}{S} + \log \frac{a_i}{a_j^{1/2}} \quad (17)$$

In the case of polymeric membrane electrodes, the interference of other sample ions is mainly due to their competitive extraction into the organic phase.[115] When ISEs have membranes containing only ion-exchangers (without ionophores), their selectivity tends to be low. This selectivity primarily relies on the free energy of ion hydration and follows the Hofmeister series:

$$Ibuprofen > Naproxen > Benzoate > SCN^- > I^- > NO_3{}^- > Br^- > Cl^- > F^- > HCO_3{}^- > Acetate > Formate > HPO_4{}^{2-} > SO_4{}^{2-}$$

Ionophore-based membranes show very different selectivity. When investigating novel ionophores, it is recommended to compare the selectivities of ISEs that incorporate ionophores in their membranes with the selectivities of ISEs that rely solely on ion-exchanger sites. In this context, Hofmeister series for anions serves as a valuable reference point.

When addressing the ionophores that have no metal centre and bind carboxylates through hydrogen bonds, acetate-ISEs have been prepared with porphyrin derivatives[116,117], uranyl salophene derivative[118], and phenylhydrazone-based ionophore[119]. To date, the determination of carboxylates using ISEs remains a challenging and largely unsolved problem.

2. EXPERIMENTAL

2.1. Instruments

The NMR measurements were conducted using either a Bruker Avance II 200 MHz NMR spectrometer or a Bruker Avance III 700 MHz NMR spectrometer. UV-Vis spectrophotometric measurements were performed using a Thermo Nicolet Evolution 300 spectrophotometer, while fluorescence spectrofluorometric measurements were carried out using a Horiba FluoroMax-4 spectrofluorometer. Cuvette holders for the spectrometer and fluorimeter were thermostatically adjustable and equipped with a magnetic stirrer. All the NMR, UV-Vis, and fluorescence measurements were carried out at 25 °C. The water content of the solvents was determined by Karl Fischer titration using a Mettler Toledo DL32 coulometer.

The potentiometric measurements were performed with a 16-channel potentiometer (Lawson Labs, Inc.) connected to a computer for data acquisition. The electrochemical impedance spectroscopy (EIS) measurements were carried out by using an Autolab General Purpose Electrochemical System and Autolab Frequency Response Analyzer System (AUT20.FRA2-AUTOLAB, Eco Chemie, B.V., The Netherlands).

2.2. Solvents and Anions

The solvents used in binding affinity measurements, DMSO and DMSO-d_6 with 0.5% of water (m/m), were prepared gravimetrically using a DMSO (Sigma Aldrich, anhydrous ≥ 99.9%) or DMSO-d_6 (Deutero, 99.8%) and water from MilliQ Advantage A10 system.

All anions (see structures in Figure 2) were used in the form of tetrabutylammonium salts. The TBA salts of acetate and benzoate were commercially available and bought from Sigma-Aldrich. TBA salts of formate, ibuprofen (as a racemate), (*S*)-(+)-ketoprofen, and D-glucuronate were self-prepared by adding the tetrabutylammonium hydroxide in methanol (Sigma-Aldrich) to a solution of the corresponding acid in methanol in 1:1 ratio. The mixture was stirred at room temperature for 24 hours, evaporated to dryness under reduced pressure, and then dried under a high vacuum at room temperature overnight. TBA salts of pivalate (trimethyl acetate) and lactate were prepared by a colleague, Kristjan Haav, using the same procedure. The salts were stored in a glove box under an argon atmosphere. The titrant solutions used in binding affinity measurements were prepared from respective tetrabutylammonium salts. For relative binding affinity measurements, the diluted anion salts were at concentration of approximately 0.25–0.75 M, while the concentrated anion salts were at concentrations of 0.63–2.20 M.

2.3. Receptors

The synthetic receptors studied in this work were selected considering their interest, structure, substituents, spectral properties, and availability. The structures of the studied receptor molecules are presented in Figure 5, and they are referenced in the text using their respective bold numbers. Several compounds are simple and can be considered building blocks of more complex receptors. The studied synthetic receptors belong to different compound families, including indolocarbazole, carbazole, indole, urea, thiourea, and amide moieties. Most of them were synthesised by a colleague, Sandip A. Kadam, at the University of Tartu. The synthesis and origin of these receptor molecules have been described in ref. [75,76,120] or in Publications I and II. For relative binding affinity measurements, the concentrations of receptors were around 0.006–0.015 M.

1,3-bis(carbazolyl)urea derivative (receptor **13**) was used as the ionophore (Ionophore **13)** for constructing SC-ISEs in Publication III.

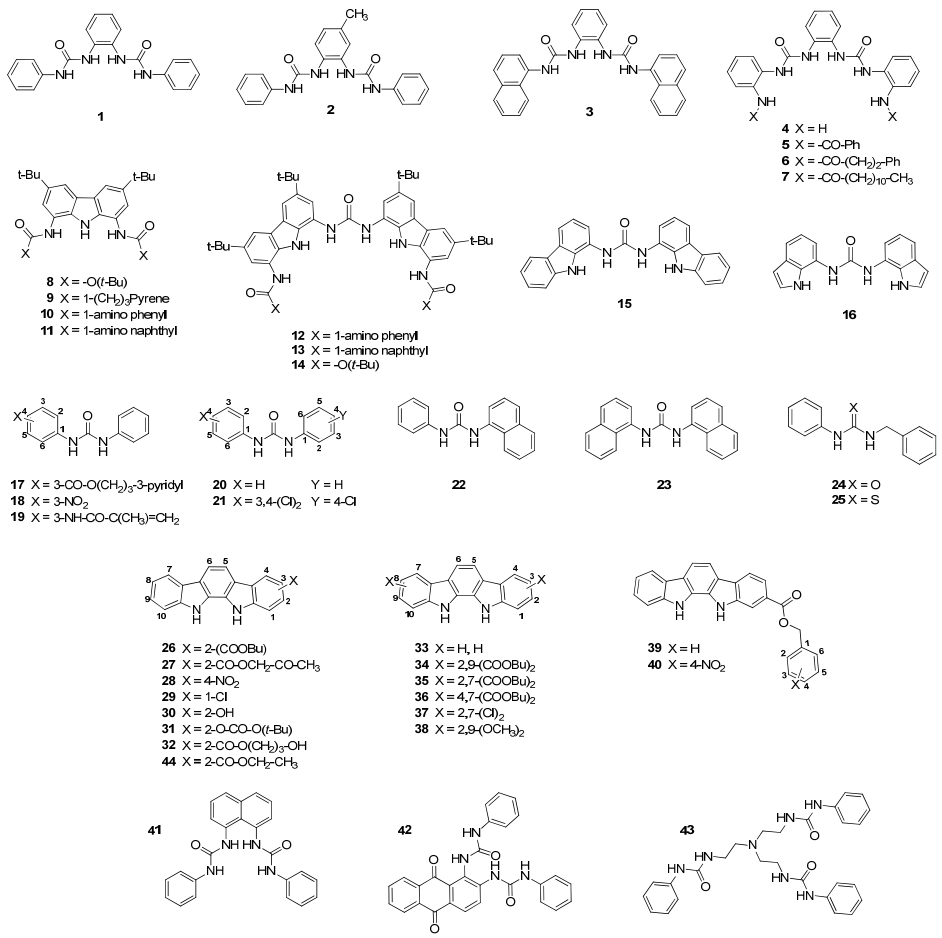

Figure 5. Structures of the studied receptor molecules.

2.4. Structure-affinity studies

The complexation of carboxylates with synthetic multidentate HBD receptors was monitored with NMR spectroscopy. The receptor-anion interaction was quantitatively characterised in terms of a binding affinity ($\log K_{ass}$) using the relative NMR-based measurement method [76]. This titration method allowed the simultaneous determination of several relative binding affinities ($\Delta\log K_{ass}$) and enabled the compilation of large-scale binding-structure-relationship plots given in Publications I and II.

^{1}H NMR-based relative binding affinity measurements

In a single experiment, two to four receptors were dissolved in DMSO-d_6 with 0.5% of water, and the ^{1}H NMR spectrum of the mixture characterising the free receptors was recorded. Next, this mixture was titrated with a carboxylate of interest, where after each addition, the ^{1}H NMR spectrum of the mixture characterising the partially complexed receptors was recorded. Having recorded approximately 17–19 spectra, and being convinced that there was no change in the chemical shift of NH signals, the titration was stopped, and the last recorded spectrum of the mixture characterising the fully complexed receptors was obtained. The experiment is also described in the following flowchart:

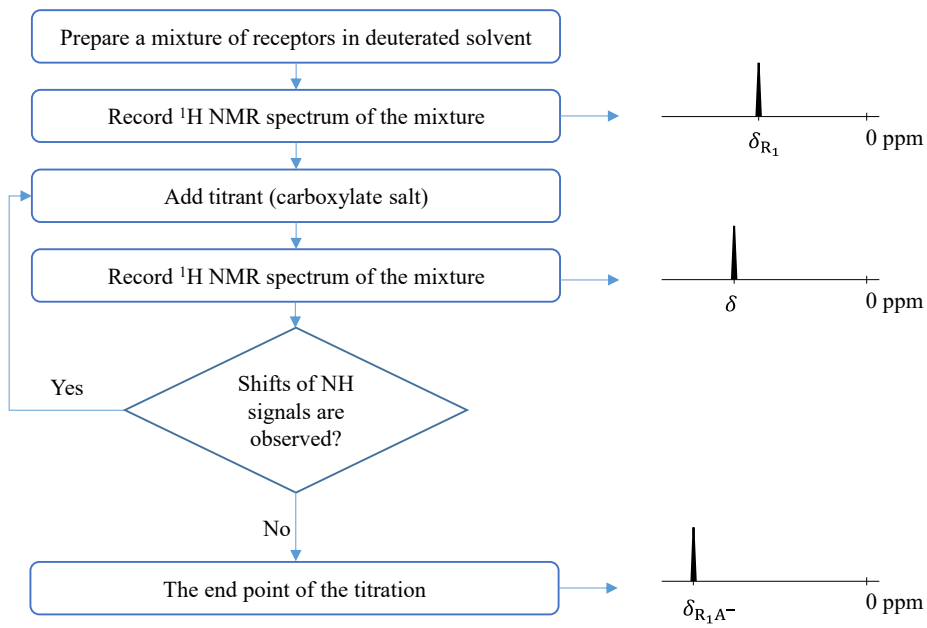

Figure 6. Steps of ^{1}H NMR titration. δ denotes the chemical shift of the NH proton at a particular titration step, and δ_{R_1} and $\delta_{R_1A^-}$ are the chemical shifts of the free receptor 1 and the receptor-anion complex, respectively.

The high selectivity of NMR measurements allowed to determine at least three $\Delta \log K_{ass}$ values from each series of titration experiments. The receptors were carefully selected such that the chemical shift values of the proton peaks for their NH groups initially differed by at least 0.2 ppm. Additionally, the rate of change in chemical shifts for the studied peaks was considered in order to address scenarios where a peak from one receptor molecule shifts more rapidly toward higher chemical values during titration, potentially overlapping with a peak from another receptor molecule that shifts more slowly or to a smaller extent.

From the NMR titration spectra, the degrees of complexation (β) for all measured receptor-anion complexes were calculated using the following equation:[76]

$$\beta = \frac{[RA^-]}{[R]+[RA^-]} = \frac{\delta - \delta_R}{\delta_{(RA^-)} - \delta_R} \quad (18)$$

The relative binding affinities ($\Delta \log K_{ass}$) were found using the Equation (19):[76]

$$\Delta \log K_{ass} = \log \frac{\beta_1(1-\beta_2)}{(1-\beta_1)\beta_2} \quad (19)$$

where β_1 and β_2 are the degrees of complexations for receptors R_1 and R_2, respectively.

In the investigation of 11 carboxylates[I,II], the relative binding affinities of 38 different receptors towards lactate, acetate, benzoate, and pivalate were determined collaboratively with one of the co-authors of Publication I, Sandip A. Kadam. Additionally, the author of this dissertation exclusively determined the relative binding affinities of 22 receptors towards formate, ibuprofen, and ketoprofen. The measurements of naproxen, sorbate and hexanoate were performed by a colleague and the second author of Publication II, Juuli Nõges.

Absolute binding affinity measurements

After determining the relative binding affinities for all the investigated synthetic receptors, some of the receptors were chosen as anchor compounds to anchor the binding scales to the absolute $\log K_{ass}$ values. The anchors' absolute binding affinities ($\log K_{ass}$) were measured directly using UV-Vis and Fluorescence spectroscopy. The absolute measurements were performed under the same conditions as the relative binding affinities measurements, and the same solvent was also used.

Previous studies have shown a good agreement between direct measurement and relative measurement.[75,76] Anchoring from the top, middle, and bottom of the scale demonstrated that there was no artificial expansion or contraction of the scale. Therefore, in this study, initially, one anchor point (absolute $\log K_{ass}$ value of Indolocarbazole **33**) was measured for lactate, benzoate, and pivalate, and later, when the binding affinity of most receptors was greater than that of unsubstituted indolocarbazole, a second anchor point (absolute $\log K_{ass}$ value of 4-NO_2-indolocarbazole **28** or 1,3-dicarbazolylurea **15**) from the upper part of the scale was added. The absolute NMR measurements and absolute $\log K_{ass}$ values of acetate given in Publication I were measured by colleague Sandip A. Kadam. Of the absolute measurements performed for Publication II, absolute $\log K_{ass}$

values of naproxen, sorbate, and hexanoate were measured by colleague Juuli Nõges.

In a single experiment, the chosen receptor was dissolved in DMSO with 0.5% of water, and the UV-Vis (or fluorescence) spectrum of the solution characterising the free receptor was recorded. Next, this solution was titrated with a carboxylate of interest, where after each addition, the UV-Vis (or fluorescence) spectrum of the solution characterising the partially complexed receptor was recorded. Having recorded approximately 12–17 spectra and being convinced that there is no change in the absorbance (or fluorescence) spectrum (the titrant was added 4–5 times more than the stoichiometric amount), the titration was stopped, and the last recorded spectrum of the solution characterising the fully complexed receptor was obtained. In contrast to measuring relative binding constants, during titration, the measuring cell was weighed before and after each addition of the titrant to calculate the exact amounts of the added titrant.

The calculations for UV-Vis absorption or fluorescence intensity were carried out at the wavelength (λ) where the change in absorbance (A) or fluorescence intensity (FI) was most pronounced in the titration spectrum. The analytical wavelengths used for different anchor compound varied and are presented in Table 1 (for UV-Vis measurements) and Table 2 (for Fluorescence measurements).

Table 1. The range of wavelengths and the analytical wavelengths in UV-Vis measurements.

Receptor	Anion	λ range (nm)	λ (nm)
Indolocarbazole **33**	Glucuronate	300-500	370
	Lactate	260-500	328
	Formate	260-460	370
	Benzoate	300-500	328
	Ibuprofen	300-500	370
	Pivalate	260-500	328
4-NO_2-indolocarbazole **28**	Glucuronate	300-700	460
	Lactate	300-700	475
	Benzoate	300-700	453
	Ketoprofen	320-700	473
	Pivalate	300-700	475
1,3-dicarbazolylurea **15**	Formate	280-500	352
	Ibuprofen	300-500	352

Table 2. The excitation wavelength (λ_{Ex}), the range of emission wavelengths (λ_{Em}), and the analytical wavelengths in Fluorescence measurements.

Receptor	Anion	λ_{Ex} (nm)	λ_{Em} range (nm)	λ (nm)
Indolocarbazole **33**	Formate	350	365-600	375
	Benzoate	350	365-500	386
	Ketoprofen	350	365-600	430
	Ibuprofen	350	365-600	377
1,3-dicarbazolylurea **15**	Formate	346	365-500	390
	Ibuprofen	346	365-600	375

From the UV-Vis titration spectra, the degrees of dissociation (α) of the receptor-anion complex were calculated using the following equation:

$$\alpha = \frac{[\mathrm{R}]}{[\mathrm{R}]+[\mathrm{RA}^-]} = \frac{A^\lambda - A^\lambda_{\mathrm{RA}^-}}{A^\lambda_{\mathrm{R}} - A^\lambda_{\mathrm{RA}^-}} \tag{20}$$

where A^λ is the absorbance at the titration step, A^λ_{R} is the absorbance of the free receptor, and $A^\lambda_{\mathrm{RA}^-}$ is the absorbance of the receptor-anion complex at analytical wavelength λ.

From the Fluorescence titration spectra, the degrees of dissociation were calculated using the following equation:

$$\alpha = \frac{[\mathrm{R}]}{[\mathrm{R}]+[\mathrm{RA}^-]} = \frac{FI^\lambda - FI^\lambda_{\mathrm{RA}^-}}{FI^\lambda_{\mathrm{R}} - FI^\lambda_{\mathrm{RA}^-}} \tag{21}$$

where FI^λ is the fluorescence intensity at the titration step, FI^λ_{R} is the fluorescence intensity of the free receptor, and $FI^\lambda_{\mathrm{RA}^-}$ is the fluorescence intensity of the receptor-anion complex.

The absolute binding affinities ($\log K_{\mathrm{ass}}$) were assigned using the average of two or three different calculation procedures, as described in more detail in ref.[75] The results from Benesi-Hildebrand linear regression method were excluded from the average calculation if they did not coincide with the results of the other two calculation methods. Mean of each $\log K_{\mathrm{ass}}$ value and its standard deviation (s) were calculated from measurements performed on different days.

Binding affinity scales

When a sufficient number of relative affinity measurements were performed with every receptor molecule and the absolute binding affinities of the anchor compounds were determined, the binding affinity scales – one for every carboxylate anion – were constructed.

In a single binding affinity scale, every relative binding affinity was presented with an arrow between two receptor molecules. The absolute $\log K_{\mathrm{ass}}$ values were obtained by anchoring the scale to the absolute binding affinities of the anchor

compounds. This was done by minimising the sum of squares (SS) of the differences between the directly measured $\Delta \log K_{\mathrm{ass}}$ values and the assigned $\log K_{\mathrm{ass}}$ values, as also described in ref. [75]:

$$SS = \sum_{\mathrm{i}=1}^{\mathrm{n_m}} \{\Delta \log K_{\mathrm{ass}}^{\mathrm{i}} - [\log K_{\mathrm{ass}}(\mathrm{R_2A^-}) - \log K_{\mathrm{ass}}(\mathrm{R_1A^-})]\}^2 \qquad (22)$$

Here $\mathrm{n_m}$ represents the number of relative affinity measurements. Every $\Delta \log K_{\mathrm{ass}}$ value is the directly measured relative carboxylate binding affinity of the receptors $\mathrm{R_1}$ and $\mathrm{R_2}$. The agreement between the assigned absolute $\log K_{\mathrm{ass}}$ values and the measured $\Delta \log K_{\mathrm{ass}}$ values was evaluated using the consistency standard deviation (s) of the scale, as expressed by the following formula:[75]

$$s = \sqrt{\frac{SS}{\mathrm{n_m} - \mathrm{n_c}}} \qquad (23)$$

where $\mathrm{n_c}$ is the number of absolute $\log K_{\mathrm{ass}}$ values determined for a given scale under investigation. Characteristic s describes the consistency of the whole binding scale. The standard uncertainties of the individual $\log K_{\mathrm{ass}}$ values assigned for every receptor were found according to Equations (24) and (25). The standard uncertainties for comparing $\log K_{\mathrm{ass}}$ values within the same scale were found according to the following equation:

$$u_{\mathrm{c}}(\log K_{\mathrm{ass}}) = \frac{SD(\Delta \log K_{\mathrm{ass}})}{\sqrt{\mathrm{n}}} \qquad (24)$$

where SD is the standard deviation of receptor's relative binding affinities and n is the number of $\Delta \log K_{\mathrm{ass}}$ values determined for a given receptor. $u_{\mathrm{c}}(\log K_{\mathrm{ass}})$ represents the random effect in $\Delta \log K_{\mathrm{ass}}$ measurements and describes the accuracy of the relative binding affinity measurement method. The standard uncertainties for comparing $\log K_{\mathrm{ass}}$ values between different scales or with those from other research groups accounts also the random and systematic effects from anchoring:

$$u_{\mathrm{c}}(\log K_{\mathrm{ass}}) = \sqrt{u\left(\frac{SD(\Delta \log K_{\mathrm{ass}})}{\sqrt{\mathrm{n}}}\right)^2 + u(\mathrm{anchoring})^2 + u(\mathrm{sys})^2} \qquad (25)$$

where $u(\mathrm{anchoring})$ is calculated as a root mean square of differences between the $\log K_{\mathrm{ass}}$ values obtained directly and using "the ladder approach", and $u(\mathrm{sys})$ is assigned a fixed value of 0.03 based on our group's long-term experience with similar measurements.

The author of this dissertation used 44 different HBD receptors and 8 carboxylate anions to construct 8 binding affinity scales.

2.5. Construction of solid-contact ion-selective electrodes

At this work stage, the focus shifted from the quantification of binding in solution to a more physical application – Receptor **13** was used as an ionophore in a SC-ISE. This part of the work is described also in Publication III.

Electrode preparation

The glassy carbon working electrodes (area = 0.07 cm^2) were polished with sandpapers (grit size from P240 to P4000), diamond paste (particle size 1 µm) and aluminium oxide (particle size 0.3 µm). Before electropolymerisation, the electrodes were cleaned chemically in 1 M HNO_3 solution and ultrasonically in ethanol and water.

An aqueous solution of polymerisation electrolyte was prepared, containing 0.01 M 3,4-ethylenedioxythiophene (EDOT) and 0.1 M KCl as the background electrolyte. The solution was stirred for 24 hours, protected from light, and before synthesis, i.e., polymerisation, the electrolyte solution was deaerated by bubbling nitrogen (N_2) through the solution for at least 30 minutes. Electrochemical synthesis of PEDOT was carried out using galvanostatic electropolymerisation by applying a constant current of 0.014 mA for 714 s.[97] The synthesis of PEDOT(Cl) is depicted in Figure 7.

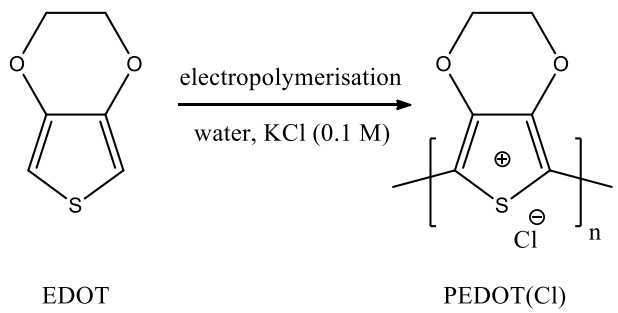

Figure 7. Electrochemical polymerisation of chloride doped PEDOT.

A conventional one-compartment three-electrode electrochemical cell was used, where the auxiliary electrode was a glassy carbon (GC) rod, an Ag/AgCl single junction electrode with an internal 3 M KCl solution was the reference, and the polished GC electrode on which the polymer films was to be deposited, was the working electrode. The experimental setup for electropolymerisation is shown schematically in Figure 8.

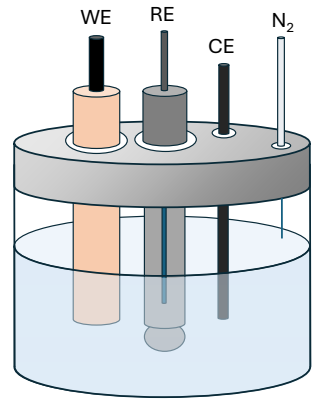

Figure 8. The experimental setup used for preparing GC/PEDOT electrodes. WE–working electrode, RE–reference electrode, CE–counter (or auxiliary) electrode, N_2–nitrogen gas flow.

During the polymerisation, N_2 gas flowed above the electrolyte solution to prevent oxidation. The formation of the PEDOT film was monitored using cyclic voltammetry. After polymerisation, the GC/PEDOT(Cl) electrodes were rinsed with purified water, the film's quality was verified visually, and the electrodes were conditioned in 0.1 M potassium acetate solution for one day before further use.

After one day of conditioning the GC/PEDOT(Cl) electrodes, they were removed from the conditioning solution, rinsed with purified water, and allowed to dry at room temperature for at least 24 hours. In the next step, two types of membrane cocktails were prepared: ISE-membranes containing Ionophore **13**, and control membranes without ionophore (see membrane compositions in Table 3). All membrane cocktails were stored at +4 °C.

Table 3. The composition of prepared membrane cocktails.

	Ion-selective membrane	**Control membrane**
Ionophore **13**	2 wt%	-
o-NPOE	65 wt%	66 wt%
PVC	33 wt%	33 wt%
TDMACl	50 mol% rel. to ionophore	0.6 wt%
THF	Dry content ~17%	Dry content ~17%

GC/PEDOT(Cl) electrodes were fixed upside down to a solid base. Half of the electrodes were coated with ISM by drop-casting 100 µl of membrane cocktail containing Ionophore **13** onto the GC/PEDOT(Cl) electrodes using a micropipette. The other half of the electrodes were coated similarly with an ionophore-free membrane cocktail for fabricating the control electrodes. Immediately after drop-casting, all the electrodes were covered with a beaker to avoid contami-

nation and too fast drying. After solvent evaporation, the constructed GC/PEDOT/ISM electrodes were conditioned in 0.1 M potassium acetate solution for at least three days before potentiometric measurements.

Electrode characterisation

The performance of each acetate-ISE or control electrode was studied by measuring its **potential** in acetate solution. The calibration curves and the limit of detection were obtained by the dilution method. The prepared SC-ISEs were connected to the measuring channels of the potentiometer. A single junction Ag/AgCl electrode with an internal 3 M KCl solution was used as a reference electrode (RE). To verify the proper functioning of the main reference electrode, a second RE of the same type was connected to a measurement channel as a control reference. The pH of the solutions was monitored simultaneously with a conventional glass pH electrode. All named electrodes were placed in the starting solution of the primary ion. A stock solution of 0.1 M potassium acetate was then serially diluted using an automatic pump, and at the same time the emf of all measuring channels was recorded in real time. At each dilution, the pump removed and replaced 34.2 mL of the electrolyte solution, so that the acetate concentration was in the range of 10^{-8}–10^{-1} M. The potentiometric response of all named electrodes was recorded in two different media: a) in a deionised water, in which case the pump replaced the removed electrolyte with deionised water, and b) in a HEPES-NaOH buffer at pH 7.0, in which case the removed electrolyte was replaced with the specified buffer solution. All experiments were performed at room temperature.

Electrochemical **impedance** spectroscopy measurements were performed by using a conventional three-electrode cell (as shown in Figure 8, but without N_2 flow) using a prepared acetate-ISE as a working electrode, a GC rod as an auxiliary electrode, and an Ag/AgCl/KCl (3 M) as a reference electrode. The measurements of impedance were performed at open-circuit potential in a 0.1 M potassium acetate solution. A sinusoidal potential modulation with 10 mV amplitude was applied in the frequency range of 10 mHz to 100 kHz. All electrodes were measured after an equally long conditioning time. Impedance data were plotted and analysed in the form of complex plane (Nyquist) plots.

The **pH effect** experiments were conducted to evaluate how **pH** influences the behaviour of acetate-ISEs. A fixed and known concentration of acetic acid (0.01 M) was monitored while systematically increasing the pH of the analyte solution from 3.4 to 10.0. Increasing the pH was done by stepwise addition of concentrated NaOH solution, which also contained 0.01 M acetate, ensuring that the total concentration of acetate anion remained constant.

Potentiometric **selectivity** coefficients ($\log K^{\mathrm{pot}}_{\mathrm{acetate,j}}$) were determined by the separate solution method (SSM) in 10^{-2} M NaF, Na_2HPO_4, Na_2SO_4, NaCl, $NaHCO_3$, HCOONa, NaBr, $NaNO_3$, NaI, NaSCN, sodium benzoate, naproxen sodium salt and ibuprofen sodium salt solutions. The solutions were first stirred until the potentials were stabilised, then the stirring was stopped and the potential

readings were taken after a few minutes. In order to eliminate the bias caused by uptake of strongly interfering ions by the membrane, the solutions were selected starting with the most discriminated ions in sequence of decreasing discrimination. Measurements with divalent ions and monovalent ions were carried out separately.

The activity coefficients for all ions were calculated according to the following formula:[81]

$$\log \gamma_{\mathrm{i}} = -\frac{Az_i^2\sqrt{I}}{1+aB\sqrt{I}} + Cz_{\mathrm{i}}I \tag{26}$$

where A, B, and C are constants with values of 0.509, 3.286, and 0.1, respectively, a is the effective hydrated radius[121] of the ion i, z_{i} is the charge of the ion i, and I is the ionic strength of the solution. The activities of monovalent ions and divalent ions were $10^{-2.04}$ and $10^{-2.21}$, respectively. Potentiometric selectivity coefficients were calculated using Equations (16) and (17).

3. RESULTS AND DISCUSSION

It would be desirable to obtain synthetic receptors capable of detecting small carboxylates like acetate and benzoate through straightforward molecular recognition processes. These receptors would serve as ideal candidates for use as ionophores in ion-selective electrodes. In my PhD project, I hypothesised that by quantifying the binding affinities of acyclic synthetic HBD receptors, it would be possible to estimate the selectivity of such receptors for monocarboxylates. In the first part of the work, I measured the affinities of 44 synthetic receptors towards 8 monocarboxylates in the same environment. During the work, a new hypothesis arose that if the used receptor framework is hydrophobic enough to be dissolved in a polymeric membrane, it can be used as an ionophore for the manufacture of ion-selective electrodes. In the study, 1,3-bis(carbazolyl)urea derivative was used as an ionophore to prepare SC-ISEs for acetate determination.

3.1. Relative binding affinities

To design a synthetic receptor that strongly and specifically binds one particular carboxylate, it is important to learn about the compatibility of different receptor structures with carboxylates with different basicity, hydrophilicity, and steric demand. In the primary receptor-anion selection, the receptor molecules were represented by different urea-, indole-, carbazole-, thiourea- and indolocarbazole-based synthetic receptors, and the carboxylates by acetate, pivalate, benzoate, and lactate. Since the chosen receptors are relatively small and instead the building blocks of more complex receptors, it was essential when choosing the measurement technique that binding constants with slight differences could be measured with high precision. The relative NMR-based measurement method[76] made it possible to study trends of the binding constant changes with carboxylate anions and different families of multidentate HBD anion receptors.[I, II]

With this titration method, in the first stage of the work, relative binding measurements were performed with lactate, benzoate, acetate, and pivalate. Figure 9 shows the stacked ^{1}H NMR spectra for the measurement series with lactate anion and receptors **3**, **27,** and **33**. The bottom spectrum corresponds to a solution to which no titrant has been added (solution of free receptors). Titration proceeds from bottom to top. The upper spectrum corresponds to a solution to which an excess of titrant has been added (solution of receptor-anion complexes).

The shifts of the NH protons in the NMR spectra characterise the degrees of complexation for these receptor-anion complexes. The stronger the binding affinity of the receptor, the more significant the proportion of the receptor-anion complex in the solution, and the faster the signal of the corresponding receptor moves during the titration. For the measurement series shown in Figure 9, the binding affinity order for the lactate anion is **27** > **3** > **33**. These stacked NMR spectra are also informative in the sense that in a situation where the NH signals

of the receptors begin to shift to the left with a new momentum, it likely indicates a 1:2 stoichiometry (after the binding of the first anion, the binding of the second anion to the same receptor initiates). This kind of binding behaviour was observed with receptors **5**–**7**[I], **12**–**13**[II], and **43**[II]. Throughout this dissertation, $\log K_{ass}$ values were always calculated using the 1:1 binding model, and only titration points with a low anion concentration were considered for these named receptors.

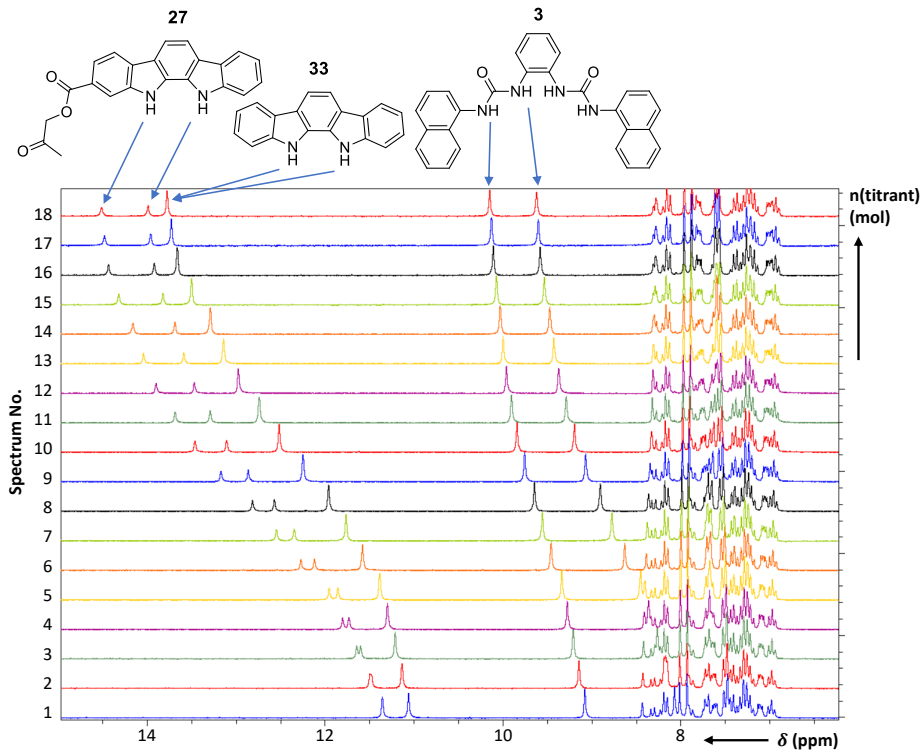

Figure 9. Stacked ^{1}H NMR spectra of the relative binding affinity measurement between receptors **3**, **27**, and **33** in DMSO-d_6:H_2O (99.5%:0.5% m/m) with TBA lactate.

All four carboxylates, in the form of their tetrabutylammonium salts, were measured against 38 different receptor molecules in DMSO-d_6 with 0.5% of water (m/m) and four binding affinity scales (one for each anion) containing all the relative binding affinities ($\Delta\log K_{ass}$) were constructed.[I] To also assign absolute binding affinities ($\log K_{ass}$) to all receptor molecules, all scales were anchored to the $\log K_{ass}$ value of the same receptor, unsubstituted Indolocarbazole **33**.

All receptors investigated in Publication I are HBD receptors, and hydrogen-bonding interactions predominantly determine their binding. The aqueous pK_a values of pivalate, acetate, benzoate, and lactate are 5.03, 4.76, 4.20, and 3.86, respectively[29,32]. Figure 10 demonstrates well how carboxylate anions' binding strength broadly follows the corresponding anions' basicity. Overall, obtaining a

binding pattern in which the most basic pivalate anion binds most strongly to the receptors was anticipated because the anion's increased negative charge density results in a stronger attraction to the partial positive charges of the HBD binding sites of the receptor molecule. Still, attention was paid to such "selectivity reversals", where the binding order of the same receptors differed for different anions. Such selectivity reversals indicate that in addition to the appropriate number and position of hydrogen bond donor sites, their size, geometry, hydrophobic interactions, and steric demand play a role even for such small receptor structures. For example, receptor **14** stands out from the upper part of Figure 10 with its interesting binding trend. While it is not the strongest receptor for the other carboxylate anions, it has the highest binding affinity towards the acetate anion ($\log K_{\mathrm{ass}}$ 4.94). This selectivity reversal is compounded by the fact that receptor **15**, which is by far the strongest pivalate anion binder ($\log K_{\mathrm{ass}}$ 5.33), is only the fourth strongest for the acetate anion ($\log K_{\mathrm{ass}}$ 4.56). Comparing the binding cavities of these two receptors, the cavity of receptor **14** is smaller and more obscured by the tert-butyloxycarbonyl (Boc) groups. This matter prevents the binding of the larger pivalate and makes the receptor **14** cavity more suitable for the smaller acetate anion. For receptor **15**, the cavity is larger and pivalate with its hydrophobic tail can fit without much steric hindrance. This explanation for the binding differences between receptors **14** and **15** was also supported by the computational geometries[I].

Significant changes in binding order also occur with receptors **3**, **8** and **9**. Their common structural feature is that they all have relatively large and hydrophobic substituents (a feature that led to their inclusion in the receptor selection) that can interact hydrophobically with the hydrophobic tails of the carboxylate anions. The binding experiments confirmed that the mentioned receptors prefer anions with larger hydrophobic moieties – benzoate and pivalate (see Figure 10).

The strongest carboxylate binders in Publication I are receptors **11**, **14**, **15**, and **16**. These receptors have multiple hydrogen-bond donor groups that are suitably positioned for anion binding, and their binding pocket is just the right size to recognise the carboxylate. An additional explanation from the calculated geometries is that an almost planar receptor-anion complex is formed upon anion binding, which experiences little steric strain.

The urea-based receptors with phenyl and/or naphthyl substitutions (receptors **20**, **22** and **23**) exhibit significantly weaker binding to carboxylate ions compared to the related urea-based receptors (receptors **14**, **15** and **16**) that have indole or carbazole substitutions. Despite the initial expectation that a receptor with additional naphthyl groups might enhance stabilising interactions with the hydrophobic regions of small carboxylates, binding studies reveal a different outcome. Each added naphthyl ring introduces steric hindrance. Consequently, when the carboxyl group binds, these receptors adopt an undesirable *anti-anti* conformation, which hinders effective molecular recognition. It follows that indole and carbazole moieties are more sensible choices near the binding site. They increase the number of hydrogen bond donor sites and form a concave structure for recognising small carboxylates.

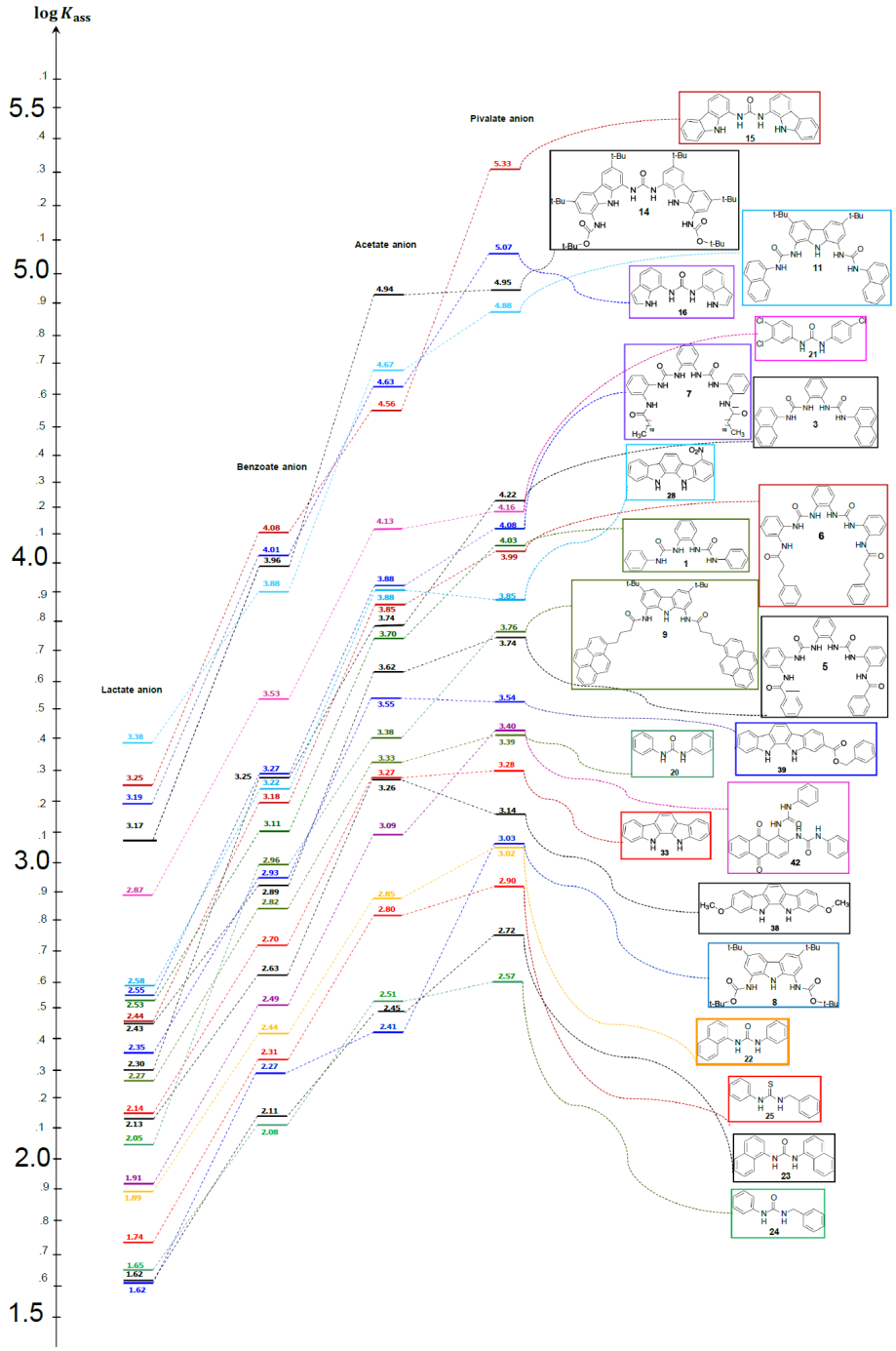

Figure 10. Binding-structure-relationship plot for pivalate, acetate, benzoate and lactate. The position of the horizontal line and the numerical value above it both indicate the absolute binding constant.

Out of the studied urea-, indole-, carbazole-, thiourea- and indolocarbazole-based synthetic receptors used in Publication I, the tetradentate systems of four suitably located NH centres were the most successful combination for binding carboxylate anions.

The described study with four carboxylates provided a good insight into how anion receptors from different compound families interact with carboxylates. In order to provide directly comparable binding constants for a larger set of receptors and anions and to describe the receptor design necessary for their selective binding, the study was expanded as follows:

> a) The number of carboxylates to be investigated was increased from four to eleven (formate, acetate, pivalate, lactate, naproxen, ibuprofen, ketoprofen, glucuronate, hexanoate, sorbate and benzoate). Such a sample of carboxylates includes both smaller and larger, more basic and less basic, more hydrophilic and hydrophobic, unsubstituted and X-substituted anions with different geometries and steric hindrance.
>
> b) From the initial 38 receptors, the 17 most promising were selected (receptors **3**, **5**, **6**, **7**, **8**, **9**, **11**, **14**, **15**, **16**, **20**, **21**, **27**, **28**, **33**, **35** and **42**), and five new receptors of interest (**10**, **12**, **13**, **41** and **43**) were added to the receptor selection. These 22 synthetic multidentate HBD receptors are all acyclic urea-, carbazole- and indolocarbazole-based receptors.

In the second stage of the work, a total of 242 $\log K_{\mathrm{ass}}$ values were determined by ^{1}H NMR-based relative binding affinity measurements. All 11 carboxylates, in the form of their tetrabutylammonium salts, were measured against 22 different receptor molecules in DMSO-d_6 with 0.5 % of water (m/m) and 11 binding affinity scales (one for each anion) containing all the relative binding affinities ($\Delta\log K_{\mathrm{ass}}$) were constructed.[II] Absolute $\log K_{\mathrm{ass}}$ values were obtained by anchoring scales to absolute $\log K_{\mathrm{ass}}$ values of receptors **15**, **27**, **28** and **33**. The summary of experimental results is presented in Figure 11.

Figure 11 illustrates how a binding pattern has emerged for almost all selected receptors and the binding affinity of anions follows the order of basicity only for some simple receptors such as Indolocarbazole (**33**) or Diphenylurea (**20**). Combinations of carbazole (or indole) and urea (receptors **10**–**16**) have the highest binding affinities and form a cluster of best binders at the upper end of the figure. Comparing the binding of these receptors to acetate, hexanoate and pivalate (aliphatic, with similar basicity), the first major binding pattern is noticeable, it appears that most of them bind acetate the weakest. Examination of the geometries of the respective complexes revealed that hexanoate and pivalate with longer alkyl chains fit better into the binding pocket of these receptors, allowing solvophobic effects between the hydrophobic residues of the anions and the receptors. Another major binding pattern in Figure 11 is the strong binding of lactate to receptors **10**–**14**. This is most probably favoured by additional hydrogen bonds with the 2-OH group of lactate and, in contrast to glucuronate, a better

spatial fit in the half-pocket of the receptors. Several other interesting relations between structure and binding cases are pinpointed and analysed in Publication II.

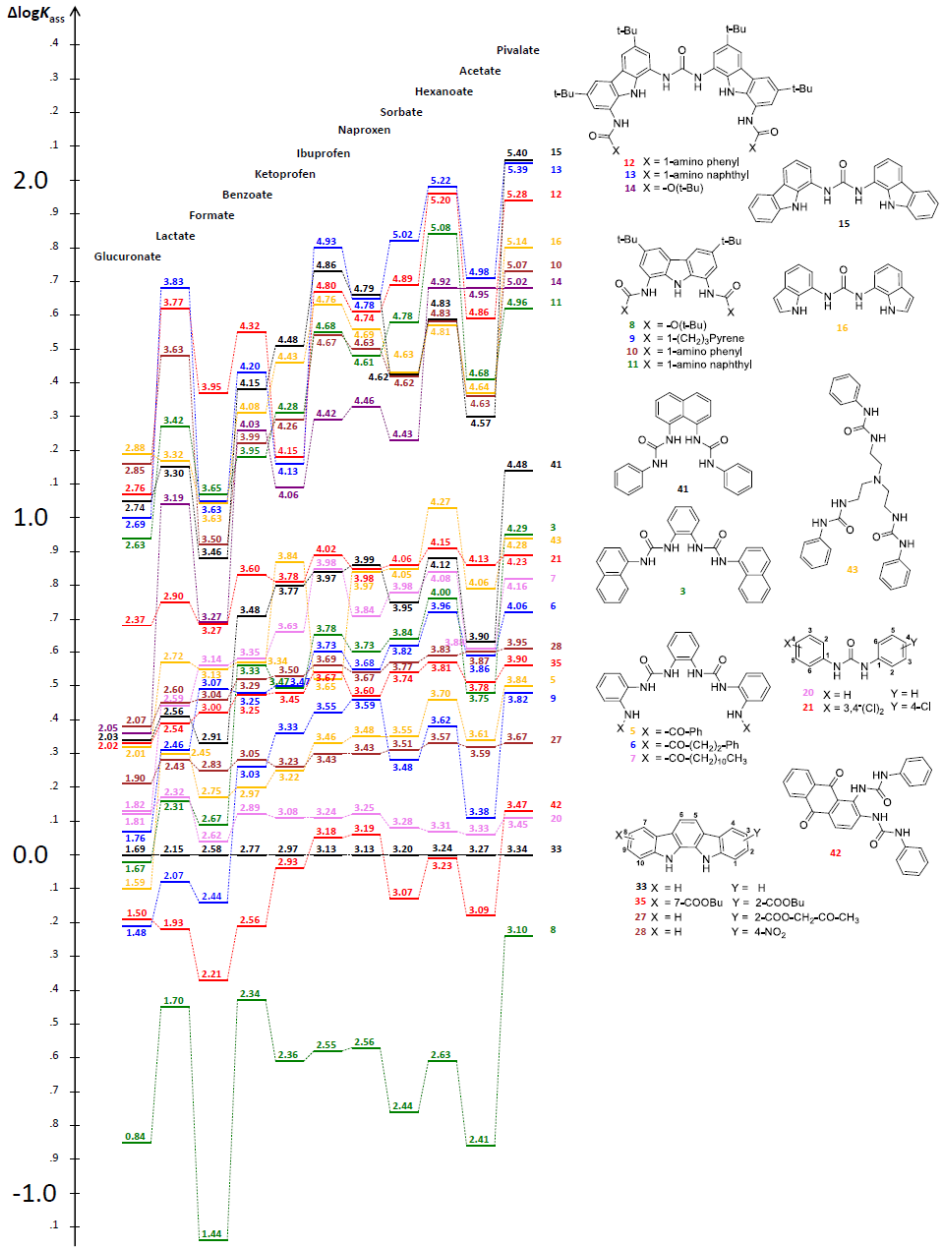

Figure 11. Binding-structure-relationship plot for 11 monocarboxylates. The position of the horizontal line indicates the difference in binding constant from the log K_{ass} value of unsubstituted Indolocarbazole (**33**) and the numerical value indicates the absolute binding constant.

1,3-bis(carbazolyl)urea-based receptors **12** and **13** exhibit the highest binding affinity for most anions in this study. They possess eight NH groups in total and computational modelling suggests that five to six NH groups are used for recognition of carboxylate group and others for the additional interactions for example with the lactate OH group.

3.2. Absolute binding affinities

Until my studies, most of the relative binding measurements in our group were performed with acetate.[75,76] Absolute binding values for acetate in DMSO with 0.5% of water (m/m) were previously determined by the first author of Publication I and were taken from ref [76]. With the addition of each new carboxylate to the study, it was necessary to determine the absolute $\log K_{\mathrm{ass}}$ value of at least one receptor with that anion to anchor the constructed scale.

The absolute $\log K_{\mathrm{ass}}$ values were measured for Indolocarbazole **33** with glucuronate, lactate, formate, benzoate, ketoprofen, ibuprofen, and pivalate. 4-NO_2-indolocarbazole **28** was used as a second anchor compound for glucuronate, lactate, benzoate, ketoprofen, and pivalate. 1,3-dicarbazolylurea **15** was used as a second anchor point for formate and ibuprofen from the upper part of the binding scale. The results of the measurements are presented in Table 4.

The binding interaction between ketoprofen and Indolocarbazole **33** was not assessed using the UV-Vis method due to the intrinsic UV-Vis absorbance of ketoprofen up to 400 nm. This would have caused spectral overlap with the absorption of the Indolocarbazole **33** receptor. However, the absorption spectrum of the 4-NO_2-indolocarbazole receptor occurs at longer wavelengths, allowing for the determination of the absolute $\log K_{\mathrm{ass}}$ value of ketoprofen via the UV-Vis method. Conversely, evaluating the binding affinity of receptor **28** using fluorescence technique was problematic because of spectral interference from the receptor's absorption. Consequently, the absolute binding constants of receptor **28** were quantified exclusively using the UV-Vis technique. The slight differences between the $\log K_{\mathrm{ass}}$ values obtained directly and using "the ladder approach" (last column of Table 4) demonstrate the excellent consistency between the absolute and the relative binding affinity measurements.

Table 4. Results of absolute log K_{ass} value measurements.

Receptor	Anion	log K_{ass} [a]	s [b]	N [b] UV-Vis	N [b] Fluoresc.	log K_{ass} from scale [c]	Δ [c]
Indolocarbazole **33**	Glucuronate	1.62	0.02	2	-	1.69	0.078
	Lactate	2.14	0.07	5	-	2.15	0.016
	Formate	2.56	0.03	2	2	2.58	0.019
	Benzoate	2.70 [d]	0.07 [d]	2	2	2.77	0.070
	Ketoprofen	3.02	0.01	-	2	2.97	-0.052
	Ibuprofen	3.07	0.01	2	2	3.13	0.057
	Pivalate	3.28 [d]	0.11 [d]	3	-	3.34	0.066
4-NO_2-indolocarbazole **28**	Glucuronate	2.15	0.02	2	-	2.07	-0.078
	Lactate	2.62	0.02	2	-	2.60	-0.016
	Benzoate	3.36	0.01	2	-	3.29	-0.070
	Ketoprofen	3.45	0.02	2	-	3.50	0.052
	Pivalate	4.01	0.02	2	-	3.95	-0.066
1,3-dicarbazolylurea **15**	Formate	3.48	0.01	2	2	3.46	-0.019
	Ibuprofen	4.92	0.01	1	2	4.86	-0.057

[a] The average of the results of all independent absolute measurements. [b] Standard deviation of all measurements and the number of measurements with UV-Vis and Fluorescence techniques. [c] log K_{ass} values obtained from the binding affinity scales by the method of least squares and the differences between the log K_{ass} values obtained directly and using "the ladder approach". [d] The absolute NMR measurements performed by colleague Sandip A. Kadam have also been used to calculate the value.

3.3. Binding affinity scales

A relative binding affinity scale was constructed for each carboxylate anion under study. On these scales ("ladders"), each double-ended arrow represents the difference in the absolute binding affinities between two receptor molecules on a logarithmic scale. In other words, one arrow represents the $\Delta \log K_{ass}$ value obtained from one measurement series. Each receptor is linked to the scale through at least two relative binding affinity values, and each additional measurement further validates the entire scale.[122] However, there are two reasons why specific receptors have been measured significantly more frequently than others on the scale: a) the respective receptor may have been synthesised in larger quantity, so it is readily available for numerous measurements, and/or b) the NH peaks of the respective receptor are positioned in the spectrum at locations less likely to overlap with the NH peaks of other measurable receptors.

The timeline of the work of the compiled scales explains why the acetate, pivalate, lactate, and benzoate scales are significantly larger than the scales of the other carboxylates used in the study. Acetate was the first anion selected by my colleague and the lead author of Publication I, Sandip A. Kadam, to develop the NMR-based relative binding affinity measurement method and characterise the binding of different HBD anion receptors.[76] The choice of receptors in Publication I builds heavily on the work that began with acetate. In order to study discrimination, binding affinities with benzoate, lactate, and pivalate were measured against the same receptors that had already been measured with acetate. However, at this point, confident choices were already made to limit the overall number of receptors, especially those that bind anions weaker. For example, indolocarbazoles with 1,10-substitutions were not included (as shown in ref. [76] that bulky groups near the binding site hinder the anion complexation), and in the case of very similar receptors (e.g. 2-NO_2-indolocarbazole vs 4-NO_2-indolocarbazole), only the receptor with the strongest affinity was selected for further study. The Publication I reported the affinities of 38 receptors for four carboxylates. The measurement results from Publication II further increased the acetate, pivalate, lactate, and benzoate binding scales.

Publication II reported the affinities of 22 receptors for 11 carboxylates. The goal was to add even more carboxylates with different properties to the research and, at the same time, more complex receptors to the selection of receptors that could be potentially suitable carboxylate binders. At the same time, the number of more superficial and less attractive receptors in terms of binding behaviour was significantly reduced.

The measurements of naproxen, sorbate and hexanoate were performed by a colleague and the second author of Publication II, Juuli Nõges, and the binding affinity scales for these anions can be found in the Supporting Information of Publication II. However, $\log K_{ass}$ values for naproxen, sorbate and hexanoate are presented on the binding affinity scale shown in Figure 11 because they are an essential part of the discrimination study and necessary for comparing and discussing the binding affinity of 11 carboxylates. Binding affinity scales for

formate, acetate, pivalate, lactate, ibuprofen, ketoprofen, glucuronate, and benzoate are presented on the following pages (Tables 5–12). The consistency standard deviation s for each scale is indicated in the corresponding table footnote. All the synthetic receptors measured by the author of this dissertation are underlined.

Table 5. Scale of relative binding constants of formate anion in DMSO-d_6:H_2O (99.5%:0.5% m/m).[a]

Receptor number	log K_{ass}	u_c[b]	u_c[c]	Δ log K_{ass}
Receptor **12**	3.95	0.01	0.04	
Receptor **11**	3.65	0.01	0.04	
Receptor **13**	3.63	0.01	0.04	
1,3-diindolylurea **16**	3.63	0.01	0.04	
Receptor **10**	3.50	0.01	0.04	
1,3-dicarbazolylurea **15**	3.46	0.01	0.04	
3,4,4-Cl_3-diphenylurea **21**	3.27	0.01	0.04	
Receptor **14**	3.27	0.01	0.04	
Receptor **7**	3.14	0.01	0.04	
Receptor **43**	3.13	0.01	0.04	
Receptor **6**	3.07	0.01	0.04	
4-NO_2-ICZ **28**	3.04	0.01	0.04	
2,7-$(BuOCO)_2$-ICZ **35**	3.00	0.01	0.04	
Receptor **41**	2.91	0.01	0.04	
CH_3-CO-CH_2-OCO-ICZ **27**	2.83	0.01	0.04	
Receptor **5**	2.75	0.01	0.04	
Receptor **3**	2.67	0.01	0.04	
1,3-diphenylurea **20**	2.62	0.01	0.04	
Indolocarbazole 33	**2.58**	0.01	0.04	
Receptor **9**	2.44	0.01	0.04	
Receptor **42**	2.21	0.01	0.04	
Receptor **8**	1.44	0.01	0.04	

[a] All log K_{ass} values correspond to the Equation (1). Consistency standard deviation (s) of the scale is 0.002. [b] Standard uncertainties for comparing log K_{ass} values within the same scale. [c] Standard uncertainties for comparing log K_{ass} values between different scales or with those from other research groups.

Table 6. Scale of relative binding constants of acetate anion in DMSO-d_6:H_2O (99.5%:0.5% m/m).[a]

Receptor number	$\log K_{ass}$	u_c[b]	u_c[c]	$\Delta \log K_{ass}$
Receptor 13	4.98	0.01	0.09	
Receptor 14	4.95	0.01	0.09	
Receptor 12	4.86	0.01	0.09	
Receptor 11	4.68	0.01	0.09	
1,3-diindolylurea 16	4.64	0.01	0.09	
Receptor 10	4.63	0.01	0.09	
1,3-dicarbazolylurea 15	4.57	0.01	0.09	
3,4,4-Cl_3-diphenylurea 21	4.13	0.01	0.09	
Receptor 43	4.06	0.01	0.09	
Receptor 18	3.90	0.01	0.09	
Receptor 41	3.90	0.01	0.09	
Receptor 7	3.88	0.01	0.09	
4-NO_2-ICZ 28	3.87	0.01	0.09	
Receptor 6	3.86	0.01	0.09	
2,9-(BuOCO)$_2$-ICZ 34	3.82	0.01	0.09	
2,7-(BuOCO)$_2$-ICZ 35	3.78	0.01	0.09	
4,7-(BuOCO)$_2$-ICZ 36	3.78	0.01	0.09	
Receptor 3	3.75	0.01	0.09	
Receptor 1	3.70	0.01	0.09	
Receptor 4	3.67	0.01	0.09	
2,7-Cl_2-ICZ 37	3.66	0.01	0.09	
Receptor 2	3.64	0.01	0.09	
Receptor 5	3.61	0.01	0.09	
CH_3-CO-CH_2-OCO-ICZ 27	3.59	0.02	0.09	
Receptor 17	3.58	0.01	0.09	
Receptor 32	3.56	0.01	0.09	
Receptor 39	3.55	0.01	0.09	
2-(BuOCO)-ICZ 26	3.54	0.02	0.09	
Receptor 9	3.38	0.01	0.09	
Receptor 31	3.36	0.01	0.09	
1,3-diphenylurea 20	3.33	0.01	0.09	
2,9-(MeO)$_2$-ICZ 38	3.27	0.01	0.09	
Indolocarbazole 33	**3.27**	0.01	0.09	
Receptor 19	3.23	0.01	0.09	
Receptor 30	3.16	0.01	0.09	
Receptor 42	3.09	0.01	0.09	
1-Cl-ICZ 29	2.89	0.01	0.09	
Receptor 22	2.85	0.01	0.09	
Receptor 25	2.80	0.01	0.09	
Receptor 24	2.51	0.01	0.09	
Receptor 23	2.45	0.01	0.09	
Receptor 8	2.41	0.01	0.09	

[a] All $\log K_{ass}$ values correspond to the Equation (1). Consistency standard deviation (s) of the scale is 0.014. [b] Standard uncertainties for comparing $\log K_{ass}$ values within the same scale. [c] Standard uncertainties for comparing $\log K_{ass}$ values between different scales or with those from other research groups.

Table 7. Scale of relative binding constants of pivalate anion in DMSO-d_6:H_2O (99.5%:0.5% m/m).[a]

Receptor number	$\log K_{ass}$	u_c[b]	u_c[c]	$\Delta \log K_{ass}$
1,3-dicarbazolylurea **15**	5.40	0.01	0.07	
Receptor **13**	5.39	0.01	0.07	
Receptor **12**	5.28	0.01	0.07	
1,3-diindolylurea **16**	5.14	0.01	0.07	
Receptor **10**	5.07	0.01	0.07	
Receptor **14**	5.02	0.01	0.07	
Receptor **11**	4.96	0.01	0.07	
Receptor **41**	4.48	0.01	0.07	
Receptor **3**	4.29	0.01	0.07	
Receptor **43**	4.28	0.01	0.07	
3,4,4-Cl_3-diphenylurea **21**	4.23	0.01	0.07	
Receptor **7**	4.16	0.01	0.07	
Receptor **1**	4.09	0.01	0.07	
Receptor **6**	4.06	0.01	0.07	
Receptor **18**	4.05	0.01	0.07	
Receptor **2**	4.02	0.01	0.07	
Receptor **4**	4.01	0.01	0.07	
4-NO_2-ICZ **28**	3.95	0.01	0.07	
2,7-(BuOCO)$_2$-ICZ **35**	3.90	0.01	0.07	
2,9-(BuOCO)$_2$-ICZ **34**	3.89	0.01	0.07	
4,7-(BuOCO)$_2$-ICZ **36**	3.88	0.01	0.07	
Receptor **5**	3.84	0.01	0.07	
Receptor **9**	3.82	0.01	0.07	
2,7-Cl_2-ICZ **37**	3.79	0.01	0.07	
Receptor **17**	3.73	0.01	0.07	
CH_3-CO-CH_2-OCO-ICZ **27**	3.67	0.01	0.07	
2-(BuOCO)-ICZ **26**	3.65	0.01	0.07	
Receptor **40**	3.65	0.01	0.07	
Receptor **32**	3.61	0.01	0.07	
Receptor **39**	3.61	0.01	0.07	
Receptor **42**	3.47	0.01	0.07	
1,3-diphenylurea **20**	3.45	0.01	0.07	
Receptor **31**	3.43	0.01	0.07	
Indolocarbazole 33	**3.34**	0.01	0.07	
Receptor **19**	3.30	0.01	0.07	
Receptor **30**	3.28	0.01	0.07	
2,9-(MeO)$_2$-ICZ **38**	3.20	0.01	0.07	
Receptor **8**	3.10	0.01	0.07	
Receptor **22**	3.08	0.01	0.07	
1-Cl-ICZ **29**	3.08	0.01	0.07	
Receptor **25**	2.96	0.01	0.07	
Receptor **23**	2.79	0.01	0.07	
Receptor **24**	2.63	0.01	0.07	

[a] All $\log K_{ass}$ values correspond to the Equation (1). Consistency standard deviation (s) of the scale is 0.011. [b] Standard uncertainties for comparing $\log K_{ass}$ values within the same scale. [c] Standard uncertainties for comparing $\log K_{ass}$ values between different scales or with those from other research groups.

Table 8. Scale of relative binding constants of lactate anion in DMSO-d_6:H_2O (99.5%:0.5% m/m).[a]

Receptor number	$\log K_{ass}$	u_c[b]	u_c[c]	$\Delta \log K_{ass}$
Receptor 13	3.83	0.01	0.04	
Receptor 12	3.77	0.01	0.04	
Receptor 10	3.63	0.01	0.04	
Receptor 11	3.42	0.01	0.04	
1,3-diindolylurea 16	3.32	0.01	0.04	
1,3-dicarbazolylurea 15	3.30	0.01	0.04	
Receptor 14	3.19	0.01	0.04	
3,4,4-Cl_3-diphenylurea 21	2.90	0.01	0.04	
Receptor 43	2.72	0.01	0.04	
Receptor 18	2.70	0.01	0.04	
4-NO_2-ICZ 28	2.60	0.01	0.04	
Receptor 1	2.60	0.03	0.05	
Receptor 7	2.59	0.01	0.04	
Receptor 41	2.56	0.01	0.04	
4,7-$(BuOCO)_2$-ICZ 36	2.56	0.01	0.04	
2,7-$(BuOCO)_2$-ICZ 35	2.54	0.01	0.04	
2,9-$(BuOCO)_2$-ICZ 34	2.53	0.01	0.04	
2,7-Cl_2-ICZ 37	2.48	0.01	0.04	
Receptor 2	2.46	0.01	0.04	
Receptor 6	2.46	0.01	0.04	
Receptor 5	2.45	0.01	0.04	
Receptor 17	2.45	0.01	0.04	
CH_3-CO-CH_2-OCO-ICZ 27	2.43	0.01	0.04	
Receptor 40	2.43	0.01	0.04	
Receptor 39	2.43	0.02	0.04	
2-(BuOCO)-ICZ 26	2.42	0.01	0.04	
Receptor 4	2.39	0.01	0.04	
Receptor 32	2.32	0.01	0.04	
1,3-diphenylurea 20	2.32	0.01	0.04	
Receptor 3	2.31	0.01	0.04	
Receptor 19	2.27	0.01	0.04	
Receptor 31	2.19	0.01	0.04	
2,9-$(MeO)_2$-ICZ 38	2.18	0.01	0.04	
Indolocarbazole 33	**2.15**	0.01	0.04	
Receptor 9	2.07	0.01	0.04	
Receptor 30	2.01	0.01	0.04	
Receptor 42	1.93	0.01	0.04	
Receptor 22	1.90	0.01	0.04	
1-Cl-ICZ 29	1.89	0.01	0.04	
Receptor 25	1.75	0.01	0.04	
Receptor 8	1.70	0.01	0.04	
Receptor 24	1.64	0.01	0.04	
Receptor 23	1.63	0.01	0.04	

[a] All $\log K_{ass}$ values correspond to the Equation (1). Consistency standard deviation (s) of the scale is 0.017. [b] Standard uncertainties for comparing $\log K_{ass}$ values within the same scale. [c] Standard uncertainties for comparing $\log K_{ass}$ values between different scales or with those from other research groups.

Table 9. Scale of relative binding constants of ibuprofen anion in DMSO-d_6:H_2O (99.5%:0.5% m/m).[a]

Receptor number	$\log K_{ass}$	u_c[b]	u_c[c]	$\Delta \log K_{ass}$
Receptor **13**	4.93	0.01	0.07	
1,3-dicarbazolylurea **15**	4.86	0.01	0.07	
Receptor **12**	4.80	0.01	0.07	
1,3-diindolylurea **16**	4.76	0.01	0.07	
Receptor **11**	4.68	0.01	0.07	
Receptor **10**	4.67	0.01	0.07	
Receptor **14**	4.42	0.01	0.07	
3,4,4-Cl_3-diphenylurea **21**	4.02	0.01	0.07	
Receptor **7**	3.98	0.01	0.07	
Receptor **41**	3.97	0.01	0.07	
Receptor **3**	3.78	0.01	0.07	
Receptor **6**	3.73	0.01	0.07	
4-NO_2-ICZ **28**	3.69	0.01	0.07	
2,7-$(BuOCO)_2$-ICZ **35**	3.67	0.01	0.07	
Receptor **43**	3.65	0.01	0.07	
Receptor **9**	3.55	0.01	0.07	
Receptor **5**	3.46	0.01	0.07	
CH_3-CO-CH_2-OCO-ICZ **27**	3.43	0.01	0.07	
CH_3-CH_2-OCO-ICZ **44**	3.42	0.01	0.07	
1,3-diphenylurea **20**	3.24	0.01	0.07	
Receptor **42**	3.18	0.01	0.07	
Indolocarbazole 33	**3.13**	0.01	0.07	
2,9-$(MeO)_2$-ICZ **38**	3.04	0.01	0.07	
Receptor **8**	2.55	0.01	0.07	

[a] All $\log K_{ass}$ values correspond to the Equation (1). Consistency standard deviation (s) of the scale is 0.004. [b] Standard uncertainties for comparing $\log K_{ass}$ values within the same scale. [c] Standard uncertainties for comparing $\log K_{ass}$ values between different scales or with those from other research groups.

Table 10. Scale of relative binding constants of ketoprofen anion in DMSO-d_6:H_2O (99.5%:0.5% m/m).[a]

Receptor number	$\log K_{ass}$	u_c[b]	u_c[c]	$\Delta \log K_{ass}$
1,3-dicarbazolylurea **15**	4.48	0.01	0.06	
1,3-diindolylurea **16**	4.43	0.01	0.06	
Receptor **11**	4.28	0.01	0.06	
Receptor **10**	4.26	0.01	0.06	
Receptor **12**	4.15	0.01	0.06	
Receptor **13**	4.13	0.01	0.06	
Receptor **14**	4.06	0.01	0.06	
Receptor **43**	3.84	0.01	0.06	
3,4,4-Cl_3-diphenylurea **21**	3.78	0.01	0.06	
Receptor **41**	3.77	0.01	0.06	
Receptor **7**	3.63	0.01	0.06	
4-NO_2-ICZ **28**	3.50	0.01	0.06	
Receptor **6**	3.47	0.01	0.06	
Receptor **3**	3.47	0.01	0.06	
2,7-$(BuOCO)_2$-ICZ **35**	3.45	0.01	0.06	
Receptor **9**	3.33	0.01	0.06	
CH_3-CO-CH_2-OCO-ICZ **27**	3.23	0.01	0.06	
Receptor **5**	3.22	0.01	0.06	
1,3-diphenylurea **20**	3.08	0.01	0.06	
Indolocarbazole 33	**2.97**	0.01	0.06	
Receptor **42**	2.93	0.01	0.06	
Receptor **8**	2.36	0.01	0.06	

[a] All $\log K_{ass}$ values correspond to the Equation (1). Consistency standard deviation (s) of the scale is 0.004. [b] Standard uncertainties for comparing $\log K_{ass}$ values within the same scale. [c] Standard uncertainties for comparing $\log K_{ass}$ values between different scales or with those from other research groups.

Table 11. Scale of relative binding constants of glucuronate anion in DMSO-d_6:H_2O (99.5%:0.5% m/m).[a]

Receptor number	$\log K_{ass}$	u_c[b]	u_c[c]	$\Delta \log K_{ass}$
1,3-diindolylurea **16**	2.88	0.01	0.08	
Receptor **10**	2.85	0.01	0.08	
Receptor **12**	2.76	0.01	0.08	
1,3-dicarbazolylurea **15**	2.74	0.01	0.08	
Receptor **13**	2.69	0.01	0.08	
Receptor **11**	2.63	0.01	0.08	
3,4,4-Cl_3-diphenylurea **21**	2.37	0.01	0.08	
4-NO_2-ICZ **28**	2.07	0.01	0.08	
Receptor **14**	2.05	0.01	0.08	
Receptor **41**	2.03	0.01	0.08	
2,7-$(BuOCO)_2$-ICZ **35**	2.02	0.01	0.08	
Receptor **43**	2.01	0.01	0.08	
CH_3-CH_2-OCO-ICZ **44**	1.92	0.01	0.08	
CH_3-CO-CH_2-OCO-ICZ **27**	1.90	0.01	0.08	
1,3-diphenylurea **20**	1.82	0.01	0.08	
Receptor **7**	1.81	0.01	0.08	
Receptor **6**	1.76	0.01	0.08	
Indolocarbazole 33	**1.69**	0.01	0.08	
Receptor **3**	1.67	0.01	0.08	
Receptor **5**	1.59	0.01	0.08	
Receptor **42**	1.50	0.01	0.08	
Receptor **9**	1.48	0.01	0.08	
Receptor **8**	0.84	0.01	0.08	

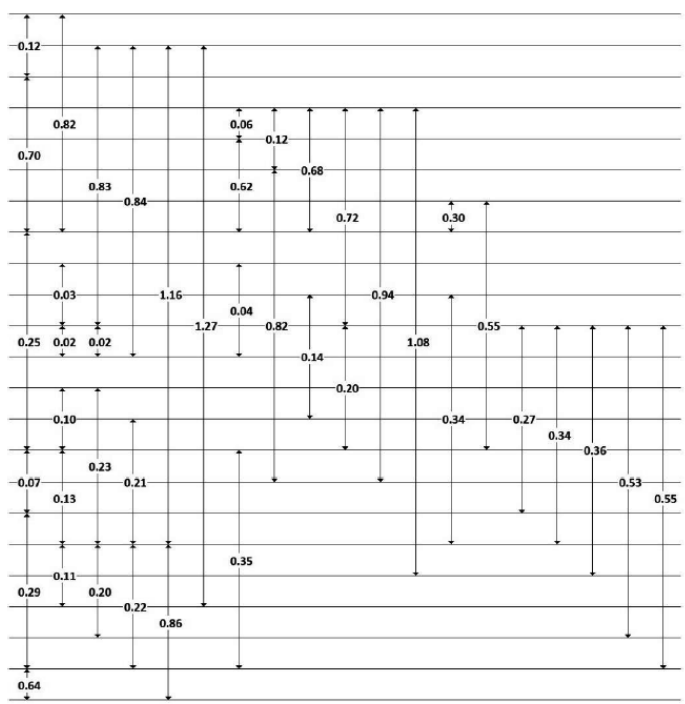

[a] All $\log K_{ass}$ values correspond to the Equation (1). Consistency standard deviation (s) of the scale is 0.002. [b] Standard uncertainties for comparing $\log K_{ass}$ values within the same scale. [c] Standard uncertainties for comparing $\log K_{ass}$ values between different scales or with those from other research groups.

Table 12. Scale of relative binding constants of benzoate anion in DMSO-d_6:H_2O (99.5%:0.5% m/m).[a]

Receptor number	log K_{ass}	u_c[b]	u_c[c]	Δ log K_{ass}
Receptor 12	4.32	0.01	0.04	
Receptor 13	4.20	0.01	0.04	
1,3-dicarbazolylurea 15	4.15	0.01	0.04	
1,3-diindolylurea 16	4.08	0.01	0.04	
Receptor 14	4.03	0.01	0.04	
Receptor 10	3.99	0.01	0.04	
Receptor 11	3.95	0.01	0.04	
3,4,4-Cl_3-diphenylurea 21	3.60	0.01	0.04	
Receptor 41	3.48	0.01	0.04	
Receptor 18	3.41	0.01	0.04	
Receptor 7	3.35	0.01	0.04	
Receptor 43	3.34	0.01	0.04	
Receptor 3	3.33	0.01	0.04	
4-NO_2-ICZ 28	3.29	0.01	0.04	
2,7-$(BuOCO)_2$-ICZ 35	3.25	0.01	0.04	
Receptor 6	3.25	0.01	0.04	
2,9-$(BuOCO)_2$-ICZ 34	3.24	0.01	0.04	
4,7-$(BuOCO)_2$-ICZ 36	3.24	0.01	0.04	
Receptor 1	3.18	0.01	0.04	
Receptor 17	3.15	0.01	0.04	
2,7-Cl_2-ICZ 37	3.14	0.01	0.04	
Receptor 4	3.07	0.02	0.04	
Receptor 2	3.06	0.01	0.04	
CH_3-CO-CH_2-OCO-ICZ 27	3.05	0.01	0.04	
Receptor 9	3.03	0.01	0.04	
2-(BuOCO)-ICZ 26	3.02	0.01	0.04	
Receptor 32	3.01	0.01	0.04	
Receptor 39	3.00	0.01	0.04	
Receptor 40	2.99	0.01	0.04	
Receptor 5	2.97	0.01	0.04	
1,3-diphenylurea 20	2.89	0.01	0.04	
Receptor 31	2.83	0.01	0.04	
Receptor 19	2.81	0.01	0.04	
Indolocarbazole 33	2.77	0.01	0.04	
Receptor 30	2.70	0.01	0.04	
2,9-$(MeO)_2$-ICZ 38	2.70	0.01	0.04	
Receptor 42	2.56	0.01	0.04	
1-Cl-ICZ 29	2.55	0.01	0.04	
Receptor 22	2.51	0.01	0.04	
Receptor 25	2.38	0.01	0.04	
Receptor 8	2.34	0.01	0.04	
Receptor 23	2.18	0.01	0.04	
Receptor 24	2.15	0.01	0.04	

[a] All $\log K_{ass}$ values correspond to the Equation (1). Consistency standard deviation (s) of the scale is 0.010. [b] Standard uncertainties for comparing $\log K_{ass}$ values within the same scale. [c] Standard uncertainties for comparing $\log K_{ass}$ values between different scales or with those from other research groups.

At this point, hundreds of $\Delta \log K_{ass}$ values were measured that are directly comparable. Among the binding patterns, there were more prominent, visible differences, and many affinities that differed very little. The question was, can the studied receptors distinguish the selected carboxylates?

3.4. Principal component analysis of the binding data

Principal component analysis (PCA) was performed to evaluate, summarise, and comparatively visualise the binding trends of the 11 selected carboxylate anions (Figure 12). The data matrix of absolute $\log K_{ass}$ values was first transformed into relative $\log K_{ass}$ values (relative to Indolocarbazole **33**). To account for the uncertainties in $\log K_{ass}$ measurements, ten $\log K_{ass}$ values were created for each receptor-anion combination by adding randomised arbitrary values within the uncertainty limits, i.e., -0.02…+0.02 $\log K_{ass}$ units (as the highest u_c value from Tables 5–12 is 0.02). The resulting data matrix comprised 110 rows (11 anions, ten points for each) and 22 columns (22 receptors depicted in Figure 11).

Principal component analysis was performed with the R freeware program package (ver. X64 3.2.0). Scaled data were used in the PCA analysis.

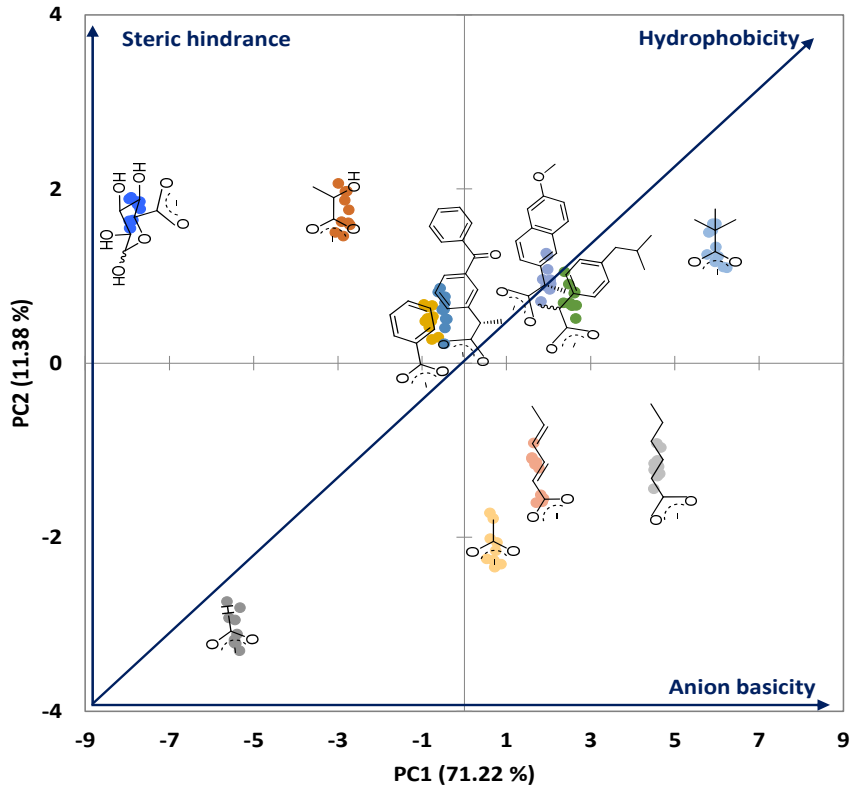

Figure 12. PCA plot of binding constant data (relative to Indolocarbazole **33**). The scatter of the dots visualises the uncertainties of the experimental $\log K_{ass}$ values.

Analysing the resulting PCA plot reveals that the anions are distributed based on three main properties: basicity, hydrophobicity, and steric hindrance. The corresponding property is strengthened in the direction of the influence arrows of the mentioned properties (see Figure 12). Bulky anions with hydrophobic moieties are directionally concentrated in the upper right quadrant, and small hydrophilic anion formate is located in the bottom left quadrant. Anions with hydrophobic moieties but without steric hindrance around the carboxylate group are located in the lower right quadrant. Finally, anions with hydrophilic moieties and some steric hindrance are in the upper left quadrant.

The first principal component (PC1) describes 71% of the variance. It represents the basicity of the anions mainly and, to some extent, their hydrophobicity. The basicity of the anions dominates the binding. However, the four hydrophobic anions located close to each other – benzoate, ketoprofen, naproxen, and ibuprofen – are arranged in the graph precisely in the order of hydrophobicity ($\log P_{\mathrm{o-w}}$ values are 1.87, 3.12, 3.34, 4.5, respectively; see Figure 2). Also, the graph separates sorbate and hexanoate more distinctively than would be expected from their similar pK_{a} values (calculated pK_{a} values in DMSO are 12.4 and 12.5, respectively; see Figure 2). The second principal component (PC2) describes 11% of the variance and expresses mainly the steric hindrance of the anionic centre. Anions with less steric hindrance (formate, acetate, sorbate, hexanoate) are located in the lower half of the PCA plot. Anions that are hindered from binding due to their substituents near the carboxylate group are located in the upper half of the plot. It is evident from the graph that the larger glucuronate anion is distinguishable from the smaller formate anion with less steric hindrance, although their basicities are not too different.

To conclude the structure-affinity study, it can be said that the selected synthetic HBD receptors can distinguish carboxylates with different structures. With similar basicity of carboxylates, the binding order is determined by the structural (hydrophilicity, substitution at the α-carbon, etc.) and steric properties of the anion and receptor. At the end of Publication II, it was obvious that instead of designing one selective HBD receptor for a specific carboxylate anion, further work could be related to sensor arrays and fingerprinting carboxylates from mixtures. This is because none of the receptors used in the work is even close to selectively binding one specific anion. Still, when several receptors are used together, clear patterns are formed, with the help of which it is possible to distinguish carboxylates from each other.

From this juncture, I oriented my study towards practical applications. The results below describe a self-made electrode in which one of the receptors used in the structure-affinity study is incorporated into the electrode's ion-selective membrane. Anticipating future research, one avenue involves integrating various investigated receptors into electrode membranes. This approach aims to create sensor arrays for carboxylate fingerprinting in mixtures.

The results described up to now have shown that I can accurately measure the binding affinities of receptors towards carboxylates in solution. The results of the structure-affinity studies unveil that receptor **13** is the strongest binder for five monocarboxylates out of 11 in DMSO:H_2O (99.5%:0.5% m/m). Thus, this receptor was selected as the ionophore for constructing SC-ISEs at Åbo Akademi University (Finland), described in Sections 2.5, 3.5, and Publication III.

3.5. Properties of prepared acetate-selective electrodes

Neutral Ionophore **13** is a profoundly lipophilic molecule ($\log P_{o-w}$ 13.9 ± 1.0[123]) capable of forming ion-to-ionophore complexes. A successful ionophore is highly lipophilic to ensure it remains in the membrane phase and does not leach into the sample. The Ionophore **13** has four tert-butyl groups and hydrophobic tails containing naphthyl groups. Due to its high lipophilicity, it is well soluble in the plasticised polymeric matrix, and no crystalline precipitates or aggregation of the membrane components were detected for the SC-ISEs.

Acetate was chosen as the primary ion for all the experiments. While ibuprofen or pivalate could have been viable choices based on the binding study, their high lipophilicity posed a significant challenge. Using these more lipophilic anions would have made it difficult to demonstrate that the binding observed was due to specific molecular recognition rather than a general preference for lipophilic anions over less lipophilic ones.

The **potentiometric response** curve of a representative acetate-ISE during serial dilutions is shown in Figure 13. In a 0.1 M potassium acetate starting solution, the acetate ion activity is $10^{-1.10}$, and the average potential value for the five acetate-ISEs was 106.1 mV ± 2.8 mV. Then, by serial dilutions, the acetate activity in the measured solution was reduced to $10^{-7.50}$. During each dilution step, the acetate ISEs were temporarily removed from the calibration solution (in air), with no signal in the potentiometric response curve at these time points. When the new dilution was ready, the electrodes were immersed back into the solution, and the average estimated response time in the activity range of $10^{-4.50}$–$10^{-1.10}$ was 105 s ± 55 s. The response time includes the time needed for mixing the solutions after each dilution step (no stirring), so it should be considered an approximate upper limit of the response time.

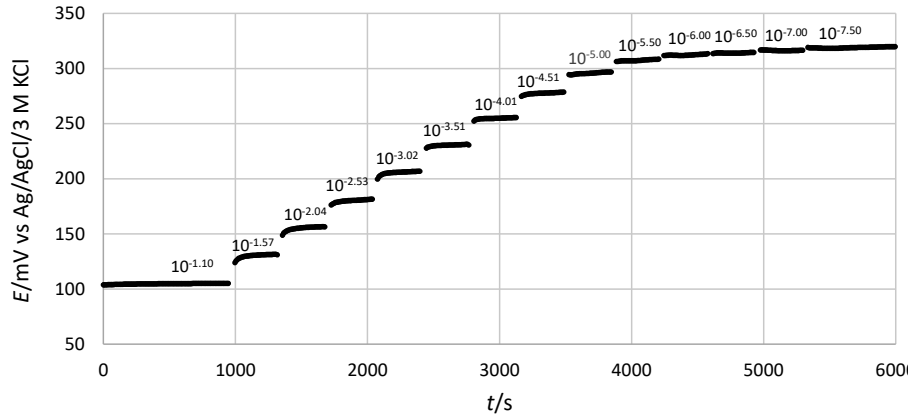

Figure 13. Potentiometric response curves of representative acetate-ISEs during sequential dilutions (acetate activities shown in the graph).

Prepared electrodes gave sub-Nernstian responses to acetate (Table 13 and Figure 14). While Nernstian behaviour is desirable, sub-Nernstian responses are common in practice and explained by assuming competitive reactions. It can be inferred that the coextraction of cations contributed to a partial breakdown of the membrane's permselectivity.

Table 13. Response characteristics for acetate-ISEs and ionophore-free control electrodes.

Electrode type	N[a]	Slope (mV/dec)[b]	$\log a_{LLL}$ [c]	$\log a_{LOD}$ [d]	R^2
Acetate-ISEs in water	5	-52.1 ± 0.4	-4.01	-5.00 ± 0.02	0.999
Control electrodes	4	-49.4 ± 0.9	-4.01	-4.15 ± 0.04	0.996
Acetate-ISEs in buffer	5	-53.9 ± 1.1	-3.02	-3.32 ± 0.04	0.997

[a] Number of electrodes. [b] Average ± standard deviation. [c] Lower limit of linearity. [d] Limit of detection ± standard deviation.

The calibration curves of acetate-ISEs and ionophore-free control electrodes are shown in Figure 14.

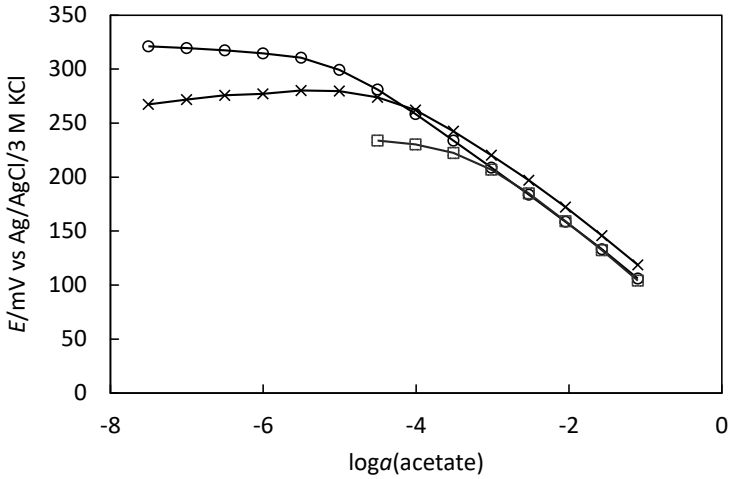

Figure 14. Calibration curves of (○) acetate-ISEs and (x) ionophore-free control electrodes measured in deionised water (without any background electrolyte or buffer). Calibration curve of (□) acetate-ISEs obtained using a HEPES-NaOH buffer at pH 7.0. The standard deviations of all potential readings were ≤ 3.5 mV.

The calibration curve obtained for acetate-ISEs in the HEPES-NaOH buffer at pH 7.0 shows a slope of -53.9 ± 1.1 mV, similar to the slope observed in measurements made in deionised water (Figure 14). However, there's a notable difference in the linear range. The linear range is significantly narrower in the HEPES-NaOH buffer at pH 7.0 (see Table 13). One potential cause could be the extraction of interfering species from the buffer into the membrane, thereby altering the acetate ion activity in the membrane phase.

Using ISEs in water without adding a pH buffer is desirable because it simplifies the analytical procedure. *In-situ* measurements, where samples are measured directly in their natural environment, adding a buffer may not be feasible. Since the HEPES buffer was found to reduce the working range of the acetate-ISEs, the decision was made to study all the prepared electrodes in unbuffered media.

Impedance measurements were performed on acetate-ISEs immersed in 0.1 M potassium acetate solution. The results obtained for five identical acetate-ISEs are shown in Figure 15.

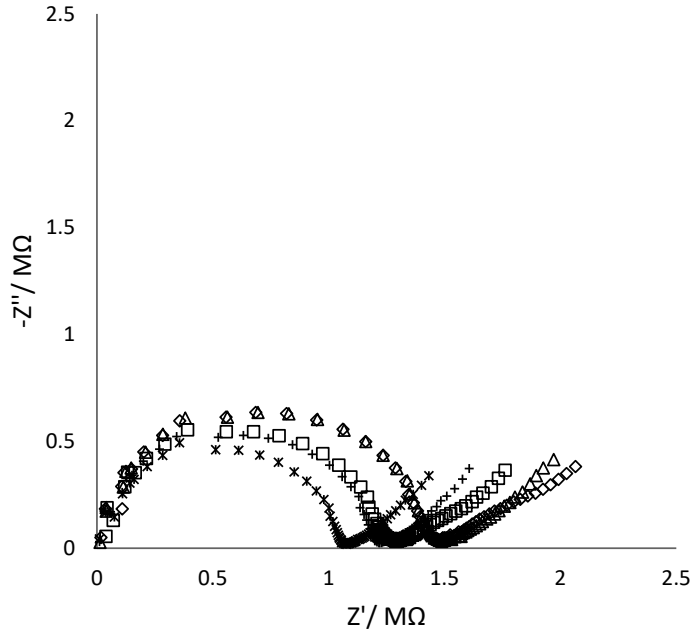

Figure 15. Electrochemical impedance spectra for five identical acetate-ISEs obtained in 0.1 M potassium acetate solution. The frequency range is from 10 mHz to 100 kHz. The five different symbols denote five replicate electrodes.

Initially, a high-frequency semicircle was observed, which can be attributed to the bulk resistance in parallel with the geometric capacitance of the ISM. Following this, a low-frequency diffusion line emerges, associated with ions' diffusion within the ISM and the PEDOT layers. Notably, variations in the bulk resistance values (ranging from 1 to 1.5 MΩ) suggest slight differences in the ISM thickness across individual electrodes. However, these thickness variations are unlikely to significantly impact the potentiometric response of the ion-selective electrodes (ISEs). Notably, the absence of a large semicircle or capacitive line at the lowest frequencies indicates that the PEDOT layer effectively mediates the ion-to-electron transduction process[97], which possesses a sufficiently high redox capacitance.

The results of the **pH effect** study are depicted in Figure 16. At the beginning of titration, where acetic acid is not fully dissociated, the potential becomes more negative due to the step-by-step deprotonation of acetic acid, i.e., an increase in acetate ion concentration. After that, between pH 6.0 and 8.0, there is minimal potential change. However, above pH 8.0, the somewhat alkaline solution leads to a minor potential change towards more negative values, possibly due to interference from OH^- ions.

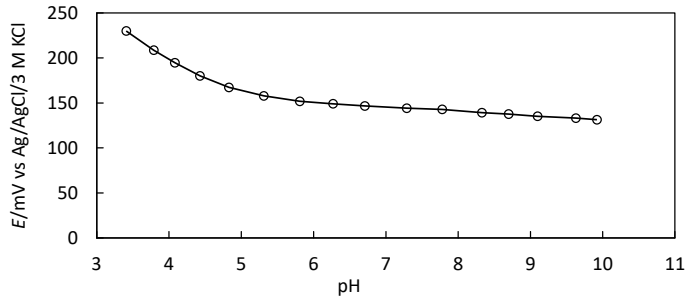

Figure 16. The pH effect on the potential response of acetate-ISEs in an acetic acid solution with a constant concentration of 0.01 M.

The **selectivity coefficient** ($\log K^{\mathrm{pot}}_{\mathrm{acetate,j}}$) for each interfering ion j was determined using the separate solution method.[80] The logarithms of selectivity coefficients calculated with respect to acetate anion for both the ISEs with membrane containing the Ionophore **13** and the ISEs with control (ionophore-free) membrane are shown in Table 14 and illustrated in Figure 17.

Table 14. The selectivity coefficients[a] of various interfering anions for acetate-ISEs and control electrodes.

ion j	$\log K^{\mathrm{pot}}_{\mathrm{acetate,j}}$				$\Delta \log K^{\mathrm{pot}}_{\mathrm{acetate,j}}$
	Acetate-ISE[b]		Control[b]		
ibuprofen	4.40	± 0.07	5.25	± 0.04	-0.85
naproxen	4.25	± 0.06	5.00	± 0.04	-0.75
benzoate	2.30	± 0.05	3.06	± 0.04	-0.76
SCN^-	1.24	± 0.05	6.48	± 0.07	-5.24
I^-	0.87	± 0.03	5.73	± 0.05	-4.86
NO_3^-	0.56	± 0.04	4.33	± 0.04	-3.77
Br^-	0.10	± 0.03	3.31	± 0.03	-3.21
$HCOO^-$	-0.15	± 0.05	0.35	± 0.01	-0.50
HCO_3^-	-0.16	± 0.03	-0.12	± 0.03	-0.04
Cl^-	-0.61	± 0.02	1.35	± 0.01	-1.96
SO_4^{2-}	-0.87	± 0.14	-0.40	± 0.03	-0.47
HPO_4^{2-}	-1.63	± 0.16	-0.74	± 0.04	-0.89
F^-	-1.94	± 0.09	-1.21	± 0.06	-0.73

[a] Selectivity coefficients measured with the separate solution method at 1×10^{-2} M sodium salts of analytes in deionised water. [b] Averages and standard deviations for five ISEs and four control electrodes.

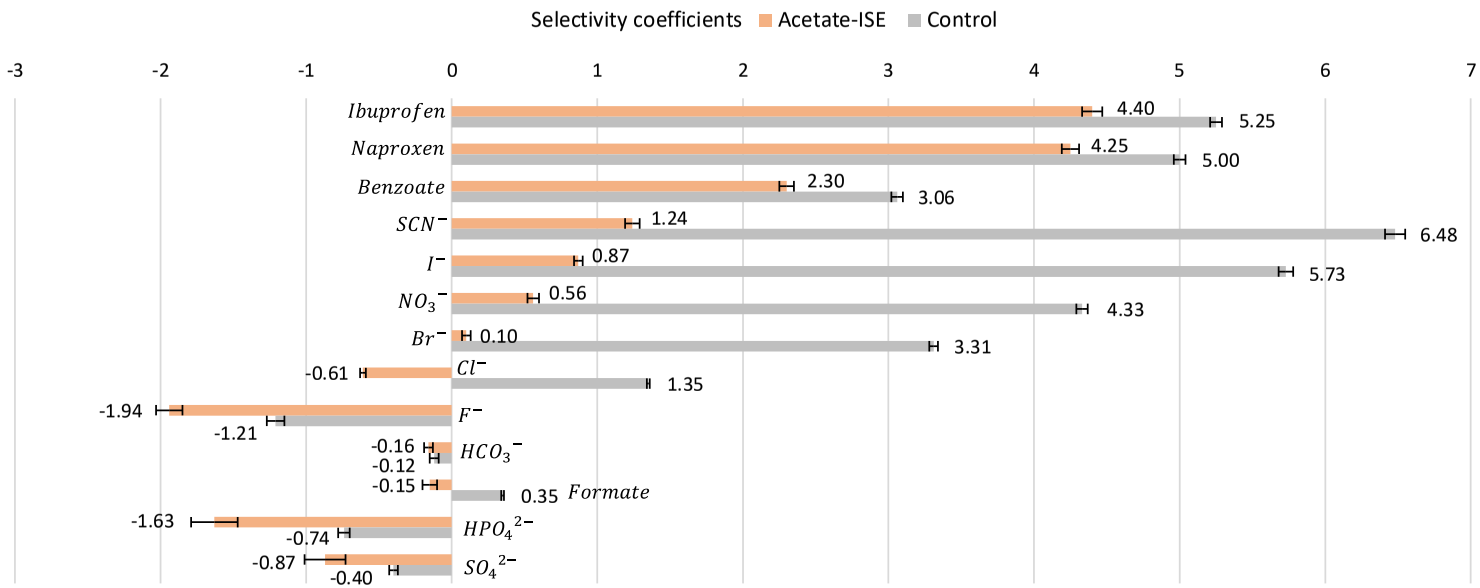

Figure 17. Comparison of selectivity coefficients: acetate-ISE vs control membrane. Anions are ranked by lipophilicity based on the Hofmeister series (lipophilicity increases from bottom to top). The average selectivity coefficients are provided numerically. Error bars describe the standard deviations.

The ionophore-free control membrane also exhibits a response to anions. However, since the ionophore does not complex these anions, a non-specific Hofmeister[124] selectivity behaviour was expected. The selectivity of ionophore-free control membranes followed the anticipated pattern, which aligns with the lipophilicity of the anions. Consequently, highly hydrophobic anions, such as SCN^- and I^-, exhibit the highest selectivity coefficients against acetate. Additionally, the response to Cl^- was significantly stronger in the control membranes than the response to acetate. Incorporating the Ionophore **13** into the membrane significantly alters the selectivity pattern, resulting in a distinctly different response order for the carboxylate anions. For example, hydrophobic carboxylates such as naproxen and ibuprofen exhibit the highest selectivity coefficients against acetate. Furthermore, the membrane containing Ionophore exhibits higher selectivity towards small carboxylates (such as acetate and formate) and HCO_3^- than to Cl^-. Remarkably, the ionophore-based electrode exhibits relatively high selectivity for bicarbonate, which is an essential analyte in clinical analysis[83]. Notably, the selectivity coefficients obtained for ISEs and control membranes vary in magnitude. It is noticeable that in the case of ionophore-containing membranes, the interferences from anions that are very hydrophobic but do not have a carboxylate group for binding with the ionophore, such as SCN^-, I^-, NO_3^- and Br^-, have become relatively small. The selectivity coefficients of SCN^-, I^-, NO_3^- and Br^- decrease by 3–5 orders of magnitude when adding ionophore to the membrane, and the selectivity coefficients of very hydrophilic anions such as F^-, HPO_4^{2-}, and SO_4^{2-} are significantly lower than in case of the ionophore-free membrane (Table 14 and Figure 17). These results show that the selectivity of an ionophore-containing membrane is, to a large extent, determined by the ionophore.

The selectivity pattern observed in electrode prototypes differs from those predicted by single-phase NMR measurements because classical binding affinity titrations overlook critical factors in receptor-anion complexation within a hydrophobic polymeric membrane. These factors include molecular lipophilicity, interfering substances, cation influence, and variations in water content.

Although the characteristics of the fabricated acetate-selective electrode prototypes have room for improvement (such as expanding the linear range, minimising the sub-Nernstian deviation toward the Nernstian behaviour, and enhancing the limit of detection), the integration of the synthetic receptor into the polymeric membrane was successful and enabled achieving functional selectivity.

SUMMARY

Carboxylate anions are pivotal in environmental, biological, and industrial contexts, necessitating their accurate determination. While various analytical methods such as chromatography, mass spectrometry, and fluorescence techniques exist, there is a growing need for synthetic receptors that can serve as carboxylate sensing ionophores in ion-selective electrode membranes. Potentiometric sensors, particularly solid-contact ion-selective electrodes, offer practical advantages due to their portability, excellent sensitivity, low energy consumption, and ease of maintenance.

This dissertation presents a systematic comparison of binding affinities of acyclic synthetic receptors towards different monocarboxylates and demonstrates the application of one such receptor as an ionophore in self-constructed solid-contact ion-selective electrodes. The binding abilities of different receptors were quantitatively characterised in terms of binding affinities (expressed as $\log K_{\mathrm{ass}}$ values) using the relative NMR-based measurement method. This titration method facilitated the creation of comprehensive binding-structure-relationship plots, allowing for direct comparison of the receptors' affinities.

Initially, the binding of small synthetic receptor molecules containing indolocarbazole, carbazole, indole, urea, thiourea, and amide moieties was studied with pivalate, acetate, benzoate, and lactate. Key findings include: (a) binding is primarily driven by hydrogen-bonding interactions and the basicity of the carboxylate anion, (b) tetradentate systems with four well-placed NH centres, such as bis-indolyl or bis-carbazolyl ureas, provide the most effective binding configuration, (c) ortho-phenylenediamine-bis-urea receptors form weaker complexes due to suboptimal spatial arrangement of NH groups, (d) tridentate carbazole-based receptors are less effective due to asymmetrical binding and (e) bidentate diphenylurea and indolocarbazole centres exhibit similar binding efficiencies due to balance between lower hydrogen-bond donicity and a more favourable bond angle for hydrogen-bond formation in diphenylurea. The main factors influencing binding efficiency are the number of hydrogen-bond donor sites, their donicity, their mutual positioning, and potential steric hindrance around the binding sites.

Further studies modified the receptor selection and expanded the number of carboxylates tested, resulting in the construction of eight binding affinity ladders and the examination of differential binding for 11 carboxylates (formate, acetate, pivalate, lactate, naproxen, ibuprofen, ketoprofen, glucuronate, hexanoate, sorbate, and benzoate). Findings revealed that: (a) anion basicity remains a crucial factor, but structural and steric factors also influence binding, (b) the carbon chain length plays a modest role in anion differentiation, (c) the binding affinity of acetate and pivalate is significantly affected by the binding site dimensions supporting solvophobic effects, and (d) carboxylates with different structures can be distinguished using a differential sensing paradigm.

Finally, a 1,3-bis(carbazolyl)urea derivative was utilised as a neutral hydrogen-bonding ionophore to construct solid-contact acetate-selective electrode proto-

types. These electrodes exhibited linearity over the activity range of $10^{-4.50}$–$10^{-1.10}$ with a sub-Nernstian slope of 51.3 mV per decade and a detection limit of $10^{-5.00}$. The prototypes demonstrated a selectivity pattern that deviated from the Hofmeister series, showing higher selectivity for small carboxylates (acetate, formate) and bicarbonate over chloride. Additionally, the ionophore-based electrodes showed reduced interference from hydrophobic inorganic anions such as SCN^-, I^-, NO_3^-, and Br^- compared to electrodes using an ion-exchanger without the ionophore. However, further advancements in the design and synthesis of synthetic anion receptors are necessary to achieve even higher levels of selectivity and sensitivity.

REFERENCES

(1) Pedersen, C. J. Cyclic Polyethers and Their Complexes with Metal Salts. *J. Am. Chem. Soc.* **1967**, *89* (26), 7017–7036. https://doi.org/10.1021/ja01002a035.

(2) Lehn, J. M. Cryptates: Inclusion Complexes of Macropolycyclic Receptor Molecules. *Pure Appl. Chem.* **1978**, *50* (9–10), 871–892. https://doi.org/10.1351/pac197850090871.

(3) Cram, D. J.; Kaneda, T.; Helgeson, R. C.; Lein, G. M. Spherands-Ligands Whose Binding of Cations Relieves Enforced Electron-Electron Repulsions. *J. Am. Chem. Soc.* **1979**, *101* (22), 6752–6754.

(4) Lehn, J.-M. Supramolecular Chemistry—Scope and Perspectives Molecules, Supermolecules, and Molecular Devices (Nobel Lecture). *Angew. Chem. Int. Ed. Engl.* **1988**, *27* (1), 89–112. https://doi.org/10.1002/anie.198800891.

(5) Cram, D. J.; Cram, J. M. Host-Guest Chemistry. *Science* **1974**, *183* (4127), 803–809.

(6) Busschaert, N.; Caltagirone, C.; Van Rossom, W.; Gale, P. A. Applications of Supramolecular Anion Recognition. *Chem. Rev.* **2015**, *115* (15), 8038–8155. https://doi.org/10.1021/acs.chemrev.5b00099.

(7) T. Williams, G.; E. Haynes, C. J.; Fares, M.; Caltagirone, C.; R. Hiscock, J.; A. Gale, P. Advances in Applied Supramolecular Technologies. *Chem. Soc. Rev.* **2021**, *50* (4), 2737–2763. https://doi.org/10.1039/D0CS00948B.

(8) Anslyn, E. V. Supramolecular Analytical Chemistry. *J. Org. Chem.* **2007**, *72* (3), 687–699. https://doi.org/10.1021/jo0617971.

(9) Steed, J. W.; Turner, D. R.; Wallace, K. J. Core Concepts in Supramolecular Chemistry and Nanochemistry. 321.

(10) Biedermann, F.; Schneider, H.-J. Experimental Binding Energies in Supramolecular Complexes. *Chem. Rev.* **2016**, *116* (9), 5216–5300. https://doi.org/10.1021/acs.chemrev.5b00583.

(11) Bonal, C.; Israëli, Y.; Morel, J.-P.; Morel-Desrosiers, N. Binding of Inorganic and Organic Cations by p -Sulfonatocalix[4]Arene in Water : A Thermodynamic Study. *J. Chem. Soc. Perkin Trans. 2* **2001**, *0* (7), 1075–1078. https://doi.org/10.1039/B102038M.

(12) Kadam, S. A.; Martin, K.; Haav, K.; Toom, L.; Mayeux, C.; Pung, A.; Gale, P. A.; Hiscock, J. R.; Brooks, S. J.; Kirby, I. L.; Busschaert, N.; Leito, I. Towards the Discrimination of Carboxylates by Hydrogen-Bond Donor Anion Receptors. *Chem. – Eur. J.* **2015**, *21* (13), 5145–5160. https://doi.org/10.1002/chem.201405858.

(13) Inokuchi, F.; Miyahara, Y.; Inazu, T.; Shinkai, S. "Cation-π Interactions" Detected by Mass Spectrometry; Selective Recognition of Alkali Metal Cations by a π-Basic Molecular Cavity. *Angew. Chem. Int. Ed. Engl.* **1995**, *34* (12), 1364–1366. https://doi.org/10.1002/anie.199513641.

(14) Hunter, C. A.; Sanders, J. K. M. The Nature of .Pi.-.Pi. Interactions. *J. Am. Chem. Soc.* **1990**, *112* (14), 5525–5534. https://doi.org/10.1021/ja00170a016.

(15) Biedermann, F.; Nau, W. M.; Schneider, H.-J. The Hydrophobic Effect Revisited-Studies with Supramolecular Complexes Imply High-Energy Water as a Noncovalent Driving Force. *Angew. Chem. Int. Ed.* **2014**, *53* (42), 11158–11171. https://doi.org/10.1002/anie.201310958.

(16) Snyder, P. W.; Lockett, M. R.; Moustakas, D. T.; Whitesides, G. M. Is It the Shape of the Cavity, or the Shape of the Water in the Cavity? *Eur. Phys. J. Spec. Top.* **2014**, *223* (5), 853–891. https://doi.org/10.1140/epjst/e2013-01818-y.

(17) Schneider, H.-J. Binding Mechanisms in Supramolecular Complexes. *Angew. Chem. Int. Ed.* **2009**, *48* (22), 3924–3977. https://doi.org/10.1002/anie.200802947.
(18) H. Hartley, J.; D. James, T.; J. Ward, C. Synthetic Receptors. *J. Chem. Soc. Perkin 1* **2000**, *0* (19), 3155–3184. https://doi.org/10.1039/A909641H.
(19) Park, C. H.; Simmons, H. E. Macrobicyclic Amines. III. Encapsulation of Halide Ions by in,in-1,(k + 2)-Diazabicyclo[k.l.m.]Alkane Ammonium Ions. *J. Am. Chem. Soc.* **1968**, *90* (9), 2431–2432. https://doi.org/10.1021/ja01011a047.
(20) Graf, E.; Lehn, J. M. Anion Cryptates: Highly Stable and Selective Macrotricyclic Anion Inclusion Complexes. 3.
(21) Gokel, G. W.; Barbour, L. *Comprehensive Supramolecular Chemistry II*; Elsevier, 2017.
(22) Schmidtchen, F. P. Artificial Host Molecules for the Sensing of Anions. In *Anion Sensing* Stibor, I., Ed.; Topics in Current Chemistry; Springer: Berlin, Heidelberg, 2005; pp 1–29. https://doi.org/10.1007/b101160.
(23) Sessler, J. L.; Gale, P. A.; Cho, W.-S. *Anion Receptor Chemistry*; Royal Society of Chemistry, 2006.
(24) Bowman-James, K.; Bianchi, A.; García-Espana, E. *Anion Coordination Chemistry*; John Wiley & Sons, 2012.
(25) Beer, P. D.; Gale, P. A. Anion Recognition and Sensing: The State of the Art and Future Perspectives. *Angew. Chem. Int. Ed.* **2001**, *40* (3), 486–516. https://doi.org/10.1002/1521-3773(20010202)40:3<486::AID-ANIE486>3.0.CO;2-P.
(26) Janata, J. *Principles of Chemical Sensors*; Springer Science & Business Media, 2010.
(27) Schneider, H.-J.; K. Yatsimirsky, A. Selectivity in Supramolecular Host –Guest Complexes. *Chem. Soc. Rev.* **2008**, *37* (2), 263–277. https://doi.org/10.1039/B612543N.
(28) Gale, P. A.; Howe, E. N. W.; Wu, X. Anion Receptor Chemistry. *Chem* **2016**, *1* (3), 351–422. https://doi.org/10.1016/j.chempr.2016.08.004.
(29) Prankerd, R. J. Critical Compilation of pKa Values for Pharmaceutical Substances. In *Profiles of Drug Substances, Excipients and Related Methodology*; Academic Press, 2007; Vol. 33, pp 1–33. https://doi.org/10.1016/S0099-5428(07)33001-3.
(30) Kelly, C. P.; Cramer, C. J.; Truhlar, D. G. Aqueous Solvation Free Energies of Ions and Ion-Water Clusters Based on an Accurate Value for the Absolute Aqueous Solvation Free Energy of the Proton. *J. Phys. Chem. B* **2006**, *110* (32), 16066–16081. https://doi.org/10.1021/jp063552y.
(31) Wang, L.-Y.; Zhang, Y.-H.; Zhao, L.-J. Raman Spectroscopic Studies on Single Supersaturated Droplets of Sodium and Magnesium Acetate. *J. Phys. Chem. A* **2005**, *109* (4), 609–614. https://doi.org/10.1021/jp0458811.
(32) Perrin, D. D.; Dempsey, B.; Serjeant, E. P. *PKa Prediction for Organic Acids and Bases*; Chapman and Hall: London, 1981.
(33) Li, X.; Cooper, M. A. Measurement of Drug Lipophilicity and pKa Using Acoustics. *Anal. Chem.* **2012**, *84* (6), 2609–2613. https://doi.org/10.1021/ac300087z.
(34) Meloun, M.; Bordovská, S.; Galla, L. The Thermodynamic Dissociation Constants of Four Non-Steroidal Anti-Inflammatory Drugs by the Least-Squares Nonlinear Regression of Multiwavelength Spectrophotometric pH-Titration Data. *J. Pharm. Biomed. Anal.* **2007**, *45* (4), 552–564. https://doi.org/10.1016/j.jpba.2007.07.029.
(35) Fini, A.; De Maria, P.; Guarnieri, A.; Varoli, L. Acidity Constants of Sparingly Water-Soluble Drugs from Potentiometric Determinations in Aqueous Dimethyl Sulfoxide. *J. Pharm. Sci.* **1987**, *76* (1), 48–52. https://doi.org/10.1002/jps.2600760114.

(36) Kohn, R.; Kovac, P. Dissociation Constants of D-Galacturonic and D-Glucuronic Acid and Their O-Methyl Derivatives. *Chem Zvesti* **1978**, *32*, 478–485.
(37) Lück, E.; Jager, M.; Raczek, N. Sorbic Acid. In *Ullmann's Encyclopedia of Industrial Chemistry*; John Wiley & Sons, Ltd, 2000. https://doi.org/10.1002/14356007.a24_507.
(38) Petrov, S. M.; Umanskii, Y. I.; Mullin, I. F.; Tertichnyi, Z. F. The Experimental pKa Values of Carboxylic Acids in DMSO. *Russ J Phys Chem* **1973**, No. 47, 363, 647.
(39) Bordwell, F. G. Equilibrium Acidities in Dimethyl Sulfoxide Solution. *Acc. Chem. Res.* **1988**, *21* (12), 456–463. https://doi.org/10.1021/ar00156a004.
(40) Koppel, I. A.; Koppel, J. B.; Pihl, V. O. Acidity of Some Carboxylic-Acids in DMSO. *Org. React.* **1988**, *25 (1)*, 77–101.
(41) Hansch, C.; Leo, A.; Hoekman, D. H. *Exploring QSAR.: Hydrophobic, Electronic, and Steric Constants*; American Chemical Society, 1995.
(42) White, D. P.; Anthony, J. C.; Oyefeso, A. O. Computational Measurement of Steric Effects: The Size of Organic Substituents Computed by Ligand Repulsive Energies. *J. Org. Chem.* **1999**, *64* (21), 7707–7716. https://doi.org/10.1021/jo982405w.
(43) Pike, S. J.; Hutchinson, J. J.; Hunter, C. A. H-Bond Acceptor Parameters for Anions. *J. Am. Chem. Soc.* **2017**, *139* (19), 6700–6706. https://doi.org/10.1021/jacs.7b02008.
(44) Lovley, D. R. Bug Juice: Harvesting Electricity with Microorganisms. *Nat. Rev. Microbiol.* **2006**, *4* (7), 497–508. https://doi.org/10.1038/nrmicro1442.
(45) Del Olmo, A.; Calzada, J.; Nuñez, M. Benzoic Acid and Its Derivatives as Naturally Occurring Compounds in Foods and as Additives: Uses, Exposure, and Controversy. *Crit. Rev. Food Sci. Nutr.* **2017**, *57* (14), 3084–3103. https://doi.org/10.1080/10408398.2015.1087964.
(46) Dehghan, P.; Mohammadi, A.; Mohammadzadeh-Aghdash, H.; Ezzati Nazhad Dolatabadi, J. Pharmacokinetic and Toxicological Aspects of Potassium Sorbate Food Additive and Its Constituents. *Trends Food Sci. Technol.* **2018**, *80*, 123–130. https://doi.org/10.1016/j.tifs.2018.07.012.
(47) Hashim, N. H.; Khan, S. J. Enantioselective Analysis of Ibuprofen, Ketoprofen and Naproxen in Wastewater and Environmental Water Samples. *J. Chromatogr. A* **2011**, *1218* (29), 4746–4754. https://doi.org/10.1016/j.chroma.2011.05.046.
(48) Chong, A. Q.; Lau, S. W.; Chin, N. L.; Talib, R. A.; Basha, R. K. Fermented Beverage Benefits: A Comprehensive Review and Comparison of Kombucha and Kefir Microbiome. *Microorganisms* **2023**, *11* (5), 1344. https://doi.org/10.3390/microorganisms11051344.
(49) Michalski, R.; Pecyna-Utylska, P.; Kernert, J. Ion Chromatography and Related Techniques in Carboxylic Acids Analysis. *Crit. Rev. Anal. Chem.* **2021**, *51* (6), 549–564. https://doi.org/10.1080/10408347.2020.1750340.
(50) Ulatowski, F.; Jurczak, J. Chiral Recognition of Carboxylates - Receptors, Analytical Tools, and More. *Asian J. Org. Chem.* **2016**. https://doi.org/10.1002/ajoc.201600093.
(51) Fujiwara, T.; Inoue, R.; Ohtawa, T.; Tsunoda, M. Liquid-Chromatographic Methods for Carboxylic Acids in Biological Samples. *Molecules* **2020**, *25* (21), 4883. https://doi.org/10.3390/molecules25214883.
(52) Ren, L.; Meng, M.; Wang, P.; Xu, Z.; Eremin, S. A.; Zhao, J.; Yin, Y.; Xi, R. Determination of Sodium Benzoate in Food Products by Fluorescence Polarization Immunoassay. *Talanta* **2014**, *121*, 136–143. https://doi.org/10.1016/j.talanta.2013.12.035.
(53) Sansone, F.; Baldini, L.; Casnati, A.; Lazzarotto, M.; Ugozzoli, F.; Ungaro, R. Biomimetic Macrocyclic Receptors for Carboxylate Anion Recognition Based on C-

Linked Peptidocalix[4]Arenes. *Proc. Natl. Acad. Sci.* **2002**, *99* (8), 4842–4847. https://doi.org/10.1073/pnas.062625499.
(54) Kang, S. O.; Powell, D.; Bowman-James, K. Anion Binding Motifs: Topicity and Charge in Amidocryptands. *J. Am. Chem. Soc.* **2005**, *127* (39), 13478–13479. https://doi.org/10.1021/ja054332l.
(55) Fan, E.; Van Arman, S. A.; Kincaid, S.; Hamilton, A. D. Molecular Recognition: Hydrogen-Bonding Receptors That Function in Highly Competitive Solvents. *J. Am. Chem. Soc.* **1993**, *115* (1), 369–370. https://doi.org/10.1021/ja00054a066.
(56) Brooks, S. J.; Gale, P. A.; Light, M. E. Carboxylate Complexation by 1,1′-(1,2-Phenylene)Bis(3-Phenylurea) in Solution and the Solid State. *Chem. Commun.* **2005**, No. 37, 4696–4698. https://doi.org/10.1039/B508144K.
(57) J. Brooks, S.; R. Edwards, P.; A. Gale, P.; E. Light, M. Carboxylate Complexation by a Family of Easy-to-Make Ortho -Phenylenediamine Based Bis-Ureas: Studies in Solution and the Solid State. *New J. Chem.* **2006**, *30* (1), 65–70. https://doi.org/10.1039/B511963D.
(58) Gale, P. A.; Anzenbacher Jr., P.; Sessler, J. L. Calixpyrroles II. *Coord. Chem. Rev.* **2001**, *222* (1), 57–102. https://doi.org/10.1016/S0010-8545(01)00346-0.
(59) Sessler, J. L.; An, D.; Cho, W.-S.; Lynch, V. Calix[2]Bipyrrole[2]Furan and Calix[2]Bipyrrole[2]Thiophene: New Pyrrolic Receptors Exhibiting a Preference for Carboxylate Anions. *J. Am. Chem. Soc.* **2003**, *125* (45), 13646–13647. https://doi.org/10.1021/ja038264j.
(60) Maeda, H.; Bando, Y. Recent Progress in Research on Anion-Responsive Pyrrole-Based π-Conjugated Acyclic Molecules. *Chem. Commun.* **2013**, *49* (39), 4100. https://doi.org/10.1039/c2cc35759c.
(61) Caltagirone, C.; Gale, P. A.; Hiscock, J. R.; Brooks, S. J.; Hursthouse, M. B.; Light, M. E. 1,3-Diindolylureas: High Affinity Dihydrogen Phosphate Receptors. *Chem. Commun.* **2008**, No. 26, 3007–3009. https://doi.org/10.1039/B806238B.
(62) A. Gale, P. Synthetic Indole, Carbazole, Biindole and Indolocarbazole-Based Receptors: Applications in Anion Complexation and Sensing. *Chem. Commun.* **2008**, *0* (38), 4525–4540. https://doi.org/10.1039/B809508F.
(63) Hiscock, J. R.; Caltagirone, C.; Light, M. E.; Hursthouse, M. B.; Gale, P. A. Fluorescent Carbazolylurea Anion Receptors. *Org. Biomol. Chem.* **2009**, *7* (9), 1781–1783. https://doi.org/10.1039/B900178F.
(64) Curiel, D.; Cowley, A.; Beer, P. D. Indolocarbazoles: A New Family of Anion Sensors. *Chem. Commun.* **2005**, No. 2, 236–238. https://doi.org/10.1039/B412363H.
(65) Sánchez, G.; Curiel, D.; Tárraga, A.; Molina, P. Anion Binding Studies on Receptors Derived from the Indolo[2,3-a]Carbazole Scaffold Having Different Binding Cavity Sizes. *Sensors* **2014**, *14* (8), 14038–14049. https://doi.org/10.3390/s140814038.
(66) Prohens, R.; Tomàs, S.; Morey, J.; Deyà, P. M.; Ballester, P.; Costa, A. Squaramido-Based Receptors: Molecular Recognition of Carboxylate Anions in Highly Competitive Media. *Tetrahedron Lett.* **1998**, *39* (9), 1063–1066. https://doi.org/10.1016/S0040-4039(97)10728-6.
(67) Fitzmaurice, R. J.; Kyne, G. M.; Douheret, D.; Kilburn, J. D. Synthetic Receptors for Carboxylic Acids and Carboxylates. *J. Chem. Soc. Perkin 1* **2002**, No. 7, 841–864. https://doi.org/10.1039/b009041g.
(68) Tshepelevitsh, S.; Trummal, A.; Haav, K.; Martin, K.; Leito, I. Hydrogen-Bond Donicity in DMSO and Gas Phase and Its Dependence on Brønsted Acidity. *J. Phys. Chem. A* **2017**, *121* (1), 357–369. https://doi.org/10.1021/acs.jpca.6b11115.
(69) Hirose, K. A Practical Guide for the Determination of Binding Constants.

(70) Freire, E.; Mayorga, O. L.; Straume, M. Isothermal Titration Calorimetry. *Anal. Chem.* **1990**, *62* (18), 950A-959A. https://doi.org/10.1021/ac00217a002.
(71) Thordarson, P. Determining Association Constants from Titration Experiments in Supramolecular Chemistry. *Chem. Soc. Rev.* **2011**, *40* (3), 1305–1323. https://doi.org/10.1039/C0CS00062K.
(72) Ackermann, Th. K. A. Connors: Binding Constants — the Measurement of Molecular Complex Stability, John Wiley & Sons, New York, Chichester, Brisbane, Toronto, Singapore 1987. 411 Seiten, Preis: £ 64.15. *Berichte Bunsenges. Für Phys. Chem.* **1987**, *91* (12), 1398–1398. https://doi.org/10.1002/bbpc.19870911223.
(73) Pung, A.; Leito, I. Predicting Relative Stability of Conformers in Solution with COSMO-RS. *J. Phys. Chem. A* **2017**, *121* (36), 6823–6829. https://doi.org/10.1021/acs.jpca.7b05197.
(74) Schalley, C. A. *Analytical Methods in Supramolecular Chemistry*; John Wiley & Sons, 2012.
(75) Haav, K.; Kadam, S. A.; Toom, L.; Gale, P. A.; Busschaert, N.; Wenzel, M.; Hiscock, J. R.; Kirby, I. L.; Haljasorg, T.; Lõkov, M.; Leito, I. Accurate Method To Quantify Binding in Supramolecular Chemistry. *J. Org. Chem.* **2013**, *78* (16), 7796–7808. https://doi.org/10.1021/jo400626p.
(76) Kadam, S. A.; Haav, K.; Toom, L.; Haljasorg, T.; Leito, I. NMR Method for Simultaneous Host–Guest Binding Constant Measurement. *J. Org. Chem.* **2014**, *79* (6), 2501–2513. https://doi.org/10.1021/jo4027963.
(77) Bazzicalupi, C.; Bianchi, A.; Giorgi, C.; Clares, M. P.; García-España, E. Addressing Selectivity Criteria in Binding Equilibria. *Coord. Chem. Rev.* **2012**, *256* (1), 13–27. https://doi.org/10.1016/j.ccr.2011.05.013.
(78) Wolfbeis, O. S. Editorial: Probes, Sensors, and Labels: Why Is Real Progress Slow? *Angew. Chem. Int. Ed.* **2013**, *52* (38), 9864–9865. https://doi.org/10.1002/anie.201305915.
(79) Mikhelson, K. N. *Ion-Selective Electrodes*; Springer, 2013.
(80) Buck, R. P.; Lindner, E. Recommendations for Nomenclature of Ionselective Electrodes (IUPAC Recommendations 1994). *Pure Appl. Chem.* **2009**, *66* (12), 2527–2536. https://doi.org/10.1351/pac199466122527.
(81) Koryta, J.; Dvořák, J.; Kavan, L. *Principles of Electrochemistry*, 2nd ed.; Wiley: Chichester ; New York, 1993.
(82) De Marco, R.; Clarke, G.; Pejcic, B. Ion-Selective Electrode Potentiometry in Environmental Analysis. *Electroanalysis* **2007**, *19* (19–20), 1987–2001. https://doi.org/10.1002/elan.200703916.
(83) Lewenstam, A. Routines and Challenges in Clinical Application of Electrochemical Ion-Sensors. *Electroanalysis* **2014**, *26* (6), 1171–1181. https://doi.org/10.1002/elan.201400061.
(84) Bobacka, J. Conducting Polymer-Based Solid-State Ion-Selective Electrodes. *Electroanalysis* **2006**, *18* (1), 7–18. https://doi.org/10.1002/elan.200503384.
(85) Wang, J. *Analytical Electrochemistry*, 1994th ed.; VCH Publishers, Inc.
(86) Wang, J. Portable Electrochemical Systems. *TrAC Trends Anal. Chem.* **2002**, *21* (4), 226–232. https://doi.org/10.1016/S0165-9936(02)00402-8.
(87) Wardak, C.; Morawska, K.; Pietrzak, K. New Materials Used for the Development of Anion-Selective Electrodes—A Review. *Materials* **2023**, *16* (17), 5779. https://doi.org/10.3390/ma16175779.

(88) Zuliani, C.; Diamond, D. Opportunities and Challenges of Using Ion-Selective Electrodes in Environmental Monitoring and Wearable Sensors. *Electrochimica Acta* **2012**, *84*, 29–34. https://doi.org/10.1016/j.electacta.2012.04.147.
(89) Cuartero, M.; Parrilla, M.; Crespo, G. A. Wearable Potentiometric Sensors for Medical Applications. *Sensors* **2019**, *19* (2), 363. https://doi.org/10.3390/s19020363.
(90) Lyu, Y.; Gan, S.; Bao, Y.; Zhong, L.; Xu, J.; Wang, W.; Liu, Z.; Ma, Y.; Yang, G.; Niu, L. Solid-Contact Ion-Selective Electrodes: Response Mechanisms, Transducer Materials and Wearable Sensors. *Membranes* **2020**, *10* (6), 128. https://doi.org/10.3390/membranes10060128.
(91) Cattrall, R. W.; Freiser, Henry. Coated Wire Ion-Selective Electrodes. *Anal. Chem.* **1971**, *43* (13), 1905–1906. https://doi.org/10.1021/ac60307a032.
(92) Bobacka, J.; Ivaska, A.; Lewenstam, A. Potentiometric Ion Sensors. *Chem. Rev.* **2008**, *108* (2), 329–351. https://doi.org/10.1021/cr068100w.
(93) Fibbioli, M.; Morf, W. E.; Badertscher, M.; de Rooij, N. F.; Pretsch, E. Potential Drifts of Solid-Contacted Ion-Selective Electrodes Due to Zero-Current Ion Fluxes Through the Sensor Membrane. *Electroanalysis* **2000**, *12* (16), 1286–1292. https://doi.org/10.1002/1521-4109(200011)12:16<1286::AID-ELAN1286>3.0.CO;2-Q.
(94) Nikolskii, B. P.; Materova, E. A. Solid Contact in Membrane Ion-Selective Electrodes. In *Ion-Selective Electrode Reviews*; Thomas, J. D. R., Ed.; Ion-Selective Electrode Reviews; Elsevier, 1985; Vol. 7, pp 3–39. https://doi.org/10.1016/B978-0-08-034150-7.50005-X.
(95) Hambly, B.; Guzinski, M.; Pendley, B.; Lindner, E. Evaluation, Pitfalls and Recommendations for the "Water Layer Test" for Solid Contact Ion-Selective Electrodes. *Electroanalysis* **2020**, *32* (4), 781–791. https://doi.org/10.1002/elan.201900637.
(96) Cadogan, Aodhmar.; Gao, Zhiqiang.; Lewenstam, Andrzej.; Ivaska, Ari.; Diamond, Dermot. All-Solid-State Sodium-Selective Electrode Based on a Calixarene Ionophore in a Poly(Vinyl Chloride) Membrane with a Polypyrrole Solid Contact. *Anal. Chem.* **1992**, *64* (21), 2496–2501. https://doi.org/10.1021/ac00045a007.
(97) Bobacka, J. Potential Stability of All-Solid-State Ion-Selective Electrodes Using Conducting Polymers as Ion-to-Electron Transducers. *Anal. Chem.* **1999**, *71* (21), 4932–4937. https://doi.org/10.1021/ac990497z.
(98) Bobacka, J.; Ivaska, A.; Lewenstam, A. Potentiometric Ion Sensors Based on Conducting Polymers. *Electroanalysis* **2003**, *15* (5–6), 366–374. https://doi.org/10.1002/ elan.200390042.
(99) Lewenstam, A.; Bobacka, J.; Ivaska, A. Mechanism of Ionic and Redox Sensitivity of P-Type Conducting Polymers: Part 1. Theory. *J. Electroanal. Chem.* **1994**, *368* (1), 23–31. https://doi.org/10.1016/0022-0728(93)03080-9.
(100) Bobacka, J.; Gao, Z.; Ivaska, A.; Lewenstam, A. Mechanism of Ionic and Redox Sensitivity of P-Type Conducting Polymers: Part 2. Experimental Study of Polypyrrole. *J. Electroanal. Chem.* **1994**, *368* (1), 33–41. https://doi.org/10.1016/0022-0728(93)03081-Y.
(101) Veder, J.-P.; De Marco, R.; Patel, K.; Si, P.; Grygolowicz-Pawlak, E.; James, M.; Alam, M. T.; Sohail, M.; Lee, J.; Pretsch, E.; Bakker, E. Evidence for a Surface Confined Ion-to-Electron Transduction Reaction in Solid-Contact Ion-Selective Electrodes Based on Poly(3-Octylthiophene). *Anal. Chem.* **2013**, *85* (21), 10495–10502. https://doi.org/10.1021/ac4024999.

(102) Lindfors, T. Light Sensitivity and Potential Stability of Electrically Conducting Polymers Commonly Used in Solid Contact Ion-Selective Electrodes. *J. Solid State Electrochem.* **2009**, *13* (1), 77–89. https://doi.org/10.1007/s10008-008-0561-z.
(103) Wardak, C.; Pietrzak, K.; Morawska, K.; Grabarczyk, M. Ion-Selective Electrodes with Solid Contact Based on Composite Materials: A Review. *Sensors* **2023**, *23* (13), 5839. https://doi.org/10.3390/s23135839.
(104) Bakker, E.; Bühlmann, P.; Pretsch, E. Carrier-Based Ion-Selective Electrodes and Bulk Optodes. 1. General Characteristics. *Chem. Rev.* **1997**, *97* (8), 3083–3132. https://doi.org/10.1021/cr940394a.
(105) Bakker, E.; Bühlmann, P.; Pretsch, E. The Phase-Boundary Potential Model. *Talanta* **2004**, *63* (1), 3–20. https://doi.org/10.1016/j.talanta.2003.10.006.
(106) Magar, H. S.; Hassan, R. Y. A.; Mulchandani, A. Electrochemical Impedance Spectroscopy (EIS): Principles, Construction, and Biosensing Applications. *Sensors* **2021**, *21* (19), 6578. https://doi.org/10.3390/s21196578.
(107) Lazanas, A. Ch.; Prodromidis, M. I. Electrochemical Impedance Spectroscopy─A Tutorial. *ACS Meas. Sci. Au* **2023**, *3* (3), 162–193. https://doi.org/10.1021/ acsmeasuresciau.2c00070.
(108) Choi, K. R.; Troudt, B. K.; Bühlmann, P. Ion-Selective Electrodes With Sensing Membranes Covalently Attached to Both the Inert Polymer Substrate and Conductive Carbon Contact. *Angew. Chem.* **2023**, *135* (28), e202304674. https://doi. org/10.1002/ange.202304674.
(109) Pechenkina, I. A.; Mikhelson, K. N. Materials for the Ionophore-Based Membranes for Ion-Selective Electrodes: Problems and Achievements (Review Paper). *Russ. J. Electrochem.* **2015**, *51* (2), 93–102. https://doi.org/10.1134/S1023193515020111.
(110) Schaller, Ulrich.; Bakker, Eric.; Spichiger, U. E.; Pretsch, Ernoe. Ionic Additives for Ion-Selective Electrodes Based on Electrically Charged Carriers. *Anal. Chem.* **1994**, *66* (3), 391–398. https://doi.org/10.1021/ac00075a013.
(111) Lindner, E.; Gyurcsányi, R. E. Quality Control Criteria for Solid-Contact, Solvent Polymeric Membrane Ion-Selective Electrodes. *J. Solid State Electrochem.* **2009**, *13* (1), 51–68. https://doi.org/10.1007/s10008-008-0608-1.
(112) Hu, J.; Stein, A.; Bühlmann, P. Rational Design of All-Solid-State Ion-Selective Electrodes and Reference Electrodes. *TrAC Trends Anal. Chem.* **2016**, *76*, 102–114. https://doi.org/10.1016/j.trac.2015.11.004.
(113) Lindner, E.; Umezawa, Y. Performance Evaluation Criteria for Preparation and Measurement of Macro- and Microfabricated Ion-Selective Electrodes (IUPAC Technical Report). *Pure Appl. Chem.* **2008**, *80* (1), 85–104. https://doi.org/10.1351/pac200880010085.
(114) Buck, R. P.; Lindner, E. Recommendations for Nomenclature of Ionselective Electrodes (IUPAC Recommendations 1994). *Pure Appl. Chem.* **1994**, *66* (12), 2527–2536. https://doi.org/10.1351/pac199466122527.
(115) Bakker, E.; Pretsch, E.; Bühlmann, P. Selectivity of Potentiometric Ion Sensors. *Anal. Chem.* **2000**, *72* (6), 1127–1133. https://doi.org/10.1021/ac991146n.
(116) Amemiya, S.; Bühlmann, P.; Umezawa, Y.; Jagessar, R. C.; Burns, D. H. An Ion-Selective Electrode for Acetate Based on a Urea-Functionalized Porphyrin as a Hydrogen-Bonding Ionophore. *Anal. Chem.* **1999**, *71* (5), 1049–1054. https://doi.org/10.1021/ac980952b.
(117) Lee, H.-K.; Song, K.; Seo, H.-R.; Jeon, S. Polymeric Acetate-Selective Electrodes Based on Meso-(α,α,α,α)-Tetrakis-[(2-Arylphenylurea)Phenyl]Porphyrins:

Electormic and pH Effects. *Bull. Korean Chem. Soc.* **2002**, *23* (10), 1409–1412. https://doi.org/10.5012/bkcs.2002.23.10.1409.
(118) Antonisse, M. M. G.; Snellink-Ruël, B. H. M.; Ion, A. C.; Engbersen, J. F. J.; Reinhoudt, D. N. Synthesis of Novel Uranyl Salophene Derivatives and Evaluation as Sensing Molecules in Chemically Modified Field Effect Transistors (CHEM-FETs). *J. Chem. Soc. Perkin Trans. 2* **1999**, No. 6, 1211–1218. https://doi.org/10.1039/a810019e.
(119) Gupta, V.; Goyal, R.; Sharma, R. Anion Recognition Using Newly Synthesized Hydrogen Bonding Disubstituted Phenylhydrazone-Based Receptors: Poly(Vinyl Chloride)-Based Sensor for Acetate. *Talanta* **2008**, *76* (4), 859–864. https://doi.org/10.1016/j.talanta.2008.04.046.
(120) Kadam, S. A.; Haav, K.; Toom, L.; Pung, A.; Mayeux, C.; Leito, I. Multidentate Anion Receptors for Binding Glyphosate Dianion: Structure and Affinity. *Eur. J. Org. Chem.* **2017**. https://doi.org/10.1002/ejoc.201601583.
(121) Harris, D. C. *Quantitative Chemical Analysis*, 7. ed., 2. print.; Freeman: New York, 2007.
(122) Leito, I.; Herodes, K.; Huopolainen, M.; Virro, K.; Künnapas, A.; Kruve, A.; Tanner, R. Towards the Electrospray Ionization Mass Spectrometry Ionization Efficiency Scale of Organic Compounds. *Rapid Commun. Mass Spectrom.* **2008**, *22* (3), 379–384. https://doi.org/10.1002/rcm.3371.
(123) Tshepelevitsh, S.; Kadam, S. A.; Darnell, A.; Bobacka, J.; Rüütel, A.; Haljasorg, T.; Leito, I. LogP Determination for Highly Lipophilic Hydrogen-Bonding Anion Receptor Molecules. *Anal. Chim. Acta* **2020**, *1132*, 123–133. https://doi.org/10.1016/j.aca.2020.07.024.
(124) Gregory, K. P.; Elliott, G. R.; Robertson, H.; Kumar, A.; Wanless, E. J.; Webber, G. B.; Craig, V. S. J.; Andersson, G. G.; Page, A. J. Understanding Specific Ion Effects and the Hofmeister Series. *Phys. Chem. Chem. Phys.* **2022**, *24* (21), 12682–12718. https://doi.org/10.1039/D2CP00847E.

SUMMARY IN ESTONIAN

Karboksülaatide tuvastamine sünteetiliste retseptorite abil – struktuur-afiinsuse uuringutest tahkiskontaktiga anioonselektiivse elektroodi prototüübini

Ioonid mängivad olulist rolli nii keskkonnasüsteemides kui ka bioloogilistes protsessides. Ioonide tasakaalu muutustel on enamasti kahjulikud mõjud: keskkonnas põhjustavad ioonide tasakaaluhäired saastet, samas kui tasakaalumuutused organismides võivad põhjustada haiguseid. Ioonide kontsentratsiooni saab määrata erinevate analüüsitehnikatega, nt ioonkromatograafiga, massispektromeetriaga või ioonselektiivsete elektroodidega. Tahkiskontaktiga ioonselektiivsetel elektroodidel on teiste meetodite ees mitmeid eeliseid – need on lihtsad, odavad, kiired, miniaturiseeritavad ja need saab asetada otse mõõdetavasse lahusesse, ilma et peaks selleks proovi eeltöötlema või laborisse viima. Kuigi väikseid katioone on polümeerse membraaniga ioonselektiivsete elektroodidega määratud juba üle 40 aasta, siis keerukamate ioonide, näiteks karboksülaatioonide määramiseks, ei ole leitud piisavalt häid ionofoore, millega elektroodi membraani valmistada.

Minu doktoritöö eesmärgiks on uurida väikeste karboksülaatide seondumist sünteetiliste retseptormolekulidega, et tuvastada retseptorite struktuuris karboksülaatioonide äratundmist soodustavaid struktuurifragmente. Uurimustöö lisaeesmärgiks on valida välja parimate seondumisomadustega retseptor ning kasutada seda ionofoorina tahkiskontaktiga ioonselektiivse elektroodide polümeerses membraanis.

Efektiivse ionofoori leidmiseks erinevate karboksüülretseptorite seast on vaja mõista supramolekulaarseid retseptor-anioon seondumisprotsesse fundamentaalsel tasemel ja määrata uuritavate retseptorite seondumisafiinsused. Varasemad uuringud on näidanud sünteetiliste retseptorite head afiinsust ja mõõdukat selektiivsust erinevate karboksülaatide suhtes. Kuid siiani ei ole avaldatud põhjalikku uurimust karboksülaatioonide struktuuride ja seondumisafiinsuste sõltuvusest. Uuringud vähese arvu retseptorite ja anioonidega erinevates lahustites seavad piirangud üldistusteks ja muudavad seondumisandmete sisuka võrdlemise keeruliseks. Seejuures on ioonselektiivsete elektroodide membraanidesse jõudnud vaid üksikud karboksülaatide retseptorid ning nende selektiivsust membraanis on uuritud väga vähe.

Oma töös iseloomustasin 44 erineva retseptori seondumisvõimekust kvantitatiivselt seondumisafiinsuste ($\log K_{\mathrm{ass}}$) kaudu, kasutades selleks meie uurimisrühmas varem väljatöötatud suhtelist tuumamagnetresonants-spektromeetrilist tiitrimismeetodit. See meetod võimaldab 0.5% veesisaldusega dimetüülsulfoksiidis eristada ka retseptormolekule, mille seondumistugevuste erinevus on vähem kui 0.05 $\log K_{\mathrm{ass}}$ ühikut ning koostada kooskõlalisi seondumisafiinsuste skaalasid uuritavatele anioonidele. Struktuur-afiinsus uuringu järelduste tegemiseks kasutasin lisaks seondumiskonstantidele ka COSMO-RS meetodil arvutatud geomeetriate ja peakomponentide analüüsi tulemusi.

Esialgu uurisin indolokarbasool-, karbasool-, indool-, uurea-, tiouurea- ja amiid-fragmente sisaldavate sünteetiliste retseptorimolekulide seondumist trimetüülatsetaadi, atsetaadi, bensoaadi ja laktaadiga. Olulisemad tulemused on järgmised: (a) seondumistugevuse määravad peamiselt vesiniksideme interaktsioonid ja karboksülaatiooni aluselisus, (b) tetradentaatsetel retseptoritel nagu bis-indolüül- või bis-karbasolüüluuread, millel on neli sobiva paigutusega NH rühma, on karboksülaatide seondumiseks kõige sobivama geomeetriaga seondumistasku, (c) orto-fenüleendiamiini-bis-urea retseptorid moodustavad nõrgemaid komplekse NH rühmade ebasoodsa ruumilise paigutuse tõttu, (d) tridentaatsete karbasooli-põhiste retseptorite madalam afiinsus on põhjustatud nende asümmeetrilisest seondumisest ning (e) bidentaatsed difenüüluureal ja indolokarbasoolil põhinevad retseptormolekulid näitavad sarnaseid seondumisafiinsusi – kuigi difenüüluurea on nõrgem vesiniksidemete doonor, on moodustatavad vesiniksidemed soodsama nurga all kui indolokarbasooli fragmendi puhul. Retseptorite seondumisafiinsust mõjutavad eelkõige NH rühmade arv, nende paigutus ja happelisus ning võimalik steeriline takistus seondumistasku läheduses.

Uurimustöö järgmises etapis jätsin uuringutest välja madalama afiinsusega retseptorid, lisasin juurde viis keerukama struktuuriga huvipakkuvat retseptorit ning laiendasin uuritavate karboksülaatide hulka. Koostasin kaheksa seondumisafiinsuste skaalat ja uurisin 11 karboksülaadi (formaat, atsetaat, trimetüülatsetaat, laktaat, naprokseen, ibuprofeen, ketoprofeen, glükuronaat, heksanoaat, sorbaat ja bensoaat) seondumist. Tulemused näitasid, et: (a) aniooni aluselisus jääb siiski võtmeteguriks, kuid seondumist mõjutavad ka aniooni asendusrühmad, steerika ja võimalikud täiendavad vastasmõjud, (b) süsinikahela pikkus mängib anioonide eristamisel tagasihoidlikku rolli, (c) atsetaadi ja trimetüülatsetaadi seondumisafiinsust mõjutavad märkimisväärselt seondumistasku mõõtmed, mis saavad olla solvofoobseid efekte soodustavad ning (d) tekkivate seondumismustrite tõttu on mitme retseptori koosmõjul võimalik erineva struktuuriga karboksülaate üksteisest eristada.

Eelnevate tulemuste põhjal valisin välja kõrge seondumisafiinsusega 1,3-bis(karbasoüül)urea derivaadi ning kasutasin seda ionofoorina tahkiskontaktiga atsetaat-selektiivsete elektroodide prototüüpide valmistamiseks. Need elektroodid näitasid lineaarsust aktiivsusvahemikus $10^{-4.50}$–$10^{-1.10}$, sub-Nernstiaalset tõusu 51,3 mV kümnendi kohta ja avastamispiiri $10^{-5.00}$. Valmistatud elektroodiprototüüpide selektiivsus erineb oluliselt Hofmeisteri seeriast, näidates suuremat selektiivsust väikeste karboksülaatide (atsetaat, formaat) ja vesinikkarbonaadi suhtes võrreldes kloriidiooniga. Ilma ionofoorita kontrollelektroodidega võrreldes vähenes hüdrofoobsete anorgaaniliste anioonide nagu SCN^-, I^-, NO_3^- ja Br^- segav mõju. Valitud retseptormolekuli kasutamine ionofoorina õnnestus, kuid veelgi kõrgema selektiivsuse ja tundlikkuse saavutamiseks on vaja sünteetiliste anioonretseptorite disaini ja sünteesi edasi arendada.

ACKNOWLEDGEMENTS

I would like to express my gratitude to the University of Tartu, Institute of Chemistry, the Chair of Bioorganic Chemistry, and the Chair of Analytical Chemistry for providing me with an excellent education and extensive knowledge throughout my studies.

This work was carried out using the instrumentation of the Estonian Center of Analytical Chemistry (www.akki.ee) and was supported by the EU through the European Regional Development Fund (project TK141 "Advanced materials and high-technology devices for energy recuperation systems" and Graduate School of Functional Materials and Technologies), as well as by the institutional research grant IUT20-14 from the Estonian Research Council.

This work is also part of the activities of the Johan Gadolin Process Chemistry Centre at Åbo Akademi University, Finland. I am deeply appreciative of the financial support provided through a Johan Gadolin Scholarship.

I would like to express my deepest gratitude to my supervisor, Professor Ivo Leito, for all the advice, help, and guidance. Prof. Leito enthusiasm and motivation are truly inspiring. Every conversation with him leaves me energised and focused on my goals. I greatly admire his hard work, productivity, quick problem-solving skills, and his constant availability to his supervisees. It has been a privilege to learn from him.

I am deeply grateful to Professor Johan Bobacka for giving me the opportunity to work in the analytical chemistry laboratory at Åbo Akademi University. Despite my limited prior exposure to electrochemistry, I had the chance to learn from the best in the field. I am so thankful for Professor Bobacka's support, helpful advice, suggestions, and discussions throughout my stay at Åbo.

I would like to thank my colleagues Sandip A. Kadam, Kristjan Haav, Astrid Darnell, Lauri Toom, Tõiv Haljasorg, Juuli Nõges, Sofja Tshepelevitsh, and Alo Rüütel, all of whom have contributed to this work. Additionally, I am grateful to Ulriika Vanamo and Associate Professor Tom Lindfors from Professor Bobacka's group. They helped me with the use of electrochemistry equipment and software, and their friendly support made me feel very much at home at the Analyten.

I also thank my colleagues at TBD Pharmatech, Piia Liigand, Jürgen Vahter, and Andi Kipper, who have provided advice and comfort during the last few months of writing this dissertation.

I would like to thank my family and friends for all their love and support. Your encouragement and belief in me have been a constant source of strength.

Finally, I thank my Taavi from the bottom of my heart. You have supported me in everything over the years, from writing programs to help with data analysis (Ladder Builder saved so much time!) to stocking my cupboard with chocolates and spending countless hours with our little daughters so that I could complete this dissertation. Your unwavering support, patience, and love have been my anchor. Thank you so much!

PUBLICATIONS

CURRICULUM VITAE

Name: Kerli Martin
Date of birth: May 26, 1990
Citizenship: Estonian
E-mail: kerly.martin@gmail.com

Education:

2017	Åbo Akademi University, Johan Gadolin PCC Fellow in Prof. Johan Bobacka's research group
2014–present	University of Tartu, PhD student in Analytical Chemistry
2012–2014	University of Tartu, M.Sc *cum laude* in Analytical Chemistry, "Building binding scales of simple carboxylate anions by synthetic receptors"
2009–2012	University of Tartu, B.Sc in Bioorganic Chemistry, "Orexin-1 receptor characterization using fluorescence methods"
2006–2009	Nõo Real Gymnasium, Secondary education
1997–2006	Käina Gymnasium, Primary education
1996–2004	Käina School of Fine Arts, Musical primary education

Work experience:

2018–present	TBD Pharmatech (formerly TBD-Biodiscovery), Quality Control Laboratory Manager
2017–2018	TBD-Biodiscovery, Analyst
2014–2017	University of Tartu, Chair of Analytical Chemistry, Chemist
2013–2014	Estonian University of Life Sciences, Department of Nutrition and Animal Products Quality, Chemist

Research Focus:
Supramolecular chemistry, with an emphasis on characterising molecular receptors and integrating them into sensor systems.

Scientific publications:

1. Kadam, S. A.; **Martin, K.**; Haav, K.; Toom, L.; Mayeux, C.; Pung, A.; Gale, P. A.; Hiscock, J. R.; Brooks, S. J.; Kirby, I. L.; Busschaert, N.; Leito, I. Towards the Discrimination of Carboxylates by Hydrogen-Bond Donor Anion Receptors. *Chem. Eur. J.* **2015**, *21* (13), 5145–5160. https://doi.org/10.1002/chem.201405858.
2. Tshepelevitsh, S.; Trummal, A.; Haav, K.; **Martin, K.**; Leito, I. Hydrogen-Bond Donicity in DMSO and Gas Phase and Its Dependence on Brønsted Acidity. *J. Phys. Chem. A* **2017**, *121* (1), 357–369. https://doi.org/10.1021/acs.jpca.6b11115.
3. **Martin, K.**; Nõges, J.; Haav, K.; Kadam, S. A.; Pung, A.; Leito, I. Exploring Selectivity of 22 Acyclic Urea-, Carbazole- and Indolocarbazole-Based

Receptors towards 11 Monocarboxylates: Exploring Selectivity of 22 Acyclic Urea-, Carbazole- and Indolocarbazole-Based Receptors towards 11 Monocarboxylates. *Eur. J. Org. Chem.* **2017**, *2017* (35), 5231–5237. https://doi.org/10.1002/ejoc.201700931.

4. **Martin, K.**; Kadam, S. A.; Mattinen, U.; Bobacka, J.; Leito, I. Solid-Contact Acetate-Selective Electrode Based on a 1,3-Bis(Carbazolyl)Urea-Ionophore. *Electroanalysis* **2019**, *31* (6), 1061–1066. https://doi.org/10.1002/elan. 201800790.

Teaching:

- Instructor for NMR practicum in "LOKT.06.015 Analytical Chemistry Practicum II" (2017)
- Instructor for NMR practicum in "LOKT.06.014 Analytical Chemistry Seminar II" (2017)
- Web content creator for the Analytical Chemistry Chair website (analytical.chem.ut.ee, 2017)
- Instructor for Group C in "LOKT.06.015 Analytical Chemistry Practicum II" (Spring 2016)
- Instructor for Group B in "LOKT.06.015 Analytical Chemistry Practicum II" (Spring 2015)
- Assessor for practical chemical analysis during the high school student selection competition camp in April 2015.

ELULOOKIRJELDUS

Nimi: Kerli Martin
Sünniaeg: 26. mai 1990
Kodakondsus: Eesti
E-post: kerly.martin@gmail.com

Haridus:

2017	Åbo Akademi Ülikool, Johan Gadolin PCC stipendiaat prof Johan Bobacka uurimisrühmas
alates 2014	Tartu Ülikool, analüütilise keemia doktorant
2012–2014	Tartu Ülikool, analüütilise keemia magister *cum laude*, „Sünteetiliste retseptorite seondumisskaalade koostamine lihtsamatele karboksülaatioonidele“
2009–2012	Tartu Ülikool, bioorgaanilise keemia bakalaureus, „Oreksiin-1 retseptori uurimine fluorestsentsmeetoditega“
2006–2009	Nõo Reaalgümnaasium, keskharidus
1997–2006	Käina Gümnaasium, põhiharidus
1996–2004	Käina Kaunite Kunstide Kool, muusikaline põhiharidus

Töökogemus:

alates 2018	TBD Pharmatech (varasem TBD-Biodiscovery), kvaliteedikontrolli labori juhataja
2017–2018	TBD-Biodiscovery, analüütik
2014–2017	Tartu Ülikool, Analüütilise keemia õppetool, keemik
2013–2014	Eesti Maaülikool, Sööda ja ainevahetuse uurimise labor, keemik

Uurimistöö põhisuund:
Supramolekulaarne keemia, molekulaarsete retseptorite iseloomustus ja nende integreerimine sensorsüsteemidesse.

Teaduspublikatsioonid:

1. Kadam, S. A.; **Martin, K.**; Haav, K.; Toom, L.; Mayeux, C.; Pung, A.; Gale, P. A.; Hiscock, J. R.; Brooks, S. J.; Kirby, I. L.; Busschaert, N.; Leito, I. Towards the Discrimination of Carboxylates by Hydrogen-Bond Donor Anion Receptors. *Chem. Eur. J.* **2015**, *21* (13), 5145–5160. https://doi.org/10.1002/chem.201405858.
2. Tshepelevitsh, S.; Trummal, A.; Haav, K.; **Martin, K.**; Leito, I. Hydrogen-Bond Donicity in DMSO and Gas Phase and Its Dependence on Brønsted Acidity. *J. Phys. Chem. A* **2017**, *121* (1), 357–369. https://doi.org/10.1021/acs.jpca.6b11115.
3. **Martin, K.**; Nõges, J.; Haav, K.; Kadam, S. A.; Pung, A.; Leito, I. Exploring Selectivity of 22 Acyclic Urea-, Carbazole- and Indolocarbazole-Based Receptors towards 11 Monocarboxylates: Exploring Selectivity of 22 Acyclic

Urea-, Carbazole- and Indolocarbazole-Based Receptors towards 11 Monocarboxylates. *Eur. J. Org. Chem.* **2017**, *2017* (35), 5231–5237. https://doi.org/10.1002/ejoc.201700931.

4. **Martin, K.**; Kadam, S. A.; Mattinen, U.; Bobacka, J.; Leito, I. Solid-Contact Acetate-Selective Electrode Based on a 1,3-Bis(Carbazolyl)Urea-Ionophore. *Electroanalysis* **2019**, *31* (6), 1061–1066. https://doi.org/10.1002/elan.201800790.

Õppetöö:

- LOKT.06.015 Analüütilise keemia praktikum II – TMR praktikumi õppejõud (2017)
- LOKT.06.014 Analüütilise keemia seminar II – TMR seminari õppejõud (2017)
- Analüütilise keemia õppetooli veebilehe (analytical.chem.ut.ee) koostaja (2017)
- LOKT.06.015 Analüütilise keemia praktikum II – C rühma juhendaja (kevad 2016)
- LOKT.06.015 Analüütilise keemia praktikum II – B rühma juhendaja (kevad 2015)
- Hindaja 2015 aprillis toimunud keskkooliõpilaste valikvõistluse laagri raames toimunud praktilisel keemilisel analüüsil.

DISSERTATIONES CHIMICAE UNIVERSITATIS TARTUENSIS

1. **Toomas Tamm.** Quantum-chemical simulation of solvent effects. Tartu, 1993, 110 p.
2. **Peeter Burk.** Theoretical study of gas-phase acid-base equilibria. Tartu, 1994, 96 p.
3. **Victor Lobanov.** Quantitative structure-property relationships in large descriptor spaces. Tartu, 1995, 135 p.
4. **Vahur Mäemets.** The ^{17}O and ^{1}H nuclear magnetic resonance study of H_2O in individual solvents and its charged clusters in aqueous solutions of electrolytes. Tartu, 1997, 140 p.
5. **Andrus Metsala.** Microcanonical rate constant in nonequilibrium distribution of vibrational energy and in restricted intramolecular vibrational energy redistribution on the basis of slater's theory of unimolecular reactions. Tartu, 1997, 150 p.
6. **Uko Maran.** Quantum-mechanical study of potential energy surfaces in different environments. Tartu, 1997, 137 p.
7. **Alar Jänes.** Adsorption of organic compounds on antimony, bismuth and cadmium electrodes. Tartu, 1998, 219 p.
8. **Kaido Tammeveski.** Oxygen electroreduction on thin platinum films and the electrochemical detection of superoxide anion. Tartu, 1998, 139 p.
9. **Ivo Leito.** Studies of Brønsted acid-base equilibria in water and non-aqueous media. Tartu, 1998, 101 p.
10. **Jaan Leis.** Conformational dynamics and equilibria in amides. Tartu, 1998, 131 p.
11. **Toonika Rinken.** The modelling of amperometric biosensors based on oxidoreductases. Tartu, 2000, 108 p.
12. **Dmitri Panov.** Partially solvated Grignard reagents. Tartu, 2000, 64 p.
13. **Kaja Orupõld.** Treatment and analysis of phenolic wastewater with microorganisms. Tartu, 2000, 123 p.
14. **Jüri Ivask.** Ion Chromatographic determination of major anions and cations in polar ice core. Tartu, 2000, 85 p.
15. **Lauri Vares.** Stereoselective Synthesis of Tetrahydrofuran and Tetrahydropyran Derivatives by Use of Asymmetric Horner-Wadsworth-Emmons and Ring Closure Reactions. Tartu, 2000, 184 p.
16. **Martin Lepiku.** Kinetic aspects of dopamine D_2 receptor interactions with specific ligands. Tartu, 2000, 81 p.
17. **Katrin Sak.** Some aspects of ligand specificity of P2Y receptors. Tartu, 2000, 106 p.
18. **Vello Pällin.** The role of solvation in the formation of iotsitch complexes. Tartu, 2001, 95 p.
19. **Katrin Kollist.** Interactions between polycyclic aromatic compounds and humic substances. Tartu, 2001, 93 p.

20. **Ivar Koppel.** Quantum chemical study of acidity of strong and superstrong Brønsted acids. Tartu, 2001, 104 p.
21. **Viljar Pihl.** The study of the substituent and solvent effects on the acidity of OH and CH acids. Tartu, 2001, 132 p.
22. **Natalia Palm.** Specification of the minimum, sufficient and significant set of descriptors for general description of solvent effects. Tartu, 2001, 134 p.
23. **Sulev Sild.** QSPR/QSAR approaches for complex molecular systems. Tartu, 2001, 134 p.
24. **Ruslan Petrukhin.** Industrial applications of the quantitative structure-property relationships. Tartu, 2001, 162 p.
25. **Boris V. Rogovoy.** Synthesis of (benzotriazolyl)carboximidamides and their application in relations with *N*- and *S*-nucleophyles. Tartu, 2002, 84 p.
26. **Koit Herodes.** Solvent effects on UV-vis absorption spectra of some solvatochromic substances in binary solvent mixtures: the preferential solvation model. Tartu, 2002, 102 p.
27. **Anti Perkson.** Synthesis and characterisation of nanostructured carbon. Tartu, 2002, 152 p.
28. **Ivari Kaljurand.** Self-consistent acidity scales of neutral and cationic Brønsted acids in acetonitrile and tetrahydrofuran. Tartu, 2003, 108 p.
29. **Karmen Lust.** Adsorption of anions on bismuth single crystal electrodes. Tartu, 2003, 128 p.
30. **Mare Piirsalu.** Substituent, temperature and solvent effects on the alkaline hydrolysis of substituted phenyl and alkyl esters of benzoic acid. Tartu, 2003, 156 p.
31. **Meeri Sassian.** Reactions of partially solvated Grignard reagents. Tartu, 2003, 78 p.
32. **Tarmo Tamm.** Quantum chemical modelling of polypyrrole. Tartu, 2003. 100 p.
33. **Erik Teinemaa.** The environmental fate of the particulate matter and organic pollutants from an oil shale power plant. Tartu, 2003. 102 p.
34. **Jaana Tammiku-Taul.** Quantum chemical study of the properties of Grignard reagents. Tartu, 2003. 120 p.
35. **Andre Lomaka.** Biomedical applications of predictive computational chemistry. Tartu, 2003. 132 p.
36. **Kostyantyn Kirichenko.** Benzotriazole – Mediated Carbon–Carbon Bond Formation. Tartu, 2003. 132 p.
37. **Gunnar Nurk.** Adsorption kinetics of some organic compounds on bismuth single crystal electrodes. Tartu, 2003, 170 p.
38. **Mati Arulepp.** Electrochemical characteristics of porous carbon materials and electrical double layer capacitors. Tartu, 2003, 196 p.
39. **Dan Cornel Fara.** QSPR modeling of complexation and distribution of organic compounds. Tartu, 2004, 126 p.
40. **Riina Mahlapuu.** Signalling of galanin and amyloid precursor protein through adenylate cyclase. Tartu, 2004, 124 p.

41. **Mihkel Kerikmäe.** Some luminescent materials for dosimetric applications and physical research. Tartu, 2004, 143 p.
42. **Jaanus Kruusma.** Determination of some important trace metal ions in human blood. Tartu, 2004, 115 p.
43. **Urmas Johanson.** Investigations of the electrochemical properties of polypyrrole modified electrodes. Tartu, 2004, 91 p.
44. **Kaido Sillar.** Computational study of the acid sites in zeolite ZSM-5. Tartu, 2004, 80 p.
45. **Aldo Oras.** Kinetic aspects of dATPαS interaction with $P2Y_1$ receptor. Tartu, 2004, 75 p.
46. **Erik Mölder.** Measurement of the oxygen mass transfer through the air-water interface. Tartu, 2005, 73 p.
47. **Thomas Thomberg.** The kinetics of electroreduction of peroxodisulfate anion on cadmium (0001) single crystal electrode. Tartu, 2005, 95 p.
48. **Olavi Loog.** Aspects of condensations of carbonyl compounds and their imine analogues. Tartu, 2005, 83 p.
49. **Siim Salmar.** Effect of ultrasound on ester hydrolysis in aqueous ethanol. Tartu, 2006, 73 p.
50. **Ain Uustare.** Modulation of signal transduction of heptahelical receptors by other receptors and G proteins. Tartu, 2006, 121 p.
51. **Sergei Yurchenko.** Determination of some carcinogenic contaminants in food. Tartu, 2006, 143 p.
52. **Kaido Tämm.** QSPR modeling of some properties of organic compounds. Tartu, 2006, 67 p.
53. **Olga Tšubrik.** New methods in the synthesis of multisubstituted hydrazines. Tartu. 2006, 183 p.
54. **Lilli Sooväli.** Spectrophotometric measurements and their uncertainty in chemical analysis and dissociation constant measurements. Tartu, 2006, 125 p.
55. **Eve Koort.** Uncertainty estimation of potentiometrically measured ph and pK_a values. Tartu, 2006, 139 p.
56. **Sergei Kopanchuk.** Regulation of ligand binding to melanocortin receptor subtypes. Tartu, 2006, 119 p.
57. **Silvar Kallip.** Surface structure of some bismuth and antimony single crystal electrodes. Tartu, 2006, 107 p.
58. **Kristjan Saal.** Surface silanization and its application in biomolecule coupling. Tartu, 2006, 77 p.
59. **Tanel Tätte.** High viscosity $Sn(OBu)_4$ oligomeric concentrates and their applications in technology. Tartu, 2006, 91 p.
60. **Dimitar Atanasov Dobchev**. Robust QSAR methods for the prediction of properties from molecular structure. Tartu, 2006, 118 p.
61. **Hannes Hagu**. Impact of ultrasound on hydrophobic interactions in solutions. Tartu, 2007, 81 p.
62. **Rutha Jäger.** Electroreduction of peroxodisulfate anion on bismuth electrodes. Tartu, 2007, 142 p.

63. **Kaido Viht.** Immobilizable bisubstrate-analogue inhibitors of basophilic protein kinases: development and application in biosensors. Tartu, 2007, 88 p.
64. **Eva-Ingrid Rõõm.** Acid-base equilibria in nonpolar media. Tartu, 2007, 156 p.
65. **Sven Tamp.** DFT study of the cesium cation containing complexes relevant to the cesium cation binding by the humic acids. Tartu, 2007, 102 p.
66. **Jaak Nerut.** Electroreduction of hexacyanoferrate(III) anion on Cadmium (0001) single crystal electrode. Tartu, 2007, 180 p.
67. **Lauri Jalukse.** Measurement uncertainty estimation in amperometric dissolved oxygen concentration measurement. Tartu, 2007, 112 p.
68. **Aime Lust.** Charge state of dopants and ordered clusters formation in CaF_2:Mn and CaF_2:Eu luminophors. Tartu, 2007, 100 p.
69. **Iiris Kahn**. Quantitative Structure-Activity Relationships of environmentally relevant properties. Tartu, 2007, 98 p.
70. **Mari Reinik.** Nitrates, nitrites, N-nitrosamines and polycyclic aromatic hydrocarbons in food: analytical methods, occurrence and dietary intake. Tartu, 2007, 172 p.
71. **Heili Kasuk.** Thermodynamic parameters and adsorption kinetics of organic compounds forming the compact adsorption layer at Bi single crystal electrodes. Tartu, 2007, 212 p.
72. **Erki Enkvist.** Synthesis of adenosine-peptide conjugates for biological applications. Tartu, 2007, 114 p.
73. **Svetoslav Hristov Slavov**. Biomedical applications of the QSAR approach. Tartu, 2007, 146 p.
74. **Eneli Härk.** Electroreduction of complex cations on electrochemically polished Bi(*hkl*) single crystal electrodes. Tartu, 2008, 158 p.
75. **Priit Möller.** Electrochemical characteristics of some cathodes for medium temperature solid oxide fuel cells, synthesized by solid state reaction technique. Tartu, 2008, 90 p.
76. **Signe Viggor.** Impact of biochemical parameters of genetically different pseudomonads at the degradation of phenolic compounds. Tartu, 2008, 122 p.
77. **Ave Sarapuu.** Electrochemical reduction of oxygen on quinone-modified carbon electrodes and on thin films of platinum and gold. Tartu, 2008, 134 p.
78. **Agnes Kütt.** Studies of acid-base equilibria in non-aqueous media. Tartu, 2008, 198 p.
79. **Rouvim Kadis.** Evaluation of measurement uncertainty in analytical chemistry: related concepts and some points of misinterpretation. Tartu, 2008, 118 p.
80. **Valter Reedo.** Elaboration of IVB group metal oxide structures and their possible applications. Tartu, 2008, 98 p.
81. **Aleksei Kuznetsov.** Allosteric effects in reactions catalyzed by the cAMP-dependent protein kinase catalytic subunit. Tartu, 2009, 133 p.

82. **Aleksei Bredihhin.** Use of mono- and polyanions in the synthesis of multisubstituted hydrazine derivatives. Tartu, 2009, 105 p.
83. **Anu Ploom.** Quantitative structure-reactivity analysis in organosilicon chemistry. Tartu, 2009, 99 p.
84. **Argo Vonk.** Determination of adenosine A_{2A}- and dopamine D_1 receptor-specific modulation of adenylate cyclase activity in rat striatum. Tartu, 2009, 129 p.
85. **Indrek Kivi.** Synthesis and electrochemical characterization of porous cathode materials for intermediate temperature solid oxide fuel cells. Tartu, 2009, 177 p.
86. **Jaanus Eskusson.** Synthesis and characterisation of diamond-like carbon thin films prepared by pulsed laser deposition method. Tartu, 2009, 117 p.
87. **Marko Lätt.** Carbide derived microporous carbon and electrical double layer capacitors. Tartu, 2009, 107 p.
88. **Vladimir Stepanov.** Slow conformational changes in dopamine transporter interaction with its ligands. Tartu, 2009, 103 p.
89. **Aleksander Trummal.** Computational Study of Structural and Solvent Effects on Acidities of Some Brønsted Acids. Tartu, 2009, 103 p.
90. **Eerold Vellemäe.** Applications of mischmetal in organic synthesis. Tartu, 2009, 93 p.
91. **Sven Parkel.** Ligand binding to 5-HT_{1A} receptors and its regulation by Mg^{2+} and Mn^{2+}. Tartu, 2010, 99 p.
92. **Signe Vahur.** Expanding the possibilities of ATR-FT-IR spectroscopy in determination of inorganic pigments. Tartu, 2010, 184 p.
93. **Tavo Romann**. Preparation and surface modification of bismuth thin film, porous, and microelectrodes. Tartu, 2010, 155 p.
94. **Nadežda Aleksejeva.** Electrocatalytic reduction of oxygen on carbon nanotube-based nanocomposite materials. Tartu, 2010, 147 p.
95. **Marko Kullapere.** Electrochemical properties of glassy carbon, nickel and gold electrodes modified with aryl groups. Tartu, 2010, 233 p.
96. **Liis Siinor.** Adsorption kinetics of ions at Bi single crystal planes from aqueous electrolyte solutions and room-temperature ionic liquids. Tartu, 2010, 101 p.
97. **Angela Vaasa.** Development of fluorescence-based kinetic and binding assays for characterization of protein kinases and their inhibitors. Tartu 2010, 101 p.
98. **Indrek Tulp.** Multivariate analysis of chemical and biological properties. Tartu 2010, 105 p.
99. **Aare Selberg.** Evaluation of environmental quality in Northern Estonia by the analysis of leachate. Tartu 2010, 117 p.
100. **Darja Lavõgina.** Development of protein kinase inhibitors based on adenosine analogue-oligoarginine conjugates. Tartu 2010, 248 p.
101. **Laura Herm.** Biochemistry of dopamine D_2 receptors and its association with motivated behaviour. Tartu 2010, 156 p.

102. **Terje Raudsepp.** Influence of dopant anions on the electrochemical properties of polypyrrole films. Tartu 2010, 112 p.
103. **Margus Marandi.** Electroformation of Polypyrrole Films: *In-situ* AFM and STM Study. Tartu 2011, 116 p.
104. **Kairi Kivirand.** Diamine oxidase-based biosensors: construction and working principles. Tartu, 2011, 140 p.
105. **Anneli Kruve.** Matrix effects in liquid-chromatography electrospray mass-spectrometry. Tartu, 2011, 156 p.
106. **Gary Urb.** Assessment of environmental impact of oil shale fly ash from PF and CFB combustion. Tartu, 2011, 108 p.
107. **Nikita Oskolkov.** A novel strategy for peptide-mediated cellular delivery and induction of endosomal escape. Tartu, 2011, 106 p.
108. **Dana Martin.** The QSPR/QSAR approach for the prediction of properties of fullerene derivatives. Tartu, 2011, 98 p.
109. **Säde Viirlaid.** Novel glutathione analogues and their antioxidant activity. Tartu, 2011, 106 p.
110. **Ülis Sõukand.** Simultaneous adsorption of Cd^{2+}, Ni^{2+}, and Pb^{2+} on peat. Tartu, 2011, 124 p.
111. **Lauri Lipping.** The acidity of strong and superstrong Brønsted acids, an outreach for the "limits of growth": a quantum chemical study. Tartu, 2011, 124 p.
112. **Heisi Kurig.** Electrical double-layer capacitors based on ionic liquids as electrolytes. Tartu, 2011, 146 p.
113. **Marje Kasari.** Bisubstrate luminescent probes, optical sensors and affinity adsorbents for measurement of active protein kinases in biological samples. Tartu, 2012, 126 p.
114. **Kalev Takkis.** Virtual screening of chemical databases for bioactive molecules. Tartu, 2012, 122 p.
115. **Ksenija Kisseljova**. Synthesis of aza-β^3-amino acid containing peptides and kinetic study of their phosphorylation by protein kinase A. Tartu, 2012, 104 p.
116. **Riin Rebane.** Advanced method development strategy for derivatization LC/ESI/MS. Tartu, 2012, 184 p.
117. **Vladislav Ivaništšev.** Double layer structure and adsorption kinetics of ions at metal electrodes in room temperature ionic liquids. Tartu, 2012, 128 p.
118. **Irja Helm.** High accuracy gravimetric Winkler method for determination of dissolved oxygen. Tartu, 2012, 139 p.
119. **Karin Kipper.** Fluoroalcohols as Components of LC-ESI-MS Eluents: Usage and Applications. Tartu, 2012, 164 p.
120. **Arno Ratas.** Energy storage and transfer in dosimetric luminescent materials. Tartu, 2012, 163 p.
121. **Reet Reinart-Okugbeni**. Assay systems for characterisation of subtype-selective binding and functional activity of ligands on dopamine receptors. Tartu, 2012, 159 p.

122. **Lauri Sikk.** Computational study of the Sonogashira cross-coupling reaction. Tartu, 2012, 81 p.
123. **Karita Raudkivi.** Neurochemical studies on inter-individual differences in affect-related behaviour of the laboratory rat. Tartu, 2012, 161 p.
124. **Indrek Saar.** Design of GalR2 subtype specific ligands: their role in depression-like behavior and feeding regulation. Tartu, 2013, 126 p.
125. **Ann Laheäär.** Electrochemical characterization of alkali metal salt based non-aqueous electrolytes for supercapacitors. Tartu, 2013, 127 p.
126. **Kerli Tõnurist.** Influence of electrospun separator materials properties on electrochemical performance of electrical double-layer capacitors. Tartu, 2013, 147 p.
127. **Kaija Põhako-Esko.** Novel organic and inorganic ionogels: preparation and characterization. Tartu, 2013, 124 p.
128. **Ivar Kruusenberg.** Electroreduction of oxygen on carbon nanomaterial-based catalysts. Tartu, 2013, 191 p.
129. **Sander Piiskop.** Kinetic effects of ultrasound in aqueous acetonitrile solutions. Tartu, 2013, 95 p.
130. **Ilona Faustova**. Regulatory role of L-type pyruvate kinase N-terminal domain. Tartu, 2013, 109 p.
131. **Kadi Tamm.** Synthesis and characterization of the micro-mesoporous anode materials and testing of the medium temperature solid oxide fuel cell single cells. Tartu, 2013, 138 p.
132. **Iva Bozhidarova Stoyanova-Slavova.** Validation of QSAR/QSPR for regulatory purposes. Tartu, 2013, 109 p.
133. **Vitali Grozovski**. Adsorption of organic molecules at single crystal electrodes studied by *in situ* STM method. Tartu, 2014, 146 p.
134. **Santa Veikšina**. Development of assay systems for characterisation of ligand binding properties to melanocortin 4 receptors. Tartu, 2014, 151 p.
135. **Jüri Liiv.** PVDF (polyvinylidene difluoride) as material for active element of twisting-ball displays. Tartu, 2014, 111 p.
136. **Kersti Vaarmets.** Electrochemical and physical characterization of pristine and activated molybdenum carbide-derived carbon electrodes for the oxygen electroreduction reaction. Tartu, 2014, 131 p.
137. **Lauri Tõntson**. Regulation of G-protein subtypes by receptors, guanine nucleotides and Mn^{2+}. Tartu, 2014, 105 p.
138. **Aiko Adamson.** Properties of amine-boranes and phosphorus analogues in the gas phase. Tartu, 2014, 78 p.
139. **Elo Kibena**. Electrochemical grafting of glassy carbon, gold, highly oriented pyrolytic graphite and chemical vapour deposition-grown graphene electrodes by diazonium reduction method. Tartu, 2014, 184 p.
140. **Teemu Näykki.** Novel Tools for Water Quality Monitoring – From Field to Laboratory. Tartu, 2014, 202 p.
141. **Karl Kaupmees.** Acidity and basicity in non-aqueous media: importance of solvent properties and purity. Tartu, 2014, 128 p.

142. **Oleg Lebedev**. Hydrazine polyanions: different strategies in the synthesis of heterocycles. Tartu, 2015, 118 p.
143. **Geven Piir.** Environmental risk assessment of chemicals using QSAR methods. Tartu, 2015, 123 p.
144. **Olga Mazina.** Development and application of the biosensor assay for measurements of cyclic adenosine monophosphate in studies of G protein-coupled receptor signalinga. Tartu, 2015, 116 p.
145. **Sandip Ashokrao Kadam.** Anion receptors: synthesis and accurate binding measurements. Tartu, 2015, 116 p.
146. **Indrek Tallo.** Synthesis and characterization of new micro-mesoporous carbide derived carbon materials for high energy and power density electrical double layer capacitors. Tartu, 2015, 148 p.
147. **Heiki Erikson.** Electrochemical reduction of oxygen on nanostructured palladium and gold catalysts. Tartu, 2015, 204 p.
148. **Erik Anderson.** *In situ* Scanning Tunnelling Microscopy studies of the interfacial structure between Bi(111) electrode and a room temperature ionic liquid. Tartu, 2015, 118 p.
149. **Girinath G. Pillai.** Computational Modelling of Diverse Chemical, Biochemical and Biomedical Properties. Tartu, 2015, 140 p.
150. **Piret Pikma.** Interfacial structure and adsorption of organic compounds at Cd(0001) and Sb(111) electrodes from ionic liquid and aqueous electrolytes: an *in situ* STM study. Tartu, 2015, 126 p.
151. **Ganesh babu Manoharan.** Combining chemical and genetic approaches for photoluminescence assays of protein kinases. Tartu, 2016, 126 p.
152. **Carolin Siimenson**. Electrochemical characterization of halide ion adsorption from liquid mixtures at Bi(111) and pyrolytic graphite electrode surface. Tartu, 2016, 110 p.
153. **Asko Laaniste.** Comparison and optimisation of novel mass spectrometry ionisation sources. Tartu, 2016, 156 p.
154. **Hanno Evard.** Estimating limit of detection for mass spectrometric analysis methods. Tartu, 2016, 224 p.
155. **Kadri Ligi.** Characterization and application of protein kinase-responsive organic probes with triplet-singlet energy transfer. Tartu, 2016, 122 p.
156. **Margarita Kagan.** Biosensing penicillins' residues in milk flows. Tartu, 2016, 130 p.
157. **Marie Kriisa.** Development of protein kinase-responsive photoluminescent probes and cellular regulators of protein phosphorylation. Tartu, 2016, 106 p.
158. **Mihkel Vestli.** Ultrasonic spray pyrolysis deposited electrolyte layers for intermediate temperature solid oxide fuel cells. Tartu, 2016, 156 p.
159. **Silver Sepp**. Influence of porosity of the carbide-derived carbon on the properties of the composite electrocatalysts and characteristics of polymer electrolyte fuel cells. Tartu, 2016, 137 p.
160. **Kristjan Haav**. Quantitative relative equilibrium constant measurements in supramolecular chemistry. Tartu, 2017, 158 p.

161. **Anu Teearu**. Development of MALDI-FT-ICR-MS methodology for the analysis of resinous materials. Tartu, 2017, 205 p.
162. **Taavi Ivan**. Bifunctional inhibitors and photoluminescent probes for studies on protein complexes. Tartu, 2017, 140 p.
163. **Maarja-Liisa Oldekop**. Characterization of amino acid derivatization reagents for LC-MS analysis. Tartu, 2017, 147 p.
164. **Kristel Jukk**. Electrochemical reduction of oxygen on platinum- and palladium-based nanocatalysts. Tartu, 2017, 250 p.
165. **Siim Kukk**. Kinetic aspects of interaction between dopamine transporter and *N*-substituted nortropane derivatives. Tartu, 2017, 107 p.
166. **Birgit Viira**. Design and modelling in early drug development in targeting HIV-1 reverse transcriptase and Malaria. Tartu, 2017, 172 p.
167. **Rait Kivi**. Allostery in cAMP dependent protein kinase catalytic subunit. Tartu, 2017, 115 p.
168. **Agnes Heering**. Experimental realization and applications of the unified acidity scale. Tartu, 2017, 123 p.
169. **Delia Juronen**. Biosensing system for the rapid multiplex detection of mastitis-causing pathogens in milk. Tartu, 2018, 85 p.
170. **Hedi Rahnel.** ARC-inhibitors: from reliable biochemical assays to regulators of physiology of cells. Tartu, 2018, 176 p.
171. **Anton Ruzanov.** Computational investigation of the electrical double layer at metal–aqueous solution and metal–ionic liquid interfaces. Tartu, 2018, 129 p.
172. **Katrin Kestav.** Crystal Structure-Guided Development of Bisubstrate-Analogue Inhibitors of Mitotic Protein Kinase Haspin. Tartu, 2018, 166 p.
173. **Mihkel Ilisson.** Synthesis of novel heterocyclic hydrazine derivatives and their conjugates. Tartu, 2018, 101 p.
174. **Anni Allikalt.** Development of assay systems for studying ligand binding to dopamine receptors. Tartu, 2018, 160 p.
175. **Ove Oll.** Electrical double layer structure and energy storage characteristics of ionic liquid based capacitors. Tartu, 2018, 187 p.
176. **Rasmus Palm.** Carbon materials for energy storage applications. Tartu, 2018, 114 p.
177. **Jörgen Metsik.** Preparation and stability of poly(3,4-ethylenedioxythiophene) thin films for transparent electrode applications. Tartu, 2018, 111 p.
178. **Sofja Tšepelevitš.** Experimental studies and modeling of solute-solvent interactions. Tartu, 2018, 109 p.
179. **Märt Lõkov.** Basicity of some nitrogen, phosphorus and carbon bases in acetonitrile. Tartu, 2018, 104 p.
180. **Anton Mastitski**. Preparation of α-aza-amino acid precursors and related compounds by novel methods of reductive one-pot alkylation and direct alkylation. Tartu, 2018, 155 p.
181. **Jürgen Vahter**. Development of bisubstrate inhibitors for protein kinase CK2. Tartu, 2019, 186 p.

182. **Piia Liigand.** Expanding and improving methodology and applications of ionization efficiency measurements. Tartu, 2019, 189 p.
183. **Sigrid Selberg.** Synthesis and properties of lipophilic phosphazene-based indicator molecules. Tartu, 2019, 74 p.
184. **Jaanus Liigand.** Standard substance free quantification for LC/ESI/MS analysis based on the predicted ionization efficiencies. Tartu, 2019, 254 p.
185. **Marek Mooste.** Surface and electrochemical characterisation of aryl film and nanocomposite material modified carbon and metal-based electrodes. Tartu, 2019, 304 p.
186. **Mare Oja.** Experimental investigation and modelling of pH profiles for effective membrane permeability of drug substances. Tartu, 2019, 306 p.
187. **Sajid Hussain.** Electrochemical reduction of oxygen on supported Pt catalysts. Tartu, 2019, 220 p.
188. **Ronald Väli.** Glucose-derived hard carbon electrode materials for sodium-ion batteries. Tartu, 2019, 180 p.
189. **Ester Tee.** Analysis and development of selective synthesis methods of hierarchical micro- and mesoporous carbons. Tartu, 2019, 210 p.
190. **Martin Maide.** Influence of the microstructure and chemical composition of the fuel electrode on the electrochemical performance of reversible solid oxide fuel cell. Tartu, 2020, 144 p.
191. **Edith Viirlaid.** Biosensing Pesticides in Water Samples. Tartu, 2020, 102 p.
192. **Maike Käärik.** Nanoporous carbon: the controlled nanostructure, and structure-property relationships. Tartu, 2020, 162 p.
193. **Artur Gornischeff.** Study of ionization efficiencies for derivatized compounds in LC/ESI/MS and their application for targeted analysis. Tartu, 2020, 124 p.
194. **Reet Link.** Ligand binding, allosteric modulation and constitutive activity of melanocortin-4 receptors. Tartu, 2020, 108 p.
195. **Pilleriin Peets.** Development of instrumental methods for the analysis of textile fibres and dyes. Tartu, 2020, 150 p.
196. **Larisa Ivanova.** Design of active compounds against neurodegenerative diseases. Tartu, 2020, 152 p.
197. **Meelis Härmas.** Impact of activated carbon microstructure and porosity on electrochemical performance of electrical double-layer capacitors. Tartu, 2020, 122 p.
198. **Ruta Hecht.** Novel Eluent Additives for LC-MS Based Bioanalytical Methods. Tartu, 2020, 202 p.
199. **Max Hecht.** Advances in the Development of a Point-of-Care Mass Spectrometer Test. Tartu, 2020, 168 p.
200. **Ida Rahu.** Bromine formation in inorganic bromide/nitrate mixtures and its application for oxidative aromatic bromination. Tartu, 2020, 116 p.
201. **Sander Ratso**. Electrocatalysis of oxygen reduction on non-precious metal catalysts. Tartu, 2020, 371 p.
202. **Astrid Darnell.** Computational design of anion receptors and evaluation of host-guest binding. Tartu, 2021, 150 p.

203. **Ove Korjus.** The development of ceramic fuel electrode for solid oxide cells. Tartu, 2021, 150 p.
204. **Merit Oss.** Ionization efficiency in electrospray ionization source and its relations to compounds' physico-chemical properties. Tartu, 2021, 124 p.
205. **Madis Lüsi**. Electroreduction of oxygen on nanostructured palladium catalysts. Tartu, 2021, 180 p.
206. **Eliise Tammekivi.** Derivatization and quantitative gas-chromatographic analysis of oils. Tartu, 2021, 122 p.
207. **Simona Selberg.** Development of Small-Molecule Regulators of Epi-transcriptomic Processes. Tartu, 2021, 122 p.
208. **Olivier Etebe Nonga.** Inhibitors and photoluminescent probes for in vitro studies on protein kinases PKA and PIM. Tartu, 2021, 189 p.
209. **Riinu Härmas.** The structure and H2 diffusion in porous carbide-derived carbon particles. Tartu, 2022, 123 p.
210. **Maarja Paalo.** Synthesis and characterization of novel carbon electrodes for high power density electrochemical capacitors. Tartu, 2022, 144 p.
211. **Jinfeng Zhao.** Electrochemical characteristics of Bi(hkl) and micro-meso-porous carbon electrodes in ionic liquid based electrolytes. Tartu, 2022, 134 p.
212. **Alar Heinsaar.** Investigation of oxygen electrode materials for high-temperature solid oxide cells in natural conditions. Tartu, 2022, 120 p.
213. **Jaana Lilloja.** Transition metal and nitrogen doped nanocarbon cathode catalysts for anion exchange membrane fuel cells. Tartu, 2022, 202 p.
214. **Maris-Johanna Tahk.** Novel fluorescence-based methods for illuminating transmembrane signal transduction by G-protein coupled receptors. Tartu, 2022, 200 p.
215. **Eerik Jõgi.** Development and Applications of E. coli Immunosensor. Tartu, 2022, 103 p.
216. **Alo Rüütel.** Design principles of synthetic molecular receptors for anion-selective electrodes. Tartu, 2022, 109 p.
217. **Tanel Sõrmus.** Development of stimuli-responsive and covalent bisubstrate inhibitors of protein kinases. Tartu, 2022, 148 p.
218. **Oleg Artemchuk.** Autotrophic nitrogen removal processes for nutrient removal from sidestream and mainstream wastewater. Tartu, 2022, 115 p.
219. **Andre Leesment.** Quantitative studies of Brønsted acidity in biphasic systems and gas-phase. Tartu, 2023, 83 p.
220. **Meeli Arujõe-Sado.** Structural effects in aza-peptide bond formation reaction. Tartu, 2023, 83 p.
221. **Jonas Mart Linge.** Electrochemical reduction of oxygen on silver-based catalysts. Tartu, 2023, 269 p.
222. **Tõnis Laasfeld.** Integrating Image Analysis and Quantitative Modeling for a Holistic View of GPCR Ligand Binding Dynamics. Tartu, 2023, 226 p.
223. **Ernesto de Jesus Zapata Flores.** Derivatization Reagents used in negative mode electrospray LC-MS. Tartu, 2023, 107 p.

224. **Patrick Teppor.** Obtaining platinum-free oxygen reduction catalysts through biomass valorization: a case study of peat. Tartu, 2023, 161 p.
225. **Peeter Valk.** Methanol Oxidation on Platinum-Rare-Earth Metal Oxide Activated Catalysts. Tartu, 2023, 162 p.
226. **Shidong Chen.** Unravelling prehistoric plant exploitation in eastern Baltic: organic residue analysis of plant-based materials by multi-method approach. Tartu, 2023, 245 p.
227. **Yogesh Kumar.** M-N_4 macrocycle-based catalysts for electrocatalysis of oxygen reduction and oxygen evolution. Tartu, 2023, 224 p.